TIP-1, A NEW BIOMARKER FOR RADIOTHERAPY, REGULATES MIGRATION AND INVASION OF HUMAN GLIOMAS THROUGH RHO GTPASES

By

Hailun Wang

Dissertation

Submitted to the Faculty of the

Graduate School of Vanderbilt University

in partial fulfillment of the requirements

for the degree of

DOCTOR OF PHILOSOPHY

In

Cancer Biology

May, 2011

Nashville, Tennessee

Approved:

Assistant Professor Josiane Eid

Assistant Professor Barbara Fingleton

Professor Michael Freeman

Assistant Professor Kevin Haas

Assistant Professor Zhaozhong Han

Professor Dennis E. Hallahan

Dedicated to my amazing parents, sister and Miaojun Han

for their endless support, encouragement and inspiration

ACKNOWLEDGEMENTS

First and foremost, I would like to thank my mentor Dr. Dennis E. Hallahan. His enthusiasm and passion for science and his insightful thoughts really inspired me to explore the biomedical science. I feel lucky to join his lab and start my thesis research on one of his brilliant discovery project. Although it is a highly challenging project, his guidance and consistent support helped me go through all these tough times and finish the project. I am also grateful for all the training opportunities I have been given to become a better scientist. The experience I gained under Dr. Hallahan's guidance will become an invaluable treasure in my life.

I would also like to thank my mentor Dr. Zhaozhong Han for teaching me all these wonderful techniques in phage display. He has always been available for brainstorming. His constructive advises and supports provided me a great help in finishing the thesis projects.

I would like to express my gratitude to all my committee members, Dr. Josiane Eid, Dr. Barbara Fingleton, Dr. Michael Freeman and Dr. Kevin Haas, for serving on my thesis committee and being supportive and constructive.

I am grateful to all members of the Hallahan lab, especially Dr. Lin Geng, Allie Fu and Halina M. Onishko for training me on animal studies. I am particularly grateful to Dr. Heping Yan for helping me produce the TIP-1 antibody. The thesis work would not have been possible without the antibody.

In the end, I want to express my deepest gratitude to my parents, my sister and my beloved Miaojun Han, for their understanding and encouragement and inspiration.

This thesis work was supported in part by NIH grants R01CA127482 (Z Han), P50 CA128323 (J.Gore), R01CA112385, R01CA89674 and R01CA125757 (DE Hallahan)

TABLE OF CONTENTS

LIST OF TABLES

LIST OF FIGURES

CHAPTER I

INTRODUCTION

Overview

Cancer targeted imaging plays an important role in cancer diagnosis. It allows us to rapidly evaluate tumor responses to certain treatments. Peptide-based imaging probes have been widely used in cancer targeted imaging (Aloj and Morelli, 2004; Okarvi, 2004; Reubi and Maecke, 2008). With the development of phage display technology, a great number of peptides have been identified specifically targeting to tumor cells *in vitro* and *in vivo*. However, due to peptides small size and relatively low binding affinity, it is difficult to identify the target of peptides. This thesis research is focused on: **i)**. identifying the target of a specific peptide – HVGGSSV, which binds to radiation responsive tumors, by utilizing several affinity purification techniques especially phage display screening, and validating the target as a marker for evaluation of radiation treatment; **ii)**. exploring the biological functions of the targeting protein.

Tumor Targeted Imaging and Therapy

Cancer is the uncontrolled growth of cells coupled with invasion and metastasis. It is a highly malignant disease. It is the leading cause of death worldwide. Despite the recent facts that cancer incidence and death rates for men and women in the United States

continue to decline, deaths from cancer worldwide are projected to continue rising, with an estimated 12 million deaths in 2030 (World Health Organization). Besides surgery, radiation therapy and chemotherapy are the mostly used methods to treat cancers.

Radiation therapy

Radiation therapy is the medical use of ionizing radiation as part of cancer treatment to control malignant cells. Radiation therapy may be used to treat localized solid tumors, such as cancers of the skin, tongue, larynx, brain, breast, lung, prostate or uterine cervix. It can also be used to treat leukemia and lymphoma. It works by damaging the DNA of cancerous cells through the use of one of two types of high energy radiation, photon or charged particle. This damage is either direct or indirect ionizing the atoms which make up the DNA chain. Indirect damage happens as a result of the ionization of water by high energy radiations, such as X-ray or gamma ray, forming free radicals, notably hydroxyl radicals, which then damage the DNA and form single- or double-stranded DNA breaks. Direct damage to DNA occurs through charged particles such as proton, boron, carbon or neon ions. Due to their relatively large mass, charged particles directly strike DNA and transfer high energy to DNA molecules and usually cause double-stranded DNA breaks. Tumor cells usually have impaired ability to repair DNA damage compared to normal cells. Therefore, the accumulating damages to cancer cells' DNA cause them to die or proliferate more slowly. To minimize the damage to normal cells, the total dose of radiation therapy is usually fractionated into several smaller doses to allow normal cells time to recover. In clinics, to spare normal tissues from the treatment, shaped radiation beams are aimed from several angles of exposure to intersect at the tumor, providing a

much larger absorbed dose in the tumors than in the surrounding tissues. Brachytherapy, in which a radiation source is placed inside or next to the cancer area, is another technique to minimize exposure to healthy tissues during treatment of cancers in the breast, prostate and other organs. It is also common to combine radiotherapy with surgery, chemotherapy, hormone therapy or immunotherapy to maximize treatment efficiency.

Chemotherapy

Chemotherapy is the use of drugs to treat cancers throughout the body. Most chemotherapy drugs work by impairing mitosis, and killing actively dividing cancer cells. Based on their structure and the mechanism they use to attack cancer cells, the majority of chemotherapy drugs can be divided into the following classes (Oslo, 2010): 1). Alkylating agents, which are the oldest and most commonly used class of chemotherapy drugs. They work by attaching an alkyl group to DNA molecules and impairing cell functions. Some examples include: cisplatin, carboplatin and oxaliplatin (Scott, 1970). 2). Anti-metabolites. By imitating purines or pyrimidines, the anti-metabolic drugs become the building blocks of DNA or RNA. They prevent the real purines or pyrimidines from being incorporated into DNA during the "S" phase and stop the cell division. Some of the important drugs include: methotrexate, fludarabine and cytarabine (Peters et al., 2000). 3). Plant alkaloids. These alkaloids are derived from plants and block cell division by preventing microtubule function. The main examples are vinca alkaloids and taxanes (Takimoto CH, 2008). 4). Topoisomerase inhibitors. Inhibition of type I or type II topoisomerases interferes with proper DNA unwinding and blocks both transcription and replication of DNA. Some mostly used examples include camptothecin and etoposide

(Takimoto CH, 2008; Wall et al., 1966). 5). Anthracycline. This class of drugs can intercalate between base pairs of DNA/RNA and prevent the replication of rapidly growing cancer cells. The first anthracycline discovered was daunorubicin, which was produced naturally by Streptomyces bacteria. Doxorubicin was developed shortly after, and many other related compounds have followed (Weiss, 1992).

Targeted therapy

In recent years, with increased understanding of cancer biology and signaling networks, newer chemotherapy agents that do not directly interfere with DNA were developed to target specifically to cancer cells. One major target is the tyrosine kinase. Tyrosine kinases play key roles in cell proliferation, differentiation, migration and apoptosis in response to external and internal stimuli (Schlessinger, 2000). Recent advances have implicated the role of tyrosine kinases in tumor development and progression. They may acquire transforming functions due to mutation(s) or overexpression (Blume-Jensen and Hunter, 2001). For examples, somatic mutations in the EGFR have been associated with human bladder and cervical cancers. Point mutations in FGFR that results in abnormal receptor dimerization and activation were identified in multiple myeloma (Zwick et al., 2002). The aberrant fusion of tyrosine kinase c-ABL with its partner protein BCR causes the kinase hyperactivation found in Chronic myelogenous leukemia (Ben-Neriah et al., 1986; Daley et al., 1990; Goga et al., 1995). Overexpression of wild type or mutated forms of EGFR is documented in 40% of cases of glioblastoma multiforme (Wong et al., 1987) and 40%-50 % of bladder cancer patient (Smith et al., 1989). The constitutive oncogenic activation of tyrosine kinases can be blocked by specific tyrosine kinase

inhibitors. Most small molecular inhibitors generated so far have been ATP mimics. They compete with ATP for binding to tyrosine kinases and inhibit their functions (Davies et al., 2000; Gazit et al., 1989). The most successful examples are Gleevec, Iressa and Tarceva. The extracellular domain of the receptor tyrosine kinase provides an excellent target for monoclonal antibodies. The revolution in antibody technology now allows us to produce humanized, chimeric or bispecific antibody for targeted cancer therapy (Bennasroune et al., 2004; Houshmand and Zlotnik, 2003). Several McAbs have already been approved by the FDA, which include Cetuximab and Panitumumab targeted to EGFR/Erbb1; and Traztuzumab and Pertuzumab targeted to Her2/Erbb2 in breast cancer. Bevacizumab (Avastin) is another McAb that blocks VEGF-A and VEGFR interaction and was the first clinically available angiogenesis inhibitor to treat colon, lung and breast cancers. The targeted therapies are less harmful to normal cells and greatly increased the efficacy of cancer treatments.

Evaluation of cancer treatment efficacy

However, different types of cancers possess different mutations. Even cancers of the same type show different growth characteristics at different locations and in different patients. The heterogeneity of cancers underlies their variable responses to the same treatment. Currently, cancer response is measured by imaging assessment of tumor volumes or by repeated biopsy to analyze tumor pharmacodynamics. Those processes are time consuming and inefficient. Speed and accuracy in detecting a cancer's response to treatment is critical for successfully combating it. Therefore, new technologies are needed for doctors to decide almost immediately whether a chosen treatment is working

or not for one patient. Recently, advances in phage display-related technologies have facilitated the use of small peptide derivatives as probes for recognition and targeting tumors. We employed this technique and identified several peptides that specifically homed to radiation or drug treatment responsive tumors (Han et al., 2008; Passarella et al., 2009). After being conjugated to optically active imaging agents, those peptides can be used to rapidly assess the pharmacodynamic response of cancer to treatments. In this thesis work, by using several molecular biological techniques, I identified the receptor of one of those peptides (HVGGSSV peptide) and explored its functions in the cell.

Principle of phage display

A phage is a type of virus that infects bacteria. Typically, phage consist of an outer protein capsid enclosing genetic material and a tail (Fig. 1A). Due to their simple structure, phage have been developed into a powerful tool in biological studies. Phage display was originally invented by George P. Smith in 1985, and he demonstrated the display of exogenous peptides on the surface of filamentous phage by fusing the DNA of the peptide on to the capsid gene of filamentous phages (Smith, 1985) (Fig. 1B). This technology was further developed and improved to display large proteins such as enzymes and antibodies (Fernandez-Gacio et al., 2003; McCafferty et al., 1990). The connection between genotype and phenotype enables large libraries of peptides or proteins to be screened in a relatively fast and economic way. The most common phage used in phage display are the M13 filamentous phage and the T7 phage (Krumpe et al., 2006; Smith and Petrenko, 1997).

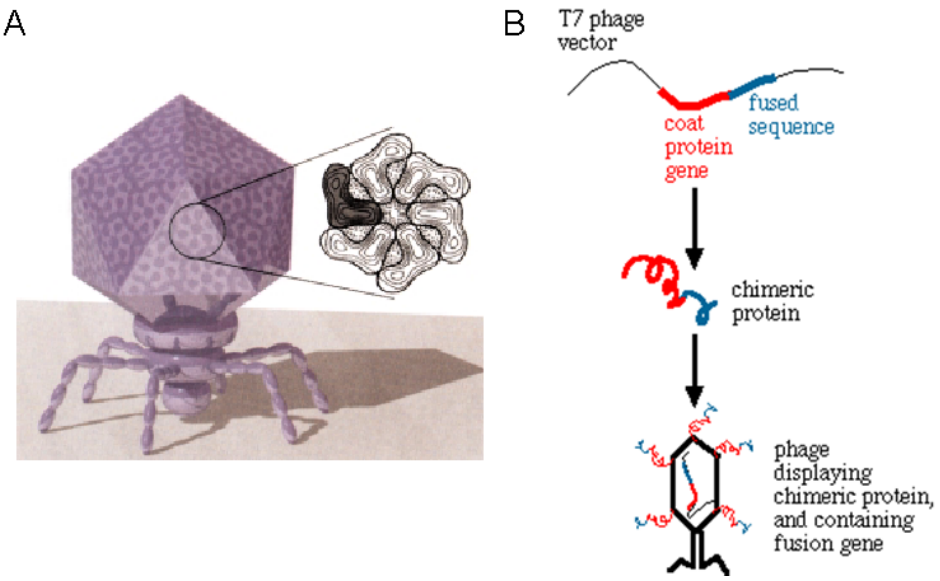

Figure 1: Phage Structure and the principle of using phage to display foreign peptide on phage surface

The principle of phage display is based on affinity purification. First, DNAs encoding the proteins or peptides of interest are ligated into certain phage coat proteins genes to create a phage library. Then the phage library is mixed with a relevant target. By immobilizing the target to the surface of a well or beads, a phage that displays a protein or peptide that binds to the target on its surface will remain while others are removed by washing. Those that remain can be eluted, used to produce more phage (by bacterial infection) and so produce a phage mixture that is enriched with the binding phage. The repeated cycling of these steps is referred to as 'panning', in reference to the enrichment of a sample of gold by removing undesirable materials. The DNAs within phage eluted in the final step are collected and sequenced to identify the interacting proteins or protein fragments.

Application of phage display

The applications of phage display technology include determination of binding partners of proteins, peptides or DNAs (Gommans et al., 2005). The technique is also used to study enzyme evolution *in vitro* for engineering biocatalysts (Pedersen et al., 1998). Phage display is also a widely used method in drug discovery. It can be used for finding new ligands, such as enzyme inhibitors, receptor agonists and antagonists, to target proteins (Pasqualini et al., 1995; Perea et al., 2004; Ruoslahti, 1996; Su et al., 2005). Invention of antibody phage display revolutionized drug discovery (McCafferty et al., 1990). Millions of different single chain antibodies on phages are used for isolating highly specific therapeutic antibody leads. One of the most successful examples was adalimumab (Abbott Laboratories), the first fully human antibody targeted to TNF alpha (Lorenz, 2002).

In vivo phage display

Because isolating or producing recombinant membrane proteins for use as target molecules in phage library screening often faced insurmountable obstacles, innovative selection strategies such as panning against whole cells or tissues were devised (Molek et al., 2011). Since cells inside the body may express different surface markers and possess different characteristics from cells cultured *in vitro*, *in vivo* phage bio-panning was developed to identify more physiologically relevant biomarkers (Pasqualini and Ruoslahti, 1996). Since its invention, *in vivo* phage display has been extensively used to screen for novel targets for tumor therapy. The majority of those studies focused on analyzing the

structure and molecular diversity of tumor vasculature and selecting tumor stage- and type-specific markers on tumor blood vessels (Arap et al., 2002a; Arap et al., 2002b; Rajotte et al., 1998; Sugahara et al., 2010; Valadon et al., 2006). Recently, the use of this technique was expanded to the discovery of new cancer biomarkers to evaluate treatment efficacy. In this research, the authors first treated tumors in mice with either radiation or tyrosine kinase inhibitors. Then a peptide phage library was injected via the tail vein to determine and measure tumor binding. After several rounds of screening and enrichment of phage isolated from the treated tumors (Fig. 2), two phage clones were identified, encoding HVGGSSV or GIRLRG peptides. Both peptides tend to target to treatment responsive tumors. These binding was further confirmed by fluorescent labeling and imaging (Han et al., 2008; Passarella et al., 2009).

Peptides as probes for tumor targeted imaging

Antibodies, especially monoclonal antibodies, have been successfully utilized as cancer therapeutic and diagnostic agents due to their high target specificity and affinity. However, due to the large size of antibody (150kDa) and limited target permeability, non-specific uptake into the reticuloendothelial system, and immunogenicity, most antibody-based therapeutics are of limited efficacy (Lin et al., 2005; Stern and Herrmann, 2005). In contrast to antibodies, peptides are much smaller molecules (1-2 kDa). Peptides have favorable biodistribution profiles compared to antibodies, as they are characterized by high uptake in the tumor tissue and rapid clearance from the blood. In addition, peptides have increased

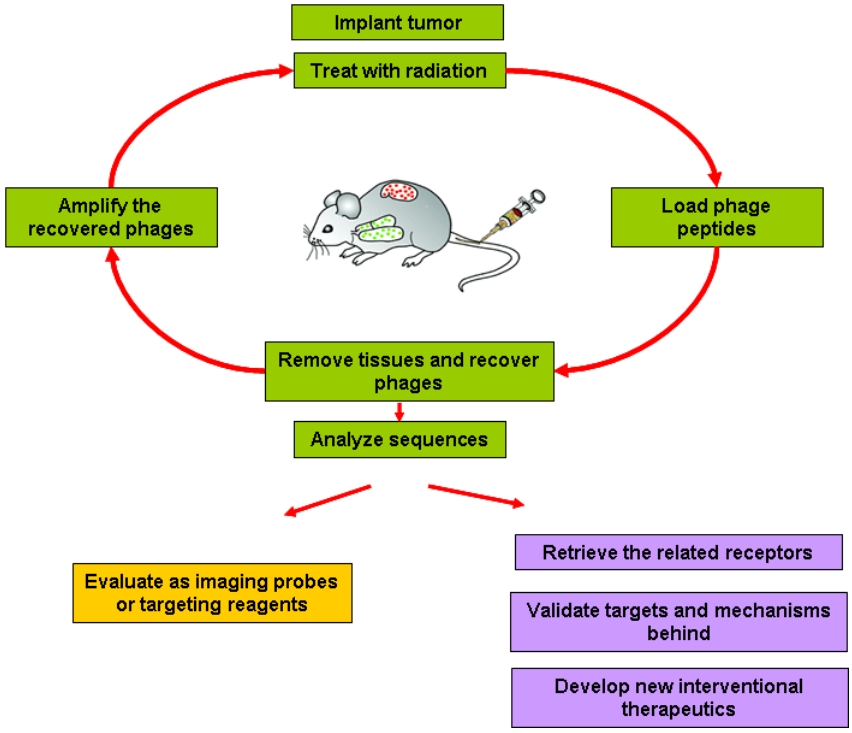

Figure 2: The processes of *in vivo* phage display, for screening peptides that specifically target to radiation or drug treated tumors.

capillary permeability, allowing more efficient penetration into tumor tissues. Also peptides are easy to make and safe to use, they will not elicit an immune response (Ladner et al., 2004). With all these advantages, peptides have been increasingly considered as a good tumor targeted imaging probes (Aloj and Morelli, 2004; Okarvi, 2004; Reubi and Maecke, 2008). To date, a large number of peptides targeting tumor receptors have already been successfully identified and characterized for tumor imaging, such as integrin (RGD), somatostatin, gastrin-releasing peptide, cholecystokinin,

glucagon-like peptides-1 and neuropeptide-Y (Cai et al., 2008; Hallahan et al., 2003; Korner et al., 2007; Miao and Quinn, 2007; Reubi, 2003; Reubi, 2007).

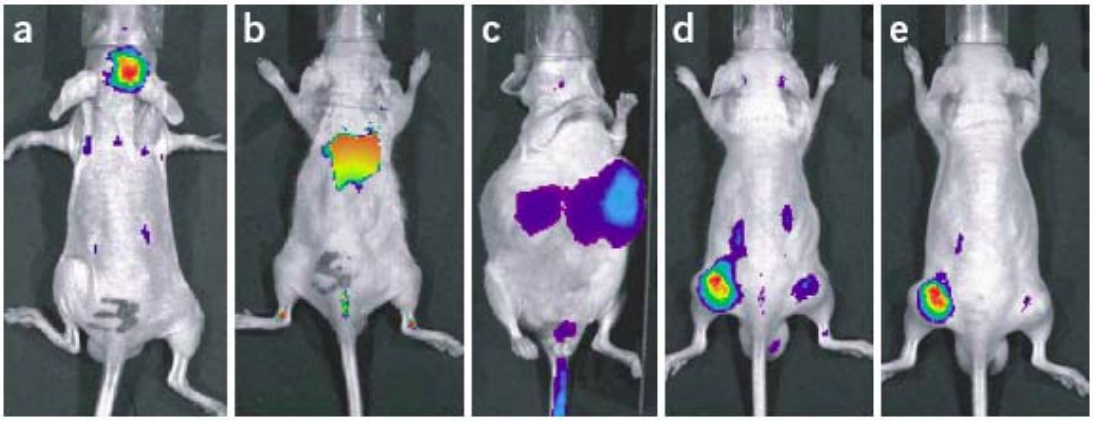

Figure 3. HVGGSSV peptide labeled with near-infrared (NIR) fluorescent dyes specifically located to irradiation treated tumors. a). brain tumor (D54 human glioblastoma cell), b). lung tumor (H460 cell), c) colon cancer liver metastasis (HT22 cell), d). prostate cancer subcutaneous model (PC-3 cell), e). breast cancer subcutaneous model (MDA-MB-231 cell). (Adapted from Han et al., 2008).

For use as *in vivo* imaging probes, peptides can be directly or indirectly labeled with a wide range of imaging moieties according to the imaging modality. For instance, near-infrared (NIR) fluorescent dyes or quantum dots have been labeled for optical imaging (Fig. 3), several radionuclides have been employed for positron emission tomography (PET) or single-photon emission computed tomography (SPECT), and paramagnetic agents have been used for magnetic resonance imaging (MRI) (Frangioni, 2003; Reubi and Maecke, 2008). Peptides can also be conjugated to other tumor targeted polymers or nanoparticles and dramatically increase their tumor targeted selectivity and efficiency (Hariri et al., 2010a; Hariri et al., 2010b; Lowery et al., 2010; Passarella et al., 2010).

Peptide receptor identification

Peptide-based probes have great potential in clinical cancer diagnostics and treatment. To understand the physiology underlying peptide binding, we need to identify its molecular targets. However, peptides are usually unstable. Their surface charges and structures are dramatically altered environmental conditions. In addition, their small size confers low binding affinity. Therefore, traditional affinity purification methods are of little use due to extensive non-specific binding. To date, there are very few identified receptors for peptides in contrast to the great number of discovered cancer targeting peptides (Teesalu et al., 2009). New strategies are needed for identifying a peptide's receptors. In our recent studies of one peptide (HVGGSSV), we utilized a phage cDNA library screening to search for the peptide's receptors. Because several rounds of phage display screening can significantly enrich the low-affinity or low-abundance proteins, we successfully identified a PDZ protein - TIP-1 as the target of HVGGSSV peptide (Wang et al., 2010). This result demonstrated the potential of screening phage-displayed cDNA library in the discovery of molecular targets of the peptides with simple structure and low affinity.

PDZ Proteins and Rho GTPases

PDZ domain structure

The PDZ domain is a very common structural domain involved in protein-protein interactions. In the mouse genome, for example, 928 PDZ domains have been recognized in 328 proteins (Spaller, 2006). It is a highly evolutionally conserved domain and can be

found in bacteria, yeast, plants, and animals (Ponting, 1997). The name 'PDZ' is an acronym combining the first letters of three proteins – post synaptic density proteins (PSD95), Drosophila disc large tumor suppressor (DlgA), and zonula occludens-1 protein (ZO-1) – which were the first three proteins discovered to share the domain. PDZ domains usually consists of 80-90 amino acids forming two alpha-helices and six beta-strands structure. The groove formed between the alpha2-helix and the beta6-strand can accommodate the peptide from its interacting proteins (Fig. 4A).

PDZ domain binding specificity

Most PDZ domains recognize short amino acid motifs at the C-termini of target proteins. Based on their recognized amino acid patterns, PDZ domains are classified into three major classes: (1) class I domains, which recognize the motif S/T-X-I/L/V; (2) class II domains, which recognize the motif Φ-X-Φ; and (3) class III domains, which recognize the motif D/E-X- Φ, where Φ represents a hydrophobic residue. Although the last three amino acids on the PDZ ligands play critical roles in PDZ domain binding, a recent large-scale specificity map of the PDZ domain family revealed that the family is surprisingly complex and diverse, recognizing up to seven C-terminal ligand residues and forming at least 16 unique specificity classes across human and worm (Tonikian et al., 2007; Tonikian et al., 2008). Some PDZ domains can also bind to internal sequences of target proteins. The most well-characterized example of this nature is the interaction between the PDZ domain of the syntrophin (or PSD-95) protein with the internal beta-hairpin finger structure of the nNOS protein (Brenman et al., 1996; Hillier et al., 1999). Besides interacting with peptide structures on proteins, several PDZ domains were shown to bind

to lipid molecules. The best example is the second PDZ domain of Par-3 which binds to phosphoinositides (PIPs). This interaction was shown to be critical for epithelial cell polarization (Wu et al., 2007a).

Although most PDZ domains exist as monomers, some can form dimers (Im et al., 2003a; Im et al., 2003b; Utepbergenov et al., 2006). For example, the second PDZ domain of the ZO1 protein forms a dimer by extensive symmetrical domain swapping of beta-strands. The formation of the PDZ dimer does not affect the binding to its target proteins because the peptide-binding sites of both PDZ domains remain open. Therefore, dimerization of ZO1 provides a structural basis for the polymerization of the tight junction proteins – claudins (Wu et al., 2007b).

Biological functions of PDZ proteins

PDZ proteins usually contain multiple PDZ domains or other functional domains (Fig. 4B). This structural feature enables them to function as scaffold proteins and assemble large intracellular complexes to mediate diverse cellular functions. PDZ proteins are often found at specialized subcellular locations, such as epithelial junctions (Niessen, 2007), neuronal postsynaptic densities (Kim and Sheng, 2004), and immunological synapses of T cells (Ludford-Menting et al., 2005). The various locations of PDZ proteins inside the cell indicate the diverse functions of PDZ domains. For examples, the tight junctional scaffolding molecules ZO-1 and ZO-2 are PDZ domain containing proteins. These proteins interact directly with other proteins - occludin, claudins and JAMs via their PDZ domains, and cluster these proteins at tight junctions. The C-terminus of ZO-1 and ZO-2 can associate with actin, thus providing a direct link with the cytoskeleton and

stabilizing tight junctions (Umeda et al., 2006). In the establishment and maintenance of apical-basal cell polarity, three groups of proteins play a central role: The Crumbs-Pals1-Patj and the Par3-Par6-aPKC protein complexes localize to the apical membrane and promote apical-membrane-domain identity (Margolis and Borg, 2005; Suzuki and Ohno, 2006). Their function is antagonized by the basolaterally localized Lgl-Scrib-Dlg protein complexes, which together promote basolateral membrane identity (Bilder, 2004). Among these nine proteins, six of them contain PDZ domains (Pals1, Patj, Par3, Par6, Scrib and Dlg). In the nervous system, membrane associated PDZ proteins such as PSD-95 and GRIP organize glutamate receptors (NMDAR, AMPAR) and their associated signalling proteins and determine the size and strength of synapses (Gramates and Budnik, 1999; Im et al., 2003b; Mori et al., 1998). Furthermore, PDZ proteins on the surface of cargo vesicles can bind to specific kinesins and myosins (molecular motors) and regulate protein transportation. For instance, the PDZ domains of PSD-95, SAP97 and S-SCAM interact directly with the C terminus of KIF1B (kinesin family member 1B), a kinesin motor (Mok et al., 2002). SAP97 can also bind, through its GK (guanylate kinase-like) domain, to KIF13B/GAKIN (kinesin family member 13B) (Asaba et al., 2003), and through its N-terminal L27 domain to myosin-VI (Wu et al., 2002).

Regulation of PDZ-mediated interactions

As the PDZ domain is one of the major signaling modules inside the cell, its interactions need to be finely regulated. Just like the function regulation of other domains, phosphorylation of Ser, Thr or Tyr within the PDZ ligand plays a major role in modulating PDZ-mediated interactions. For example, the interaction between the NR2B

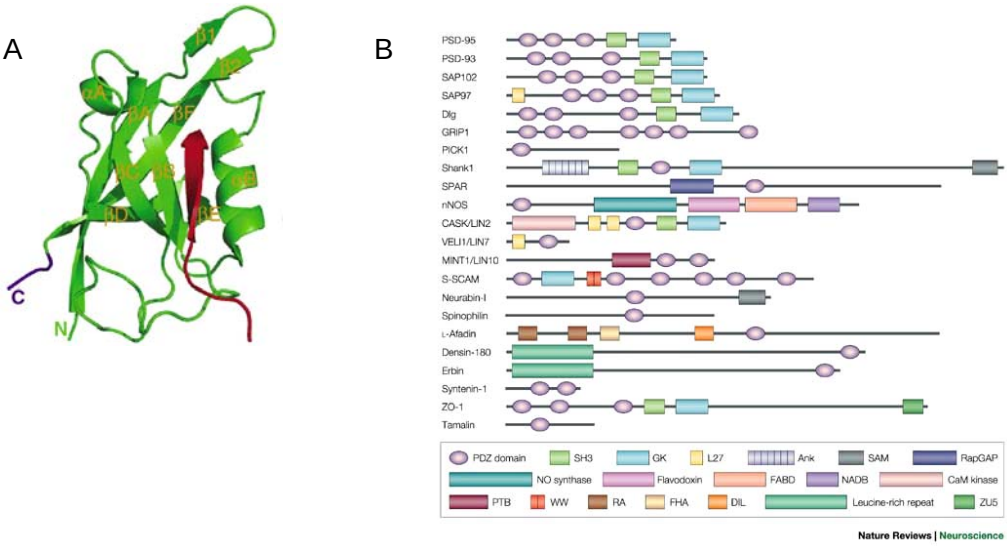

Figure 4: A). Representative structure of a PDZ domain (green) binding with a peptide (red). B). PDZ proteins often contain multiple PDZ domains and other structural domains. (Adapted from Kim and Sheng, 2004).

subunit of the NMDA receptor with PSD-95 is negatively regulated by phosphorylation on the Ser residue (LSSIE**S**DV$_{COOH}$) by CK2, which eventually decreases the surface expression of NR2B in neurons (Chung et al., 2004). Besides phosphorylation of the '-2' site within the PDZ ligand, other positions in the ligand can also be phosphorylated. The Ser residue at '-5' site in the C-terminal PDZ ligand (ERKL**S**SESQV$_{COOH}$) of LRP4 is phosphorylated by CaMKII which disrupts the interaction with PSD-95 and SAP97 (Tian et al., 2006). Although many studies have reported that phosphorylation at the C-terminus of proteins negatively modulates PDZ interactions, others have shown that phosphorylation does not affect or even promotes PDZ interactions (Adey et al., 2000; Chen et al., 2006). Several studies have also reported that phosphorylation on the PDZ

domain itself may also disrupt PDZ protein-protein interactions. For example, the activation of the NMDA receptor induces a CaMKII-dependent phosphorylation of SAP-97 or PSD-95. The phosphorylation sites are located in the alpha2-helix structure, which is the binding site of the PDZ domain. Therefore, phosphorylation causes the dissociation of NR2A from PSD-95 or SAP-97 and negatively regulates spine growth and synaptic plasticity (Mauceri et al., 2007; Steiner et al., 2008).

Although phosphorylation is important in regulating PDZ protein-protein interactions, intramolecular disulfide bond formation in PDZ domains can also modulate PDZ ligands binding. For example, the PDZ5 doamin of InaD, a PDZ scaffold protein in photoreceptor cells that can undergo a light-dependent conformational change, exists in a redox-dependent equilibrium between two conformations: the reduced form, which can bind PDZ ligands, and the oxided form, in which the ligand binding site is distorted due to the formation of a strong intramolecular disulfide bond (Mishra et al., 2007).

Some PDZ domain containing proteins also have a PDZ-binding motif at their C-terminal tail. The binding site of the PDZ domain in these proteins can be occupied by their own C-terminal sequences, thereby inhibiting the binding of other PDZ ligands. This structural feature is found in the proteins NHERF-1, PDZK1, X11α and Tamalin. The autoinhibition of PDZ domain functions can be counteracted by phosphorylation of the C-terminal sequence or the association of other PDZ proteins with the C-terminal tails (Cheng et al., 2009; LaLonde and Bretscher, 2009; Li et al., 2007; Long et al., 2005; Morales et al., 2007; Sugi et al., 2007).

PDZ proteins in carcinogenesis

PDZ proteins are involved in many cell signaling pathways. They are crucial for maintaining normal cellular functions. Disruption of PDZ interactions will lead to diseases (Montell, 2000; Obenauer et al., 2006; Rogelj et al., 2006), especially cancers. Recent evidence indicate that loss of cell polarity is a hallmark of cancer, and is correlated with more aggressive and invasive cancers (Thiery, 2002). Basic mechanisms of cell polarity are often targeted by oncogenic effectors. Several crucial cell-polarity proteins, which contain PDZ domains, are known targets of oncoproteins. For example, the E6 proteins from high-risk human papillomavirus are characterized by the presence of a PDZ binding motif in their C-terminus, through which they bind and degrade a number of PDZ proteins, including MAGI-1, Dlg, Scrib and Par-3. Degradation of these proteins disrupts cell junction integrity, promotes epithelial-to-mesenchymal transition, and eventually leads to cervical cancers (Kranjec and Banks, 2010; Tomaic et al., 2009). On the other hand, deletion of the PDZ binding motif on E6 prevents its immortalization effects (Spanos et al., 2008). Similarly, the oncogenic potential of several other oncoproteins, such as E4-ORF1 and Tax1, also depends on their ability to inactivate key cell polarity PDZ proteins (Frese et al., 2003; Hall and Fujii, 2005; Javier, 2008). Although many PDZ proteins function as tumor suppressors, some can promote tumor formation. For example, overexpression of the PDZ protein, Dishevelled, activates Wnt signaling and contributes to the pathogenesis of mesothelioma (Uematsu et al., 2003).

Rho-family GTPases

The ability of cells to move around depends upon the reorganization of the actin cytoskeleton, which includes generating protrusions at the leading edge and contraction in the body of the cell. Protrusion and contraction require different types of actin filament arrays: protrusion of the lamellipodia requires rapidly growing, branched filament arrays, whereas contractility requires myosin-rich, parallel bundles of actin filaments called stress fibers. Thus, an accurate system is needed for the cell to construct distinct actin-based structures in different sub-cellular sites simultaneously and then constantly remodel those structures as the cell moves forward. In 1992, a pair of landmark papers from Anne Ridley, Alan Hall and co-workers were published and established roles for the small guanine nucleoside triphosphatases (GTPases) in the generation of stress fibers and lamellipodia (Ridley and Hall, 1992; Ridley et al., 1992). Since then, over 20 Rho-family GTPases have been discovered (Boureux et al., 2007).

Rho GTPases functions

Rho GTPases are small (~21kDa) signaling G proteins and are highly conserved from lower eukaryotes to plants and mammals. They form a distinct family within the Ras-like protein superfamily, which also includes the Ras, Rab, Arf and Ran families. Rho GTPases differ from other Ras superfamily members by the presence of a Rho-specific insert domain.

Most Rho GTPase family members act as molecular switches, cycling between a GTP-bound active form and a GDP-bound inactive form (Jaffe and Hall, 2005). Once activated,

Rho GTPases bind different effector molecules and trigger different signaling cascades to direct cellular responses. Rho GTPases have been implicated in many cellular processes including actin and microtubule cytoskeleton organization, motility, cell adhesion, cell division, vesicle trafficking, phagocytosis and transcriptional regulation (Jaffe and Hall, 2005). Rho GTPases can be divided into 8 different subfamilies, which include the most studied Rac, Cdc and Rho families (Boureux et al., 2007). The activation of RhoA, Rac1 or Cdc42 leads to the assembly of contractile actin-myosin filaments, protrusive actin-rich lamellipodia, and protrusive actin-rich filapodia, respectively (Etienne-Manneville and Hall, 2002). Rac1 and Cdc42 initiate peripheral actin polymerization through recruiting the WASP/WAVE and Arp2/3 complex. Arp2 and Arp3 closely resemble the structure of monomeric actin and serve as nucleation sites for new actin filaments. Branched actin networks are created as a result of this nucleation of new filaments (Suetsugu et al., 2002). On the other hand, RhoA stimulates actin polymerization through the diaphanous-related formin (DRF) and mDial. mDial directly binds to the barbed end of an actin filament and initiates actin polymerization (Zigmond, 2004). In addition to elongation, RhoA can also promote phosphorylation of myosin light chain (MLC) through one of its downstream effectors – Rho-associated protein kinase (ROCK). This in turn leads to the activation of myosin II and promotes the actin filament cross-linking (Riento and Ridley, 2003). Rho GTPases can also regulate microtubule dynamics. For example, Cdc42/Rac1 dependent activation of PAK can phosphorylate Op18/stathmin and inhibit its microtubule plus ends disassembly activity (Cassimeris, 2002; Daub et al., 2001). Through IQGAP, a Rac1/Cdc42 effector, Cdc42/Rac1 can also recruit microtubule plus end binding protein – CLIP-170 to the leading edge of migrating cells, and promote

plus end capture (Fukata et al., 2002a). The effect of RhoA on microtubule dynamics is likely to be context dependent. In neurons, RhoA promote the collapse of microtubules through inactivation of CRMP-2, a microtubule assembly protein, by ROCK phosphorylation (Fukata et al., 2002b). In migrating fibroblasts, on the other hand, RhoA promotes the formation of stabilized microtubules. It is not clear how stabilization occurs, although it appears to be mediated by mDia (Palazzo et al., 2001).

In addition to their cytoskeletal effects, Rho GTPases also regulate several signaling pathways. Rho, Rac, and Cdc42 are capable of activating the JNK and p38 MAP kinase pathway, although this is dependent on cell context (Coso et al., 1995; Minden et al., 1995). RhoA, Rac1 and Cdc42 have been reported to activate NFκB in response to a variety of stimuli (Perona et al., 1997). For example, Rac1 and Cdc42 can stimulate the production of reactive oxygen species (ROS) and inflammatory cytokines, both of which are potent activators of NFκB (Bromberg et al., 1994; Joneson and Bar-Sagi, 1998; Pulecio et al., 2010; Qian et al., 2003; Tapon et al., 1998).

Regulation of Rho GTPases functions

The activation of Rho GTPases is mediated by specific guanine nucleotide exchange factors (GEFs), which promote the release of bound GDP and subsequent binding of the GTP (Fig.5). In their active state, Rho GTPases interact with their downstream effectors to modulate their activity and location. The signal is terminated by hydrolysis of GTP to GDP, a reaction that is stimulated by GTPase activating proteins (GAPs) (Bos et al., 2007). Rho proteins are also frequently post-translationally modified at their C-terminal CAAX (where C represents cysteine, A is an aliphatic amino acid, and X is a terminal

amino acid) tetrapeptide motifs with the addition of a lipidic group by prenylation or palmitoylation. This modification promotes proper subcellular localization of Rho GTPases to the plasma membrane and/or endomembranes, which is required for their biological activity (Adamson et al., 1992; Roberts et al., 2008). In addition, guanine nucleotide dissociation inhibitors (GDIs) negatively regulate the activity of Rho GTPases by binding to the C-terminal prenyl group, blocking the release of GDP form Rho GTPases, preventing their membrane association and sequestering them in the cytoplasm, and thus inhibiting their access to downstream targets (Dovas and Couchman, 2005). Rho GDIs can bind to either the GTP- or the GDP-loaded forms.

GEF activity requires a conserved domain known as the Dbl homology (DH) domain for Rho GTPases binding. Meanwhile, almost all GEFs contain a pleckstrin homology (PH) domain adjacent and C-terminal to the DH domain. These two domains provide the minimal structural unit that is required to catalyze the GTP/GDP exchange reaction *in vivo*. PH domains assist the exchange reaction and in some cases participate in binding to the GTPases, but they can also bind to phospholipids and to other proteins (Rossman et al., 2005; Schmidt and Hall, 2002). To date, more than 70 RhoGEFs, 60 RhoGAPs and 3 RhoGDIs have been identified in mammals. They outnumber their target GTPases by a factor of three, which reflects the complexity of the regulation of Rho GTPases (Rossman et al., 2005).

In recent years, several interactions between RhoGEFs and scaffold proteins containing PDZ domains have been reported (Audebert et al., 2004; Liu and Horowitz, 2006; Park et al., 2003; Penzes et al., 2001; Radziwill et al., 2003). These PDZ scaffold proteins promote the formation of multiprotein signaling complexes with RhoGEFs. They can

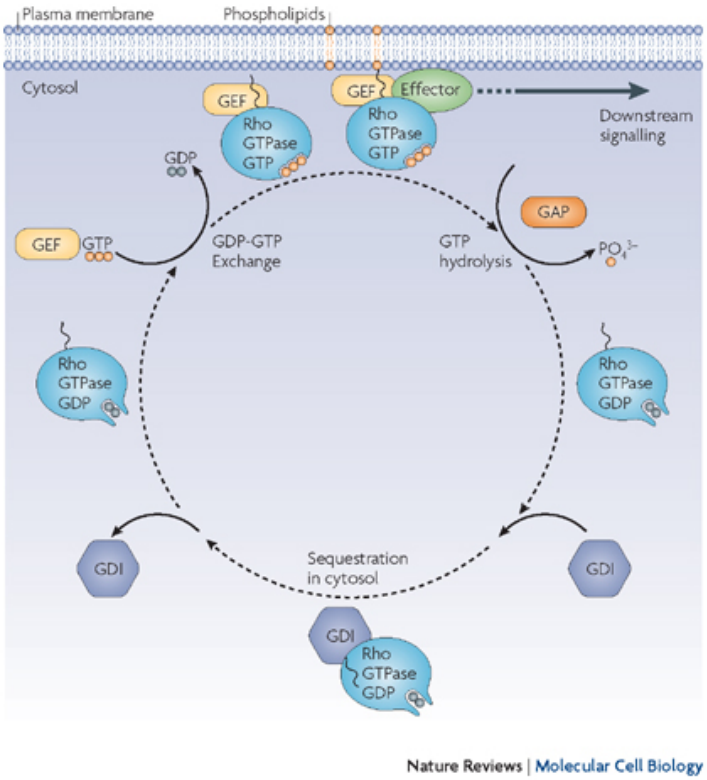

Figure 5: Regulation of the activities of Rho GTPases. GEFs activate Rho GTPases by promoting the exchange of GDP for GTP. Active Rho GTPases are associated with the plasma membrane and bind different effector proteins to trigger different downstream signaling pathways. The low intrinsic GTP hydrolysis activity of Rho GTPases is enhanced by the binding of GAPs, resulting in an inactive GDP-bound GTPase and the shutdown of signaling. GDIs sequester Rho GTPases in the cytosol and inhibit their functions (Iden and Collard, 2008).

target the RhoGEFs to specific locations in the cell, and spatially and temporally restrict their nucleotide exchange activity and subsequent GTPases activation. A recent bioinformatics analysis revealed that more than 40% of RhoGEFs contain a putative PDZ binding motif at the C-terminus (Garcia-Mata and Burridge, 2007), which further

suggested that the interaction between RhoGEFs and PDZ proteins is a general mechanism that controls RhoGEFs targeting and activation.

Rho GTPases in cancer development

As well as contributing to physiological processes, Rho GTPases have been found to contribute to pathological processes including cancer. Rho GTPases have been reported to contribute to most steps of cancer initiation and progression. Unlike the closely related Ras oncoprotein, which often contains mutations that result in constitutively activation, Rho GTPases are found only rarely mutated in tumors, whereas their expression and/or activity are frequently altered. For example, several Rho GTPases are upregulated in some human tumors, including RhoA, RhoC, Rac1, Rac2, Rac3, Cdc42, Wrch2/RhoV and RhoF (Gomez del Pulgar et al., 2005; Gouw et al., 2005).

RhoA has been implicated in virtually all stages of cancer progression. Constitutively active RhoA can stimulate transformation *in vitro* (Jaffe and Hall, 2005). RhoA activity is important for collective cell invasion (Gaggioli et al., 2007). RhoA can also regulate the production and secretion of MMPs, affecting matrix remodeling and tumor cell invasion (Lozano et al., 2003). Some reports indicate that RhoA and its downstream target ROCK are needed for cancer cell extravasation (Miles et al., 2008).

Rac1 is over-expressed in various tumors and accumulating evidence indicates that Rac1 dependent signaling is important for malignant transformation (Gomez del Pulgar et al., 2005). Rac1 is one of the few Rho GTPases mutated in some tumors (Hwang et al., 2004). A splice variant of Rac1, Rac1b, was found upregulated in colon cancers (Jordan et al., 1999). It does not bind RhoGDIs and thus is predominantly present in the GTP-bound state. It stimulates cell survival and cell cycle progression through NFκB (Matos and

Jordan, 2006; Singh et al., 2004; Visvikis et al., 2008). Rac1 can contribute to cancer cell proliferation via regulation of the cell cycle: for example, it stimulates expression of cyclin D1 and induces cell transformation in vitro (Benitah et al., 2004; Jaffe and Hall, 2005). Rac1 can also contribute to cancer cell invasion by regulating the production of MMPs and their inhibitors, the tissue-specific inhibitors of MMP (TIMPs) (Lozano et al., 2003).

Cdc42 expression is upregulated in some breast cancers (Fritz et al., 1999), however, liver-specific knockout indicates that loss of Cdc42 enhances liver cancer development (van Hengel et al., 2008), suggesting that the contribution of Cdc42 to cancer progression may be tissue-specific. By regulating trafficking of receptors and preventing their degradation, Cdc42 can stimulate transformation and contribute to Ras-induced transformation as well (Jaffe and Hall, 2005; Wu et al., 2003). Cdc42 can also affect cell cycle progression by regulating chromosome segregation during mitosis. Cdc42 knockdown was found to induce chromosome misalignment during cell division, leading to multinucleated cells (Yasuda et al., 2006).

CHAPTER II

TIP-1 TRANSLOCATION ONTO THE CELL SURFACE IS A MOLECULAR BIOMARKER OF TUMOR RESPONSE TO IONIZING RADIATION

Abstract

Even though anatomic and functional imaging have been extensively investigated and applied to assess tumor response to treatment, new biomarkers with sound biological relevance are still needed to assess tumor response to treatment in a time-efficient manner. We have previously shown in vivo that a small peptide (HVGGSSV) demonstrated the potential as a molecular imaging probe to distinguish tumors responding to ionizing radiation (IR) and/or tyrosine kinase inhibitor treatment from those of non-responding tumors. In this study we have identified Tax interacting protein 1 (TIP-1, also known as Tax1BP3) as a molecular target that enables selective binding of the HVGGSSV peptide within irradiated xenograph tumors. The peptide binding within irradiated tumors was blocked by a TIP-1 specific antibody as demonstrated by optical imaging of tumors and via immunohistochemical staining of the tumor tissues. Intracellular TIP-1 relocated to the plasma membrane surface within the first few hours after exposure to IR and before the onset of treatment associated apoptosis and cell death, suggesting a potential mechanism to assess tumor response to IR at an early time point of a treatment course. Finally, SPECT/CT imaging with 125I-labeled HVGGSSV peptide showed that TIP-1 imaging can predict tumor cell response to ionizing radiation-induced cell death. Thus,

this study suggested that TIP-1 imaging of radiation-inducible TIP-1 translocation onto the cell surface may predict tumor responsiveness to radiation in a time-efficient manner and thus tailor radiotherapy of cancer.

Introduction

Radiation therapy, in addition to surgery and chemotherapy, is one of the most commonly prescribed treatments for cancer patients. However, due to the heterogeneity of tumors, not all the tumors respond to a therapy regimen with a similar efficiency. Certain tumors respond to one treatment regimen better than others. The dose and delivery of treatments needs to be tailored to each individual patient and progression stage of the tumor (Kung et al., 2000). With current assessment approaches that mainly detect treatment-related anatomic or histological changes within the tumor (Dowsett and Dunbier, 2008), it usually takes weeks to months before therapeutic response can be detected and treatment efficacy can be determined. The long clinical delay before a response can be assessed costs patients valuable time on expensive and potentially ineffective treatments. A time efficient assessment is especially important in managing the highly malignant lung cancer. For this reason, identification of specific biomarkers for early assessment of cancer response can help personalized cancer therapy based on cancer responsiveness to a prescribed regimen.

Targeting the tumor-specific biomarkers with imaging probes allows monitoring of tumor progression even before it is anatomically detectable. Proteomic and genomic approaches have been extensively explored to detect abundance of gene transcripts or products.

Identification of tumor-specific biomarkers with those approaches relies upon precise sampling and thus requires time- and labor-consuming validation. Compared to the proteomic or genomic techniques, phage display is economic, flexible and easily executed. *In vivo* phage display technology (Pasqualini and Ruoslahti, 1996) takes advantage of high fidelity without sampling bias and allows identifying circulation-accessible markers that distinguish tumors from normal tissues by spatial location instead of expression abundance (Christian et al., 2003; Joyce et al., 2003; Zhang et al., 2005). Over the past decade, a myriad of phage display-derived peptides have been generated to bind to tumor cells and tumor-associated antigens (Joyce et al., 2003; Tenzer et al., 2004; Zurita et al., 2004). Although phage display derived peptides show promise in the *in vivo* tumor targeting and molecular imaging of cancer, due to a peptide's small size and relatively low affinity to its molecular target, it is still a great challenge to identify the molecular targets that contribute to the peptide binding *in vitro* and *in vivo*. Lack of knowledge about the biological basis of peptide binding within tumors poses limitations on further development of the tumor-binding peptides for clinical applications.

In a previous study, we have identified a small peptide (HVGGSSV) that specifically binds to tumors responding positively to ionizing radiation and tyrosine kinase inhibitors by using in vivo phage display (Han et al., 2008). Here, we report that Tax interacting protein 1 (TIP-1, also known as Tax1 binding protein 3, Tax1BP3) is a molecular target of the HVGGSSV peptide, and the radiation-inducible translocation of the predominantly intracellular TIP-1 protein onto the plasma membrane surface serves as a biomarker for tumor responsiveness to ionizing radiation.

Materials and Methods

Cell culture

Lewis Lung Carcinoma (LLC) and H460 lung carcinoma cells were obtained from American Type Culture Collection (ATCC, Rockville, MD, USA) and maintained in DMEM medium with 10% fetal calf serum and 1% penicillin/streptomycin (Thermo Scientific Inc., Waltham, MA). Primary human umbilical vein endothelial cell (HUVEC) were obtained from Lonza Biologics (Riverside, CA) and maintained in EGM endothelial cell growth medium. Boyden chambers (Becton Dickinson Labware, Franklin Lakes, NJ) were used to prepare coculture of HUVEC and cancer cells. Constructs expressing shRNA sequences with green fluorescent protein (GFP) were purchased from Open Biosystems (Thermo Fisher Scientific, Huntsville, AL,USA), the TIP-1 specific shRNA (5'-GGCTAACAGCTGATCCCAA-3') matches with TIP-1 mRNA transcripts, a non-targeting sequence was used as a control. Transfection of the cells with recombinant plasmids was conducted with standard protocols (Felgner et al., 1987). Efficiency of the shRNA knocking down was detected by western blot analysis of whole cell lysates. Cells were irradiated with 300 kV X-rays using a Pantak Therapax DXT 300 Model Xray unit (Pantak, East Haven, CT). Antibodies and chemicals were purchased from Sigma (St. Louis, MO) unless otherwise stated.

Phage Display

Screening (Han et al., 2004b; Han et al., 2002) of a cDNA library displayed on T7 bacteriophage was employed to identify proteins interacting with the HVGGSSV peptide.

In brief, the peptide-immobilized magnetic beads were prepared by incubation of 10 μl of 2 mg/ml biotin-GCNHVGGSSV-COOH peptide (Genemed Synthesis Inc., San Antonio, TX) with 100 μl of streptavidin-coated Dynabeads (Invitrogen, Carlsbad, CA) at room temperature for 30 minutes. The same amount of a scramble peptide (Biotin-GCSGVSGHGN-COOH) served as a control in all rounds of the screening. After removal of free peptides, the beads were resuspended in phosphate buffered saline (PBS, pH 7.2) containing 0.1% Tween 20 (PBST). The complex was incubated with 109 plaque-forming units (pfu) of a T7Select human lung tumor cDNA library (Novagen, Gibbstown, NJ) in PBS. The mixture was incubated on a shaker for 2 hours at room temperature. The phage bound to the beads were magnetically separated from the unbound phage within solution. After washing 5 times with PBST, the phages recovered from the HVGGSSV peptide-coated beads were amplified in E.coli BLT5615 (Novagen) for subsequent rounds of screening. In each round of the screening, 10^7 pfu of the amplified phage were used. The phages recovered from both of the HVGGSSV peptide-coated beads and control beads were also titrated; selectivity of the phage to the HVGGSSV peptide was estimated with ratio of the phage recovered from the target beads to those recovered from the control beads. The screening was repeated until significant (>1000) selectivity of the phage to the target beads was achieved.

The phage recovered from the last round of the screening were cloned and amplified for enzyme-linked immunosorbent assay (ELISA)-based plate screening. Briefly, 96-well polystyrene plates (Corning Corp., Lowell, MA) were sequentially coated with streptavidin (0.2 μg/well), blocked with 2% BSA in PBS solution, and incubated with the biotinylated HVGGSSV or scrambled peptides (50 ng/well). 50 μl of the amplified phage

were added to each well for 2 hours incubation at room temperature. After the plates were washed five times with PBST, binding of the phage to peptides was detected with a rabbit antiserum against T7 phage (a kind gift from Dr. Toshiyuki Mori at National Cancer Institute, Frederick, MD) and secondary antibodies conjugated with horse radish peroxidase (HRP) (Sigma). Following PBST washing and incubation with 100 μl of substrate solution containing 2,2'-Azinobis [3-ethylbenzothiazoline-6-sulfonic acid]-diammonium salt (ABTS, from Sigma) in 50 mM sodium citrate buffer, optical density was read at 405 nm. The insert sequences of the HVGGSSV-specific phage clones were amplified with polymerase chain reactions (PCR) by use of a forward primer (5'-GGAGCTGTCGTATCCAGTC-3') and a reverse primer (5'-TGGATTGACCGGAAGTAGAC-3'). The PCR products were purified for sequencing reaction by using a sequencing primer (5'-ATGCTCGGGGATCCGAATTC-3').

GST-TIP-1 protein production

cDNA encoding TIP-1 was amplified using PCR by use of the selected phage clone as template. A construct encoding TIP-1 mutant with a dysfunctional PDZ domain (H90A) (Alewine et al., 2006) in pcDNA3.1 plasmid was a generous gift from Dr. Paul A. Welling at University of Maryland (Baltimore, MD). The DNA fragments encoding the functional TIP-1 and mutant TIP-1 were respectively subcloned into a pGEX-4T-1 vector (GE Healthcare) between BamH I and EcoR I sites to create fusion with glutathione S-transferase (GST). The GST-fused proteins were expressed in E.coli XL-10 GOLD (Stratagene, Kirkland, WA) and purified by passing through a column packed with GST-binding resin (Thermo Scientific Inc., Waltham, MA) (Han et al., 2004a). The purified

proteins were dialyzed against PBS and quantified with Bradford methods (Bradford, 1976). Size and purity of the proteins were examined by SDS-PAGE and coomassie blue staining.

Peptide binding assay

An ELISA was used to study the interaction of peptide with the recombinant TIP-1 protein. All the biotinylated peptides were synthesized at Genemed Synthesis Inc. (San Antonio, TX), purity and molecular weight were assured with HPLC and mass spectrometry. Corning costar 96-well microtiter plates with high protein-binding capacity were coated with streptavidin (0.2 μg/well in PBS) overnight at 4°C. Plates were blocked with BSA and washed twice with PBST before incubating with the biotinylated peptides (50 ng/well) at room temperature for 1 hour. After washing with PBST, the purified GST-TIP-1 or GST-TIP-1(H90A) proteins were added to each well (100 ng/well), respectively. The recombinant proteins bound to the immobilized peptides were detected by rabbit anti-GST antibody and a secondary antibody conjugated with HRP (Sigma). After washing with PBST as described above, ABTS solution was added to each well for color development, and optical density at 405 nm was read for quantification of peptide affinity to the recombinant proteins.

Preparation of TIP-1 specific antibodies

New Zealand white rabbits (Harlan Laboratories, Prattville, AL) were initially immunized with 100 μg of purified GST-TIP-1 protein premixed in a 1:1 ratio by weight with Titermax adjuvant (CytRx Corporation, Los Angeles, CA). One month after the

initial immunization, the animals were boosted with same amount of antigen twice with 2 weeks interval without the adjuvant. Blood samples were periodically taken for antibody titration and specificity analyses by ELISA or western blot. When the anti-TIP-1 antibody reached the designated high titer, the animals were sacrificed to collect the antiserum. The antiserum was purified by passage through protein A plus protein G columns (Sigma) to purify IgGs. TIP-1 specific antibodies were prepared from the purified IgGs by tandem absorption with bacterial proteins and the purified GST protein-conjugated sepharose-4B (Sigma) to remove the IgGs that might bind proteins other than TIP-1. The final antibody was dialyzed against PBS and concentrated via Amicon centrifugal filters (Millipore, Billerica, MA). Specificity of the TIP-1 specific antibody was validated with whole cell staining and western blot analyses of whole cell lysates. All animal studies were conducted as approved by the Institutional Animal Care and Use Committee (IACUC) at Vanderbilt University.

Antibody competition assays

In vitro antibody competition experiments were performed using ELISA as described above in the peptide binding assay, except that the purified GST-TIP-1 proteins were pre-mixed with serial diluted antibodies (starting at 10 μg/ml) before incubating with the immobilized peptides. In vivo antibody competition assays were conducted as described (Han et al., 2008). In brief, $1x10^6$ LLC cells were implanted subcutaneously in both hind limbs of C57BL/6 Foxn1 null/null nude mice (4~5 weeks old, Harlan Laboratories). The tumors were allowed to grow to a size of 0.5 cm in diameter before treatment with X-ray radiation (5 Gy) on one tumor while the other tumor in the same mouse was used as an

untreated tumor control. All animals were anesthetized and shielded to only irradiate the tumors with 300 kV X-rays using a Pantak Therapax DXT 300 Model X-ray unit (Pantak, East Haven, CT). 200 μg of TIP-1 antibody or control antibody (normal rabbit IgGs) were injected through tail veins 4 hours after the radiation treatment, followed by injection of 100 μg of Alexa Fluor750 (Invitrogen)-labeled streptavidin that was complexed with the biotinlytated HVGGSSV peptides. Biodistribution of the peptide-strepavidin complex within the tumor-bearing mice was monitored with In Vivo Imaging Systems 200 (IVIS 200) (Caliper Life Sciences, Hopkinton, MA) at the Vanderbilt University Institute of Imaging Sciences 24 hours after the peptide injection.

Animal imaging

Tumor model development, tumor treatment and Peptide or antibody labeling with Alexa Fluor 750 (Invitrogen) were conducted as described in previous publication (Han et al., 2008). 20 μg of the fluorochrome-labeled antibody or peptide were intravenously administrated in each animal at 4 hours post irradiation. Optical images were taken at 24 hours post the antibody injection with Xenogen IVIS-200 Optical In Vivo Imaging System (Calipers Life Sciences, Hopkinton, MA) at the Vanderbilt University Institute of Imaging Sciences.

Flow Cytometry

Lung cancer cells LLC and H460, HUVEC, or HUVEC co-cultured with either LLC or H460 (in a Boyden Chamber) were allowed to grow to 80% confluency, and irradiated with 0, 2, 4, 6 or 8 Gy. At variable time points after the treatment, the cells were detached

with accutase (eBioscience, San Diego, CA) and collected by centrifugation at 100x g for 5 minutes. TIP-1 antibody in PBS with 2% BSA was added to the suspended cells and incubated on ice for 40 minutes. Free TIP-1 antibody was removed by centrifugation and resuspended in fresh PBS before Alexa Fluor 488-labeled goat anti-rabbit antibody (Invitrogen) was added and incubated for another 40 minutes on ice. Again the cells were washed and Annexin V-APC (BD Biosciences, Franklin Lakes, NJ) was incubated with the cells for 30 minutes on ice to detect apoptotic cells, Propidium Iodide (PI, BD Bioscience) was added in the last 10 minutes to detect cell plasma membrane integrity. Cells were scanned with a BD LSRII flow cytometer (BD Bioscience).

TIP-1-positive and -negative H460 cells were sorted from PI-negative cell populations with FACSAria (BD Bioscience) for proliferation and radiosensitivity assays. Cell proliferation was surveyed with Ki-67 staining. Briefly, the sorted TIP-1 -positive or -negative cells were cultured on glass coverslips at 37 ^{o}C for 24 hours. The cells were then fixed in 70% ethanol, permeated with 0.5% Triton X-100, and stained with Ki-67 antibody (Vector laboratories, Burlingame, CA). Cells were counterstained with DAPI (4',6-diamidino-2-phenylindole) before examination under a fluorescence microscope.

Susceptibility of the TIP-1-positive and –negative H460 cells was evaluated with a clonogenic assay in which the sorted cells were seeded and cultured with DMEM medium supplemented with 10% FCS and antibiotics in petri dishes for 4 hours before the cells were irradiated with X-ray at variable dosages. The colonies were allowed to form in 12 days. The colonies were stained with methylene blue solution and the colony numbers were counted for data analyses.

Statistical analyses

All data were analyzed with the ANOVA to determine significance (with >95% confidence) of the differences. Results are presented as mean ± S.D.

Results

TIP-1 binds to the HVGGSSV peptide

We have previously shown that one phage display-derived peptide HVGGSSV shows selective binding within a broad spectrum of tumors including lung cancers that had been treated with X-ray radiation and multiple tyrosine kinase inhibitors. The peptide binding within the treated tumors correlated to the overall efficacy of the treatment on tumor growth (Han et al., 2008). To further develop this peptide for molecular imaging and tumor-targeted drug delivery, we intended to identify the molecular target that enables the selective binding of the HVGGSSV peptide within irradiated tumors. Screening a T7 phage-displayed human lung tumor cDNA library against the HVGGSSV peptide revealed TIP-1 as one protein that enables the selective binding of the HVGGSSV peptide within irradiated tumors.

To identify the molecular target of the HVGGSSV peptide within irradiated tumors, a T7 phage-displayed human lung tumor cDNA library composed of 107 independent phage clones was screened against the HVGGSSV peptide that was immobilized onto magnetic beads. The beads with a scrambled peptide were used as a control to deplete the non-specific phage clones. The phage recovered from the HVGGSSV peptide-coated beads,

as well those recovered from the control beads, were titrated by following procedures as described (Han et al., 2004b; Han et al., 2002). After 5 rounds of such screening, it was found that total phage showed more than 1000-fold selectivity to the HVGGSSV peptide-coated beads over the control beads (Fig. 6A), indicating the screening successfully enriched some phage clones that selectively bind to the HVGGSSV peptide. Single clones from the fifth round of the biopanning were isolated for further ELISA-based plate screening. Roughly 46.8% (22/47) of the analyzed phage clones exhibited specific binding to the HVGGSSV peptide but no detectable binding was observed to the control peptide which has same amino acid composition but with a scrambled amino acid sequence (data not shown). 17 out of the 20 (85%) sequenced HVGGSSV-binding phage clones encoded amino acid sequence of the TIP-1 (Rousset et al., 1998). Specificity of the TIP-1 expressing phage to HVGGSSV peptide was shown (Fig. 6B) in the ELISA-based assays.

TIP-1 binds to the HVGGSSV peptide via PDZ domain

To further study the interaction of the HVGGSSV peptide and TIP-1 protein, gene fragments encoding TIP-1 protein were inserted into an expression plasmid to produce recombinant GST-TIP-1 proteins in E. coli. The GST tag was utilized to purify the recombinant proteins to homogeneity (Fig. 6D). Affinity of the HVGGSSV peptide with TIP-1 protein was studied with ELISA by use of the purified recombinant proteins and synthetic peptides (Fig. 6E). TIP-1 is a small protein of 124 amino acids, a PDZ-domain is the only functioning structure identified so far (Fig. 6C). The HVGGSSV peptide contains a canonical PDZ binding motif (-X-S/T-X-V/L/I, where X represents any

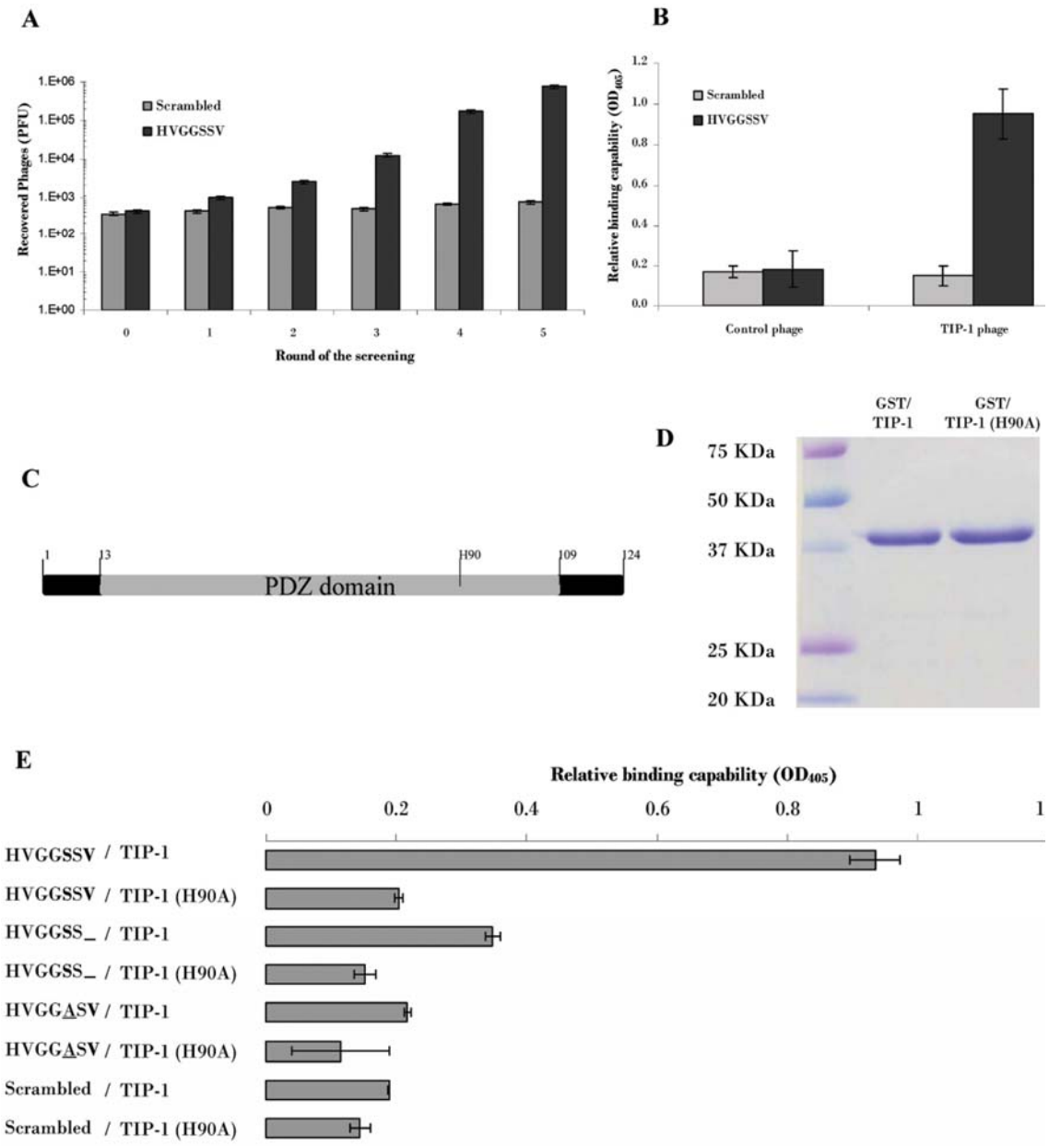
A
Recovered Phages (PFU)
1.E+06
1.E+05
1.E+04
1.E+03
1.E+02
1.E+01
1.E+00
Scrambled
HVGGSSV
0
1
2
3
4
5
Round of the screening
B
Relative binding capability (OD405)
1.2
1.0
0.8
0.6
0.4
0.2
0.0
Scrambled
HVGGSSV
Control phage
TIP-1 phage
C
1
13
H90
109
124
PDZ domain
D
GST/
TIP-1
GST/
TIP-1 (H90A)
75 KDa
50 KDa
37 KDa
25 KDa
20 KDa
E
Relative binding capability (OD405)
0
0.2
0.4
0.6
0.8
1
1
HVGGSSV / TIP-1
HVGGSSV / TIP-1 (H90A)
HVGGSS_ / TIP-1
HVGGSS_ / TIP-1 (H90A)
HVGGΔSV / TIP-1
HVGGΔSV / TIP-1 (H90A)
Scrambled / TIP-1
Scrambled / TIP-1 (H90A)

Figure 6. HVGGSSV peptide binds to PDZ domain of the TIP-1 protein. A: Enrichment of phage with selective binding to the HVGGSSV peptide. Phages recovered from the five rounds of screening and those from the original phage library were subjected to selectivity analysis on beads coated with the HVGGSSV peptide or a scrambled peptide control, respectively. Shown are number (PFU) of phage recovered from the beads after the free phage were washed off. 109 PFU of phages were used in this assay. B: Specificity of the TIP-1-expressing phage to the HVGGSSV peptide. C: Diagram of TIP-1 protein shows location of PDZ domain and the critical amino acid (H90) for PDZ ligand binding; D: SDS-PAGE image shows purity of the recombinant TIP-1 proteins and a dysfunctional mutant TIP-1 (H90A). The fusion proteins (~37 kD) were analyzed along with molecular weight markers. E: Relative association of the purified recombinant proteins to the synthetic peptides was evaluated with ELISA. In these assays, 100 ng of the purified GST/TIP-1 or GST/TIP-1(H90A) proteins were used per well, all the synthetic peptides were used as 50 ng per well. The mutations in the PDZ binding motif were underlined. Shown are representative data from triplicate experiments. * $p<0.05$, $n = 3$, the Student's t-test.

hydrophobic amino acids) (Kay and Kehoe, 2004), the peptide probably binds to TIP-1 through the PDZ domain. Therefore a TIP-1 mutant protein (H90A) with abolished PDZ ligand binding capability (Alewine et al., 2006) was included in the binding assay. Several peptides with mutation within the PDZ binding motif were also included in the ELISA-based affinity study. The data showed that the HVGGSSV peptide binds to the TIP-1 protein through the PDZ domain, it can not bind to the H90A mutant which contains a dysfunctional PDZ domain. The scrambled peptide, as well as other peptides with single mutations within the PDZ binding motif, did not show significant binding to the TIP-1 protein (Fig. 6E).

TIP-1 specific antibody competes with HVGGSSV peptide for TIP-1 binding

TIP-1 antibody was developed by immunizing rabbits with the purified GST-TIP-1 proteins. Specificity and reactivity of the TIP-1 antibody were determined by western

blot analysis of whole LLC cell lysate and immunofluorescent staining of LLC cells in which TIP-1 expression had been depleted with specific shRNA. The TIP-1 specific antibody only recognized a single band corresponding to the endogenous TIP-1 protein (~14 kD) in a western blot analysis of the LLC whole cell lysates, with minor or undetectable binding to other unrelated proteins (Fig. 7A). Cell staining further demonstrated specificity of the TIP-1 antibody. We identified one out of a panel of shRNA constructs that efficiently down-regulated TIP-1 expression within LLC cells, as shown by western blot analysis of whole cell lysate (upper panel of Fig. 7B). This TIP-1 targeting shRNA was selected for transfection of LLC cells and the transfection was tracked with GFP expression from the shRNA plasmid. Overlapping of the TIP-1 antibody (red) and GFP (green) was observed within the LLC cells that were transfected with a construct with a control shRNA (pointed with arrow heads). The TIP-1 specific antibody did not stain the LLC cells that were transfected with a construct with the TIP-1-targeting shRNA (pointed with arrows), because the target of the antibody had been depleted with the TIP-1 targeting shRNA (lower panel of Fig. 7B). These data demonstrated that the TIP-1 antibody did not bind to any protein other than TIP-1 within the cancer cells. These results confirm that this is a TIP-1 specific antibody.

The TIP-1 specific antibody inhibits the HVGGSSV peptide binding to the recombinant TIP-1 protein in a dose-dependent manner as measured by ELISA (Fig. 7C), whereas the control antibody did not interfere with the binding. The results of these experiments demonstrate that the TIP-1 specific antibody share or overlap with the HVGGSSV peptide for common interacting areas within the TIP-1 protein. Therefore, this TIP-1

antibody was used to study the contribution of TIP-1 to the selective binding of the HVGGSSV peptide within irradiated tumors.

TIP-1 mediates binding of the HVGGSSV peptide within irradiated tumors

To determine if TIP-1 binds to the HVGGSSV peptide within irradiated tumors, antibodies were intravenously administrated in LLC tumor-bearing mice prior to the injection of the fluorophore-labeled HVGGSSV peptide. Optical imaging data showed that binding of the HVGGSSV peptide within the irradiated tumors was not affected by pre-injection of the control IgGs. However, pre-injection of the TIP-1 specific IgGs dramatically attenuated the accumulation of the fluorophore-labeled peptide within the irradiated tumors (Fig. 7D). These data clearly demonstrated that, at least in part, TIP-1 mediates the selective binding of the HVGGSSV peptide within the irradiated tumors.

TIP-1 specific antibody exhibited similar binding patterns as the HVGGSSV peptide within irradiated tumors

We have previously shown that HVGGSSV peptide specifically binds to the tumors responding positively to radiation and/or tyrosine kinase inhibitors (Han et al., 2008). If TIP-1 contributes to the peptide accumulation within irradiated tumors, one logic prediction is that the TIP-1 antibody can recapitulate the biodistribution pattern of the HVGGSSV peptide in tumor-bearing mice. To test this hypothesis, nude mice bearing H460 or LLC xenografts were irradiated, Alexa Fluor-750 labeled TIP-1 antibody was injected via tail veins 4 hours after the radiation treatment by following the same protocol

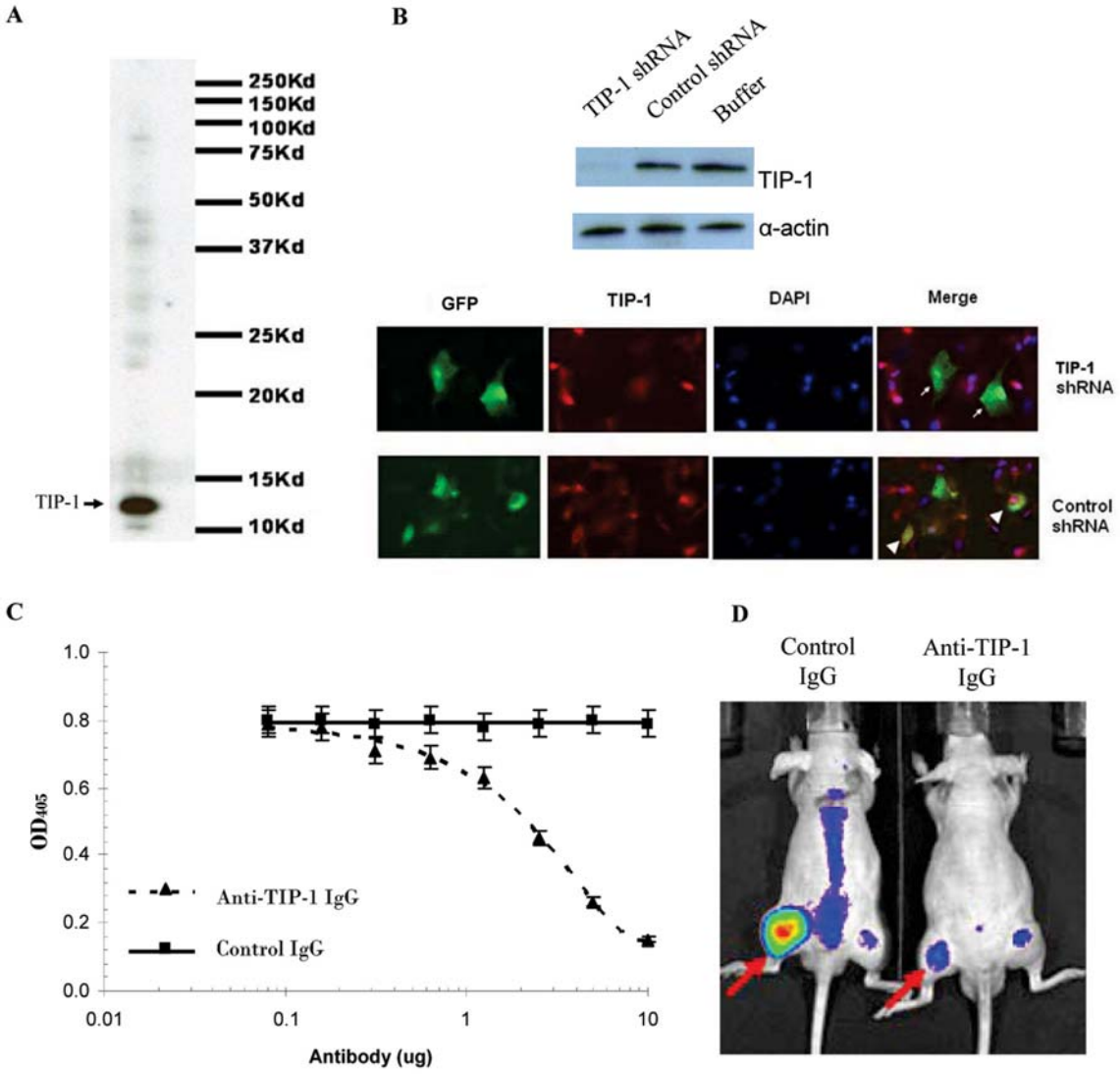
A
250Kd
150Kd
100Kd
75Kd
50Kd
37Kd
25Kd
20Kd
15Kd
10Kd
TIP-1
B
TIP-1 shRNA
Control shRNA
Buffer
TIP-1
α-actin
GFP
TIP-1
DAPI
Merge
TIP-1 shRNA
Control shRNA
C
1.0
0.8
0.6
0.4
0.2
0.0
OD405
Anti-TIP-1 IgG
Control IgG
0.01
0.1
1
10
Antibody (ug)
D
Control IgG
Anti-TIP-1 IgG

Figure 7. TIP-1 specific antibody blocked the HVGGSSV peptide binding within irradiated tumors. A: Specificity of the TIP-1 antibody as revealed with western blot analysis of whole LLC cell lysate. The endogenous TIP-1 protein (~14 kD) recognized by the antibody is identified with an arrow. B: Specificity of the TIP-1 antibody as demonstrated in immunofluorescent staining of LLC cells that were transfected with shRNA plasmids. Effect of the TIP-1 targeting shRNA on TIP-1 expression was determined with western blot analysis (upper panel). In the cell staining, the transfected cells were tracked with GFP protein expression from the shRNA plasmids. TIP-1 was stained as red with the TIP-1 antibody. Cell nuclei were stained with DAPI. The LLC cells transfected with the control shRNA that did not affect TIP-1 expression are shown with arrow head, while the cells transfected with TIP-1 targeting shRNA that abolished TIP-1 expression are identified with arrows (lower panel). C: ELISA-based in vitro competition assay. Serially diluted antibodies were pre-incubated with the purified GST/TIP-1 proteins (100 ng/well) before the complex was added to the plates coated with the HVGGSSV peptide (50 ng/well). The GST/TIP-1 protein associated to the immobilized HVGGSSV peptide was detected with GST-specific antibody. D: Optical images of LLC tumor-bearing mice that were co-administrated with the Alexa Fluor 750-labeled HVGGSSV peptide and antibodies. LLC tumors in the left hind limbs were irradiated at 5 Gy (indicated with arrows). 200 μg of the TIP-1 antibody, or the control antibody, was injected at 2 hours post the IR treatment, followed by injection of Alexa Fluor 750-labeled HVGGSSV peptide at 4 hours post the IR treatment. Optical images were acquired 24 hours after the peptide injection. The presented data represent three independent experiments.

that was used to study the biodistribution of the HVGGSSV peptide within tumor-bearing mice (Han et al., 2008). Optical images acquired 24 hours after the antibody injection indicated that the TIP-1 antibody had high selectivity to the irradiated tumors, but not the untreated tumors or normal tissues in both of the LLC and H460 tumor models (Fig. 8A). In this regard, accumulation of the TIP-1 specific antibody within the irradiated tumors was confirmed with immunohistochemical staining (Fig. 8B) of the retrieved tumor tissues after animal imaging.

Radiation induces TIP-1 translocation onto the plasma membrane surface

TIP-1 is a basically intracellular protein that is ubiquitously expressed within multiple

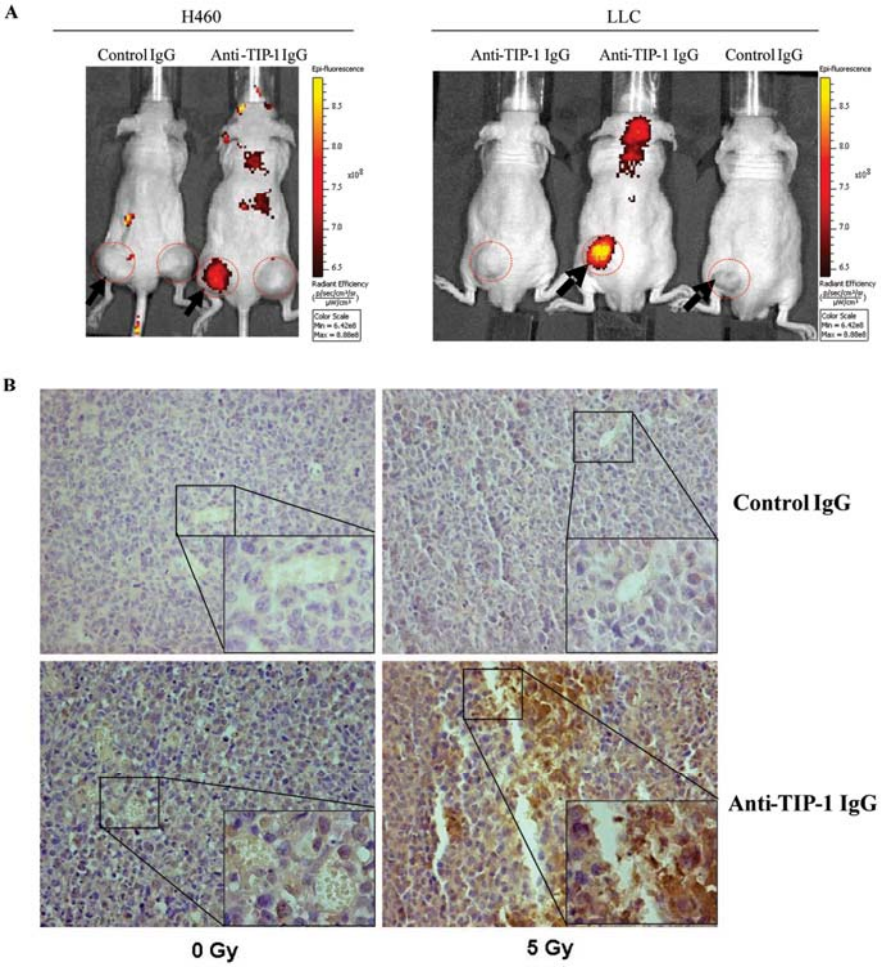

Figure 8. TIP-1 specific antibody selectively homed to the irradiated tumors. A: NIR images of the TIP-1 antibody distribution within tumor-bearing mice. H460 and LLC tumors were developed in hind limbs of nude mice, respectively. Tumors are indicated within the dashed circles. The irradiated tumors (at 5 Gy) are indicated by arrows. Alexa Fluor 750-labeled control or TIP-1 specific antibodies were injected 4 hours after the irradiation. The representative optical images shown were acquired 24 hours after the antibody injection. B: Immunohistochemical staining of the intravenously administrated antibodies within the irradiated tumors. The imaged tumors were retrieved for detection of the antibodies within the tumors. The antibodies (rabbit IgGs) were detected with HRP-conjugates and visualized with DAB (shown as brown). Hematoxylin (blue) was used for counterstaining. Representative images from H460 tumor sections are presented, high magnification (x400) images are shown as inserts.

organs (Kanamori et al., 2003). The tumor-specific and radiation-inducible binding of the HVGGSSV peptide and the TIP-1 antibody within tumor-bearing mice suggested that TIP-1 accessibility to the circulating peptide or antibody is inducible upon radiation treatment and limited within tumor cells. We used cultured LLC, H460 lung cancer cells and HUVEC cells to study the IR-induced TIP-1 translocation onto the cell surface. Western blot analysis of the whole cell lysates did not show dramatic changes in the TIP-1 protein level after IR in all the three tested cells (data not showed). However, flow cytometric analysis showed that the percentage of the H460 cells with TIP-1 expression on the cell surface was elevated from basal level (untreated cells) of 4.67% to 13.3% in 24 hours after IR treatment (Fig. 9A). This observation was supported by immunofluorescent staining of the surface-located TIP-1 on the irradiated H460 cells (Fig. 9B). It was found that the translocation of the TIP-1 protein onto the H460 cell plasma membrane surface sustained for a prolonged period of time after the irradiation (Fig. 9C). The effect of IR on TIP-1 translocation is dose-dependent (Fig. 9D), higher doses of IR were more effective at inducing the TIP-1 translocation onto the cell surface. A similar effect of radiation on the TIP-1 expression on the cell surface were also observed on the LLC cells, but not the HUVEC cells even then the endothelial cells had been co-cultured with LLC or H460 cancer cells (Fig. 9F). These data suggested that radiation induced translocation of the intracellular TIP-1 onto the plasma membrane might be limited to cancer cells.

The TIP-1 positive and negative H460 cells were sorted for western blot analysis to determine whether they represent two independent subgroups of cells with different TIP-1 protein level. The result showed that the total TIP-1 levels were similar in both of the

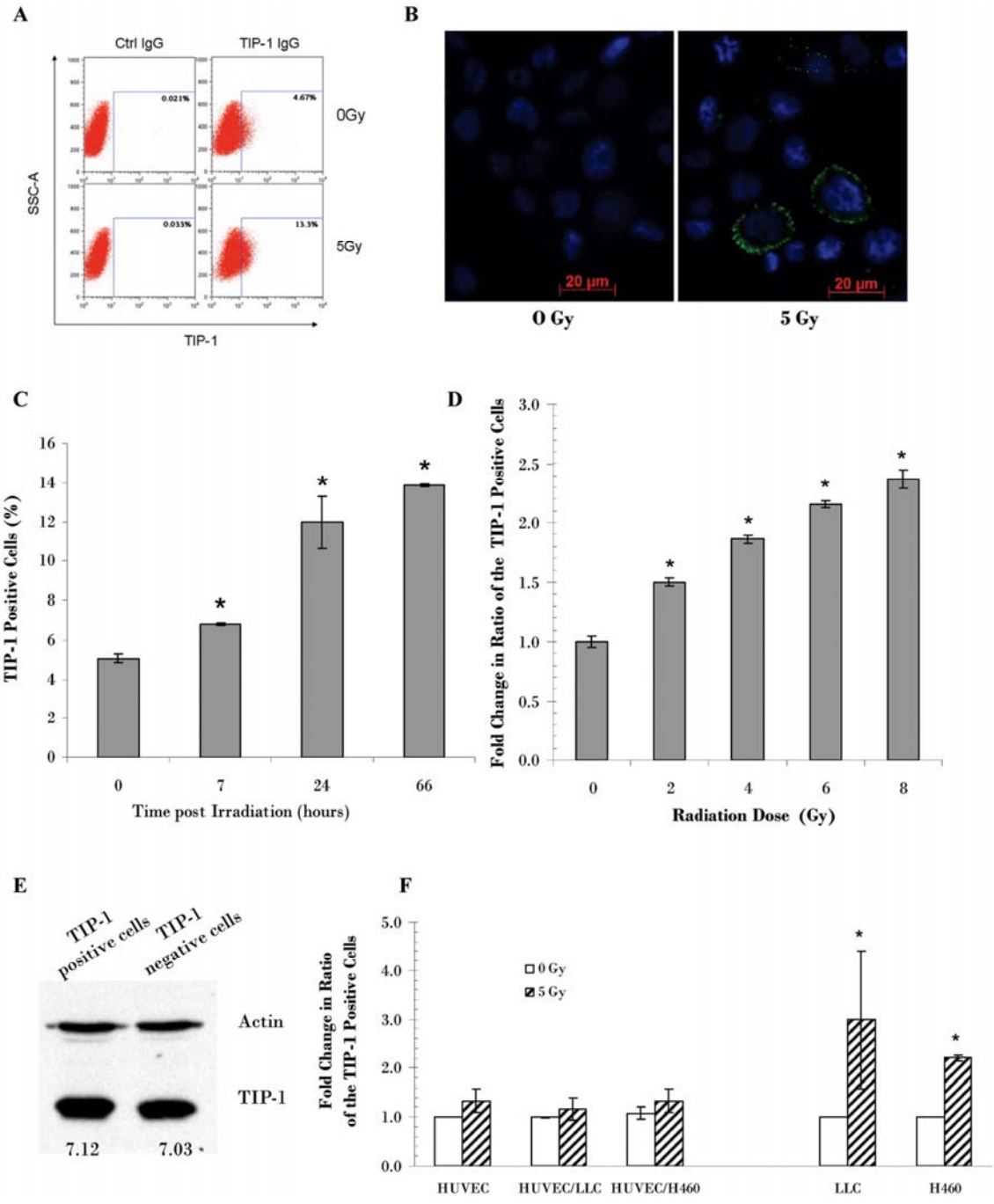
A
Ctrl IgG
TIP-1 IgG
0Gy
5Gy
SSC-A
TIP-1
B
20 μm
20 μm
0 Gy
5 Gy
C
TIP-1 Positive Cells (%)
Time post Irradiation (hours)
D
Fold Change in Ratio of the TIP-1 Positive Cells
Radiation Dose (Gy)
E
TIP-1 positive cells
TIP-1 negative cells
Actin
TIP-1
7.12
7.03
F
Fold Change in Ratio of the TIP-1 Positive Cells
0 Gy
5 Gy
HUVEC
HUVEC/LLC
HUVEC/H460
LLC
H460

Figure 9. Radiation induced TIP-1 translocation onto the plasma membrane of the cancer cells. A: Flow cytometric profile of TIP-1 expression on the H460 cell surface. TIP-1 on the cell surface was detected with the TIP-1 antibody 24 hours after radiation treatment, a control IgG was included to demonstrate the antibody specificity. B: Fluorescent staining of the TIP-1 expression (green) on the cell surface of the irradiated H460 cells. DAPI was used for counterstaining. C: Time course study. The H460 cells were irradiated at 5 Gy and then fixed at variable time points after irradiation for flow cytometric analysis of the TIP-1 expression on the cell surface. Percentage of the TIP-1 positive cells was presented. D: The dose-dependence study. The H460 cells were irradiated with variable dose of X-ray, the cells were fixed 24 hours post the irradiation for profiling the TIP-1 expression on the cell surface with flow cytometry. Fold change of the TIP-1 positive cells was calculated by comparison to the untreated cells (counted as 1). E: Western blot analysis of TIP-1 expression within the TIP-1 positive or negative cells that were sorted from the irradiated (5 Gy) H460 cells 24 hours after the irradiation. Relative TIP-1 protein level was normalized to that of the actin control (counted as 1) and shown under the image. F: Flow cytometric profile of TIP-1 expression on the cell surface of LLC, H460 or HUVEC cells. The cells were treated with 5 Gy of X-ray, TIP-1 on the cell surface was profiled 24 hours post the radiation treatment. Fold change of the TIP-1 positive cells was calculated by comparison to the untreated cells (counted as 1). * $p<0.01$, n = 3, the ANOVA, each was compared to the untreated control, respectively.

TIP-1 positive and negative cells (Fig. 9E). Combined with the observations that IR did not significantly change overall TIP-1 protein levels in the tested cells, we concluded that radiation does not alter total protein levels of TIP-1 but rather appears to promote the TIP-1 translocation onto the plasma membrane surface.

The radiation-induced TIP-1 translocation relates to reduced colony formation and proliferation potential and increased susceptibility to subsequent radiation treatment

Annexin V profiling (apoptosis) and PI staining (membrane integrity and cell death) are commonly used to detect cellular response to cytotoxic treatment. H460 cells were

irradiated (5 Gy) and dissociated 24 hours after the irradiation for flow cytometric analysis. Triple color flow cytometric profiling showed that the majority of cells with TIP-1 expressed on the cell surface (TIP-1 positive cells) are negative for both the dead cell marker (PI) and the apoptotic cell marker (Annexin V) (Fig. 10A). Among the total apoptotic cells (0.48%+1.41% = 1.89%), only one third (0.48% out of 1.89%) of them were TIP-1 positive. Among the TIP-1 positive cells (13.5%+0.48% = 13.98%), the majority (13.5% out of 13.98%) were Annexin V negative. Among all the dead cells (0.98%+6.19% = 7.17%), only a small portion (0.98% out of 7.17%) of the dead cells were stained as TIP-1 positive. Among all the TIP-1 positive cells (13%+0.98% = 13.98%), the majority (13% out of 13.98%) were PI-negative. These data suggest that radiation-inducible TIP-1 translocation onto the cell surface does not overlap with treatment associated apoptosis or cell death.

The TIP-1 positive and negative H460 cells were sorted from the irradiated H460 cells for in vitro colony formation, proliferation and radiation susceptibility studies. Although both irradiated TIP-1 positive and negative cells showed very low capability to form visible colonies on petri dishes, a statistically significant difference was observed between the two subgroups of cells with respect to the capability of colony formation (Fig. 10B). Ki-67 staining (Fig. 10C) further showed that fewer TIP-1-positive cells were undergoing proliferation than the TIP-1-negative cells. Clonogenic assays (Fig. 10D) indicated that fewer TIP-1 -positive cells survived after subsequent radiation treatment than the TIP-1 -negative cells. All these data suggested that the radiation-inducible TIP-1 translocation onto the cancer cell surface serves as a biomarker for identifying radiation-responding cancers before the onset of apoptosis and cell death.

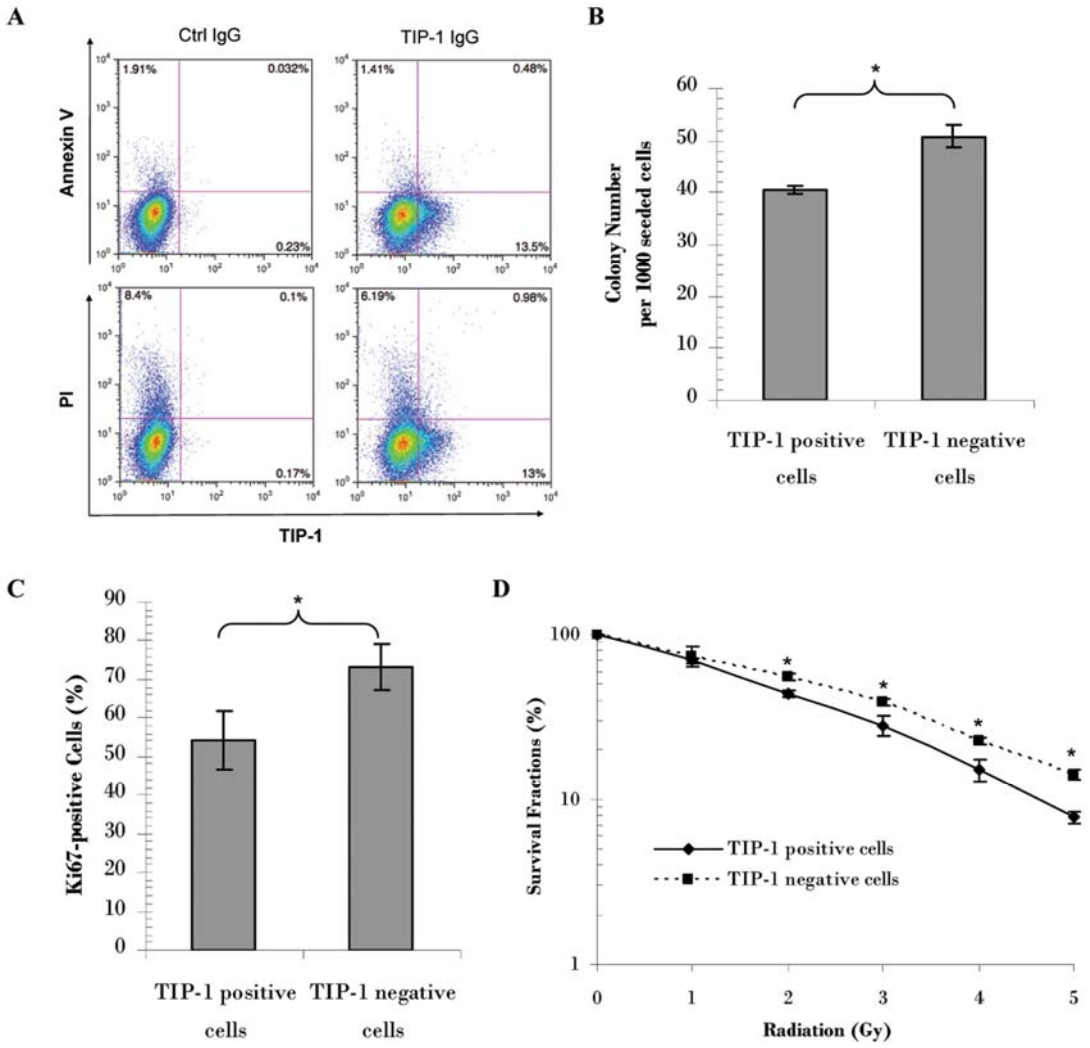

Figure 10. TIP-1 translocation onto the cell surface is a biomarker distince from those for cell death and apoptosis. A: Flow cytometric profile of TIP-1 expression on the cell surface, apoptosis (Annexin V) and cell death or membrane integrity (PI) at 24 hours after the radiation (5 Gy) treatment of the H460 cells. Percentage of the cells in each section was shown in the representative profile images from three independent experiments. B: Colony formation on petri dishes of the TIP-1 positive and negative cells sorted from the irradiated H460 cells. The H460 cells were irradiated at 5 Gy. The TIP-1 positive and negative cells were sorted 24 hours post the radiation treatment. Colony formation capability of the two subgroups of cells was shown as colony number per 1000 seeded cells. C: Proliferation capability of the sorted cells as determined with Ki-67 staining. Percentage of the proliferative cells among the counted cells was shown. D: Susceptibility of the sorted H460 cells to subsequent irradiation. Shown are data from clonogenic assays. Survival fractions are presented to show the difference of the radiation susceptibility between the TIP-1 positive and negative cells. * $p<0.05$, n = 3, the Student's t-test.

Discussion

Not all tumors, not even within the same classifications, respond to a treatment in the same way. Personalized or tailored treatment of tumor calls for efficient and reliable assessment of tumor responsiveness. Even though anatomic and functional imaging have been extensively investigated and applied to assess tumor response to treatment, new biomarkers with sound biological relevance are still needed to assess tumor response to treatment in a time-efficient manner.

In an effort to identify such biomarkers, we previously identified a short peptide (HVGGSSV) using in vivo phage display technology. The peptide demonstrated potential in assessing the tumor responsiveness to radiation and tyrosine kinase inhibitors at an early stage of treatment courses (Han et al., 2008). As demonstrated within multiple heterotopic and orthotopic tumor models, the peptide selectively binds to the responding tumors, and the peptide accumulation within the treated tumors correlates to the overall biological effects of the treatment on the tumor growth control. In this study, TIP-1 was identified as one molecular target of the HVGGSSV peptide. TIP-1 specific antibody competed with the HVGGSSV peptide for binding within irradiated tumors, and exhibited similar binding patterns as the peptide in tumor-bearing mice. It was further identified that radiation induced translocation of the basically intracellular TIP-1 protein onto the cell surface occurred in a dose-dependent manner. The treatment-induced TIP-1 expression on the cell surface is detectable in the first few hours after the treatment and before the onset of treatment associated apoptosis or cell death. In fact, the majority of

the cells expressing TIP-1 on the cell surface are the live but still responding cancer cells, albeit such cells are less potent in proliferation and more susceptible to subsequent radiation treatment. Although it still under investigation to understand the mechanism and biological consequence of the radiation-induced TIP-1 translocation, these data support one conclusion that the radiation-inducible translocation of TIP-1 onto the cell surface holds promise as one surrogate biomarker in assessing the tumor responsiveness to ionizing radiation.

Discovery of the TIP-1 translocation onto the cell surface as one biomarker of tumor response to radiation took advantage of phage display technologies. Firstly, a peptide HVGGSSV was identified with selective binding to the tumors responding to IR and tyrosine kinase inhibitors by *in vivo* phage display (Han et al., 2008). Cancer cells distinguish themselves from normal cells by expressing proteins or receptor on the cell surface, imaging of such surface proteins such as EGFR has been studied to track the tumor progression or even monitor tumor response to treatment (Manning et al., 2008). We envision that the treatment-inducible protein expression on the cancer cell surface holds promise as a surrogate biomarker for imaging-based assessment of the tumor responsiveness to treatment. Compared to genomic and proteomic profiling (Han et al., 2006) that focus on the gene structure and overall expression abundance, in vivo phage display prefers the molecules that are localized on the cell surface and circulation accessible. Moreover, unlike the subcellular proteomic profiling (Oh et al., 2004) that has been explored in biomarker discovery in vivo, the in vivo phage display takes advantage of minimal sample bias and the real time in vivo binding within the sophisticated tissues

and cell structures. Secondly, TIP-1 was identified as the molecular target of the HVGGSSV peptide through biopanning a phage-displayed cDNA library. In an effort to identify the molecular target(s) of the HVGGSSV peptide, no meaningful data was generated through BLAST search for homologous sequences (Zurita et al., 2004), affinity purification accompanied with mass spectrometric identification (Christian et al., 2003), or yeast-two hybrid screening of cDNA libraries (Zhang et al., 2005). Low affinity or low abundance of the corresponding molecular target(s) might contribute to the difficulty in identification of the molecular target(s) of the short peptide. A phage-displayed cDNA library was screened against the HVGGSSSV peptide, rounds of biological amplification and affinity selection significantly enriched the peptide-binding clones that lead to the TIP-1 identification. This study further demonstrated the potential of screening phage-displayed cDNA library for the discovery of molecular targets of peptides with simple structure and low affinity.

TIP-1 is ubiquitously expressed within multiple organs (Besser et al., 2007). It is predominantly localized in the cytoplasma (Besser et al., 2007; Reynaud et al., 2000), with rare or undetectable expression in the nucleus or on the cell plasma membrane under normal culturing condition. It has been studied as a PDZ antagonist in modulating cell proliferation, polarity, migration and stress response (Alewine et al., 2006; Hampson et al., 2004; Kanamori et al., 2003; Reynaud et al., 2000). However, its biological functions in cancer biology and cell stress response are still under investigation. Our flow cytometry and cell imaging data showed that the TIP-1 translocation onto the cell surface after X-ray irradiation was dominantly observed in cancer cells, but did not extend to

endothelial cells as tested in this study by the use of HUVEC (Fig. 9F). This difference is not related to the abundance of the TIP-1 protein within the cells. Western blot analysis of TIP-1 expression within the whole cell lysates indicated that TIP-1 was expressed in all the cell lines including the HUVEC with comparable protein level (data not shown). Tissue staining also showed that the intravenously administrated TIP-1 antibody was dominantly associated to the tumors cells (Fig. 8B). These data suggested that the radiation-induced TIP-1 translocation onto the cell surface might be limited to the tumor cells. This conclusion is also supported by our previous observations that the HVGGSSV peptide did not bind to normal tissues that had been irradiated or inflamed with LPS and TNF-α (Han et al., 2008). Conversely, radiation-induced translocation of other intracellular proteins such as P-Selectin (Hallahan et al., 1998) and intercellular adhesion molecule-1 (ICAM-1) (Hallahan et al., 1996) are reportedly associated with inflammatory response to ionizing radiation and thus not specific to tumor response to the radiation treatment. In this regard, the radiation-induced TIP-1 translocation onto the cancer cell surface is a unique biomarker of tumor response to radiation.

Although further investigation is needed to elucidate the mechanism(s) by which X-ray irradiation induces the TIP-1 translocation onto the cell surface and the biological relevance of the TIP-1 translocation in the tumor response to radiation, we revealed that the cells responding to radiation by relocating TIP-1 onto the cell surface are live but have reduced capability to proliferate and form colonies. The cells with TIP-1 expression on the cell surface are more susceptible to subsequent radiation treatment, compared to the counterparts of the cells without TIP-1 expression on the cell surface. These data

partially explain why TIP-1 imaging with the HVGGSSV peptide is predictive in assessing the tumor responsiveness to radiation (Han et al., 2008). The TIP-1 translocation was detectable in the first few hours after radiation treatment and before the onset of the treatment associated apoptosis and cell death, suggesting a potential mechanism to assess tumor response to IR at an early time point of a treatment course.

CHAPTER III

MIGRATION AND INVASION OF HUMAN GLIOMAS IS CONTROLLED BY TIP-1-MEDIATED SPATIAL AND TEMPORAL REGULATION OF RHO GTPASE ACTIVATION

Abstract

Unlike other PDZ domain containing proteins that usually are composed of multiple structural and functional domains, Tax interacting protein (TIP-1) is unique in that almost the entire protein forms a single PDZ domain. Therefore, TIP-1 is predicted to play different roles from the classic PDZ proteins. In this study, we report a positive correlation between TIP-1 expression and human glioma malignancy based on tissue array analysis. The correlation between TIP-1 expression and glioma progression was further supported by mouse model studies using orthotopic glioma xenografts in which down-regulation of TIP-1 with shRNA was found to increase animal survival significantly. Upon histological examination of tumor tissues, we found that TIP-1 knockdown inhibited tumor invasion into normal brain tissues, which was confirmed by in vitro glioma cells migration and invasion assays. Downregulation of TIP-1 also caused cellular morphology changes, with more membrane 'spike' protrusions and fewer matured lamellipodia, as well as slower reorientation of the microtubule-organizing center (MTOC). Using recently released protein structures, we discovered that TIP-1 interacts with beta-PIX and rhotekin with high affinity through the PDZ domain. These

two proteins are GEF/Effectors for Rho GTPases. Knockdown of TIP-1 significantly increased the interactions of beta-PIX and rhotekin with a PDZ scaffold protein, scribble, that plays critical roles in directional cell migration. Consequently, TIP-1 deficiency resulted in mislocalization of rhotekin and beta-PIX within the migrating cells. The mislocalization of rhotekin and beta-PIX lead to abnormal activation of RhoA and Rac1/Cdc42 in the TIP-1 knockdown cells. Taken together, our study indicates that TIP-1 is required for malignant glioma invasion. It revealed that TIP-1 controls cells migration and invasion through regulating the intracellular localization of beta-PIX and rhotekin and the activation of RhoA, Rac1 and Cdc42. Furthermore, TIP-1 regulation provides a novel mechanism of coordinately regulating Rho GTPases activities.

Introduction

The ability of cancer cells to invade surrounding normal tissues requires a series of early events, including the formation of membrane protrusions in response to chemotactic signals, extension of membrane protrusions at the leading edge and retraction of the cell body at the trailing edge. This coordinated reorganization of cell cytoskeleton is primarily driven by the Rho GTPases (Jaffe and Hall, 2005). Rho GTPases act as molecular switches, cycling between a GTP-bound active form and GDP-bound inactive form. The activation of Rho GTPases is mediated by guanine-nucleotide exchange factors (GEFs). Once activated, Rho GTPases bind to and regulate a spectrum of functionally diverse downstream effectors, initiating a network of cytoplasmic and nuclear signaling cascades.

The spatially and temporally orchestrated regulation of Rho GTPases functions is critical for cell migration (Machacek et al., 2009; Pertz et al., 2006).

Rho GTPases have been reported to contribute to most steps of cancer initiation and progression (Gomez del Pulgar et al., 2005). Several Rho GTPases are upregulated in some human tumors, including gliomas (Benitah et al., 2004; Hwang et al., 2004; Oellers et al., 2009; Zavarella et al., 2009; Zhai et al., 2006). Malignant gliomas are highly aggressive cancers, clinical treatment of these tumors is challenging due to extensive infiltration of individual tumor cells into adjacent brain tissue. These invading cells render these cancers resistant to current treatments of surgical removal in combination with radiation, chemo- and immuno-therapies.

In our previous studies, we discovered that a small PDZ protein TIP-1 (also known as Tax1bp3) can be used as a biomarker for early evaluation of radiotherapy efficacy (Han et al., 2008; Wang et al., 2010), and TIP-1 expression protected glioma cells from radiation treatment (*Han M, unpublished*). In contrast to other PDZ proteins which usually contain multiple functioning domains and serve as scaffold proteins to assemble big structural or signaling complexes, almost the entire TIP-1 protein (124 amino acids) forms a single PDZ domain (~98 amino acids). The unique structure suggests TIP-1's different functions from the classic PDZ proteins. Until now, the molecular function of TIP-1 has remained elusive. TIP-1 is mainly a cytosolic protein, although it is also found to associate with the plasma membrane and be inside the nucleus (Kanamori et al., 2003; Olalla et al., 2008). TIP-1 is expressed in almost all tissues. Soon after its discovery,

TIP-1 was identified to interact with rhotekin, a Rho GTPase - RhoA effector protein. This interaction is involved in Rho signaling to the serum response element (Reynaud et al., 2000). TIP-1 also interacts with glutaminase L in mammalian brain. However the exact mechanisms by which TIP-1 regulates glutaminase L function is not yet elucidated (Aledo et al., 2001; Olalla et al., 2001; Olalla et al., 2008). In colon cancers, TIP-1 was found to bind to beta-catenin and inhibit beta-catenin transcriptional activity (Kanamori et al., 2003). The interaction between TIP-1 and potassium channel Kir2.3 blocks Kir2.3 membrane localization and affects cell polarity (Alewine et al., 2006). TIP-1 can also interact with NMDA receptor, which is thought to play a critical role in synaptic plasticity. Knockdown of TIP-1 increased the neurotoxicity of NMDA on neuron cells (Cui et al., 2007). In another study using a zebrafish model, TIP-1 expression level was found highest in the central nervous system of the zebrafish embryo, and TIP-1 can induce filopodia growth and is important for gastrulation movements during zebrafish development (Besser et al., 2007). TIP-1 was also the target of several virus oncoproteins, such as the Tax protein of the human T-lymphotropic virus Type I (Rousset et al., 1998), human papillomavirus E6 protein (Hampson et al., 2004) and avian influenza NS1 protein (Obenauer et al., 2006). Although the biological functions were not determined in these studies, the diversity of all these interacting proteins indicates that TIP-1 protein has a broad effect in living cells. Recently, the crystal structure of TIP-1 was resolved. Besides the classic PDZ motif binding pocket, a second binding site was identified to assist PDZ binding (Yan et al., 2009; Zhang et al., 2008).

In this study, we report that high levels of TIP-1 expression correlated with human glioma progression, and TIP-1 down-regulation inhibited glioma cell migration and invasion *in vitro* and in a mouse model of intracranially implanted human glioma xenograft. We demonstrat that TIP-1 controls cells migration and invasion through regulating the intracellular localization of beta-PIX and rhotekin and the activation of RhoA, Rac1 and Cdc42.

Materials and Methods

Cell Culture and Stable shRNA Transfection

Human glioblastoma cancer cells lines D54 and T98G were obtained from Dr. Yancie Gillespie (University of Alabama-Birmingham, Birmingham, AL), and purchased from ATCC (Manassa, VA), respectively. Both lines were maintained in DMEM/F12 media (Invitrogen, Carlsbad, CA), and stably transfected with shRNAs (Sigma-Aldrich, TRCN0000159034 and TRCN0000162886, St Louis, MO) using Lipofectamine 2000 according to the manufacturer's instructions (Invitrogen). Positive clones were selected with puromycin (Sigma-Aldrich). Tip-1 downregulation was assessed by Western blot as described previously(Wang et al., 2010).

Antibodies and Reagents

TIP-1 polyclonal antibody from rabbit was produced in our lab as described before (Wang et al., 2010). Beta-PIX antibody (SH3 domain) was obtained from Millipore (Billerica, MA). Antibodies against Rac1, beta-catenin, GM130 and paxillin were

purchased from BD Biosciences (Rockville, MD). Anti-Pericentrin, Ki67 and RhoA antibodies were obtained from Abcam (Cambridge, MA). Anti-Flag (M2), beta-Actin antibodies were purchased from Sigma. Anti-Scrib (H300), Cdc42, Rhotekin antibodies were purchased from Santa Cruz Biotechnology (Santa Cruz, CA). Alexa Fluor 594 labelled Phallotoxins and all other Alexa Fluor dye labeled secondary antibodies were obtained from Invitrogen.

Plasmids Constructs

A construct encoding cMyc tagged TIP-1 mutant with a dysfunctional PDZ domain (H90A) (13) in pcDNA3.1 plasmid was a generous gift from Dr. Paul A. Welling at University of Maryland(Baltimore, MD). The plasmid expressing flag-tagged beta-PIX (Mayhew et al., 2006) was obtained from Addgene (Cambridge, MA). To create a c-terminal PDZ binding motif mutation (from -WLQSPV to -ALQAPV) of beta-PIX, we used the QuikChange™ Site-Directed Mutagenesis Kit (Stratagene, Santa Cruz, CA) with primers 5'-atatgaacgaccctgccgcggatgaggccaatctatagctcgag-3', and 5'-ctcgagctatagattggcctcatccgcggcagggtcgttcatat-3'.

Migration and Invasion Assays

Cell migration and invasion assays were performed using 8-µm porous Boyden chambers (Corning Life Science, Lowell, MA) coated with or without Matrigel (BD Biosciences) according to the manufacturer's recommendations. Cell migration was also assayed using the wound healing assay (Etienne-Manneville, 2006).

Cell Staining and Imaging

The cells were fixed and permeabilized in 4% formaldehyde solution and stained with corresponding antibodies. For study of migrating cells at the wound edge, cells were allowed to grow to confluence on cover slips. After starving the cells overnight with serum free media, the cell monolayers were scratched with a 200ul pipette tip, and allowed to grow in fresh media for the indicated time before fixation for staining. The images were acquired using a Zeiss LSM 510 inverted confocal microscope. To quantify the percentage of individual proteins located at the cell leading edge, the fluorescent intensity of each protein was measured using Image J software (NIH). At least 50 cells were included in each measurement.

In vivo Xenograft Tumor Model of Glioma

To access the impact of TIP-1 on glioma progression, an orthotopic mouse brain tumor model was used. The intracranial tumor model was described previously (Geng et al., 2006). Briefly, D54 cells or D54 cells with TIP-1 knockdown ($n=2x10^4$) in 20uL of PBS were injected 3mm deep (from the skull surface) into the right burr hole of nude mice. The mice were monitored daily for hypomotility, absence of grooming behavior, and weight loss. All the animal work was conducted as approved by the Institutional Animal Care and Use Committee (IACUC). A Kaplan-Meier survival curve was used to graph these surrogate behaviors for survival. Statistical analysis was performed using Log Rank Test.

Immunohistochemistry of Tumor Tissues

To study histologic changes in intracranial tumor model, tumors were retrieved after survival assays, and fixed in formaldehyde and embedded in paraffin. 6μm thick tumor sections were deparaffinized in graded alcohols, rehydrated and heated in 10mM citrate buffer (pH 6.0) for antigen retrieval using a pressure cooker. The tissue slides were subsequently stained with Ki67 antibody or TIP-1 antibody and counterstained with hematoxylin.

For the study of human glioma tissues, tissue microarrays with pathological diagnosis of astrocytoma, glioblastoma, glioblastoma multiforme (GBM) and normal tissue were purchased from US Biomax (Rockville, MD). The tissue slides were processed as described above for TIP-1 staining and counterstained with hematoxylin. TIP-1 expression intensity was scored on a four point scale as either negative (1), weak (2), moderate (3), or strong (4). Mean expression scores multiplied by percent of the positive cells in the field (Quick's combined score system) are presented for normal brain, grade I, grade II, grade III and grade IV gliomas, respectively, in a graphic format using error bars with 95% confidence intervals (CI). Differences among these groups were compared using ANOVA. A p-value of ≤ 0.05 was considered statistically significant.

Rho GTPases Activation Assay

Rho GTPases activation was determined by using either RhoA Activation Assay Kit or Rac1/Cdc42 Activation Assay Kit (Cell Biolabs, San Diego, CA). Briefly, the cells were lysed in lysis buffer and centrifuged at 13,000g for 10min. The supernatant was mix with either rhotekin RBD-agarose beads (for activated RhoA) or PAK1 PBD-agarose beads

(for activated Rac1/Cdc42) for 1 hour at 4°C. The activated Rho GTPases were analyzed by Western immunoblot.

Results

High expression levels of TIP-1 correlate with glioma malignancy

A correlation between TIP-1 expression and clinical presentation of the malignant gliomas was recently revealed with reanalysis of microarray data (Han M, unpublished). In this study, we used a TIP-1 specific antibody (Wang et al., 2010) to profile TIP-1 expression and intracellular location within arrayed human brain tumor tissues that contain pathologically verified tissue samples from patients with progressive glioblastomas of different malignancy. Immunohistochemistry staining indicated that TIP-1 is mainly a cytosolic protein, with some localized to the plasma membrane (Fig. 11A). Semi-quantitative analysis of TIP-1 expression revealed a positive correlation between the expression level of TIP-1 and the malignancy of glioblastoma (Fig. 11B). The normalized mean TIP-1 expressions in the malignant glioma were much higher than those in normal brain tissues. TIP-1 level was elevated with the increased malignancy of glioma (Fig. 11B), except in grade IV gliomas which have the similar TIP-1 level as grade III glioma, and there were little or no expression of TIP-1 in normal brain tissues.

Downregulation of TIP-1 in glioma cells extended survival of mice with intracranially implanted tumors

To further investigate the positive correlation between high levels of TIP-1 expression

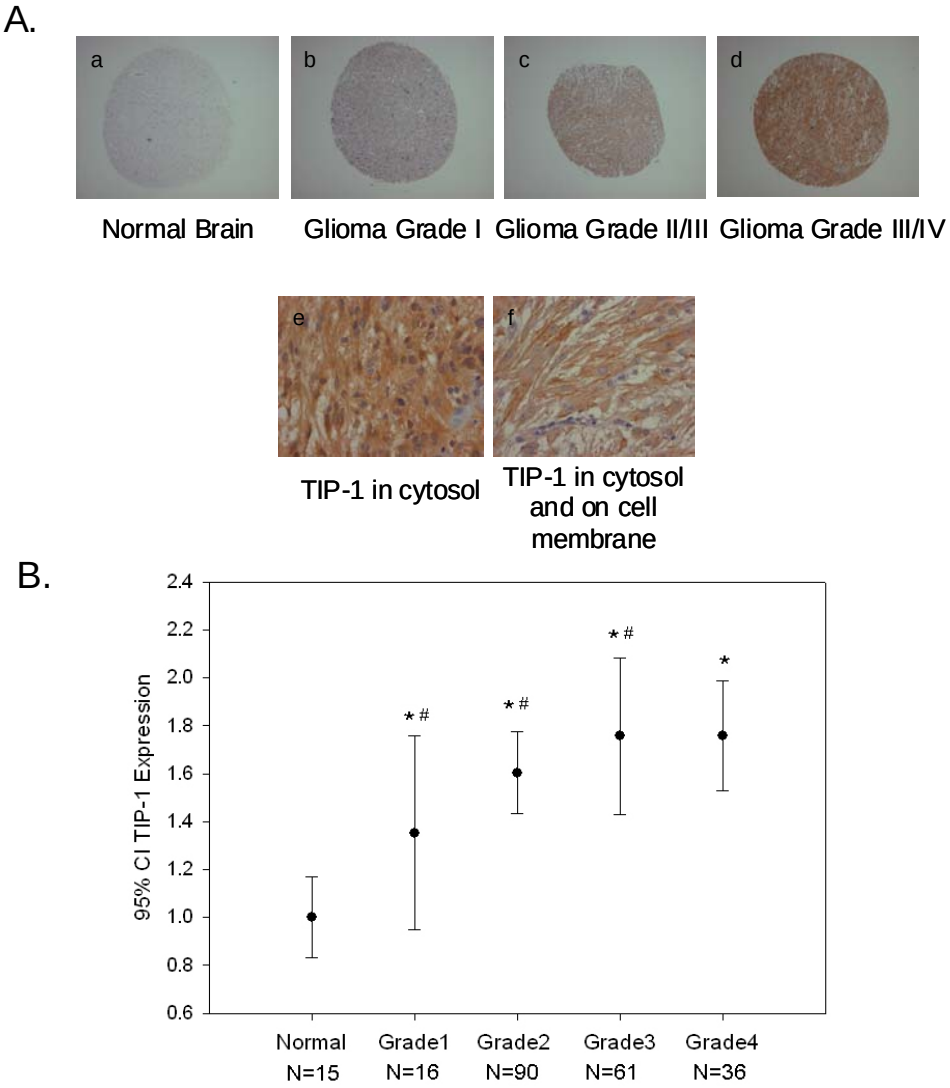

Figure 11. TIP-1 expression correlates with human gliomas malignancy. (A) TIP-1 expression in human gliomas. Representative tissue cores of a tissue microarray stained with a monospecific anti-TIP-1 polyclonal antibody demonstrate weak staining in normal brain and lower grade gliomas (panels a and b), but strong staining in higher grade gliomas (panels c and d). Higher magnification images revealed TIP-1 location in the cytosol (panel e) and on the plasma membrane (panel f). (B) Semi-quantitative histological evaluation of TIP-1 expression within human glioma tissue blocks. TIP-1 expression intensity was scored on a four point scale as either negative (1), weak (2), moderate (3), or strong (4). Mean expression scores multiplied by percentage of the positive cells in the field (Quick's combined score system) are presented for normal brain, grade I, grade II, grade III and grade IV gliomas, respectively, in a graphic format using error bars with 95% confidence intervals (CI). Statistically significant differences were noted between normal brain and gliomas of different malignant grades. *, $p < 0.001$ and between different grades gliomas; #, $p < 0.005$ (ANOVA). Case numbers for each group of tissues were marked under the bar graph.

and malignancy of glioma, we examined the impact of TIP-1 down-regulation on glioma progression using an orthotopic brain tumor model. D54 was selected as a malignant human glioma cell line for this study since mRNA sequencing and western blot analyses indicated that D54 cells express high level of wild-type TIP-1 protein (Fig. 17B and unpublished data). D54 cells with TIP-1 stably knockdown (Fig. 13A) and control cells were implanted intracranially into mice brains. Extent of survival was analyzed by the Kaplan-Meier method. In contrast to the control groups in which all mice died in 28 days, a significant increase in the survival time (about 8 more days) was observed in the TIP-1 Knockdown group (Fig 12B).

Downregulation of TIP-1 inhibited glioma cell migration and invasion

To elucidate the roles of TIP-1 in glioma progression, we first studied the impact of TIP-1 on cell proliferation. Both *in vitro* (Fig 12A) and *in vivo* (Fig 12D) experiments indicated that knockdown of TIP-1 did not change glioma cell proliferation rate. At the end of the survival experiments, the tumors were resected from mice brains. Immunohistochemical studies with TIP-1 antibody staining confirmed that TIP-1 expression was still silenced in the knockdown tumors. One significant difference between control and TIP-1 knockdown tumors was that, in contrast to the extensive invasion of tumors formed with regular D54 cells or those transfected with a control shRNA, TIP-1 downregulation dramatically reduced invasion of the D54 tumor cells into surrounding normal brain tissues (Fig 12C). Therefore, these results revealed a potential role of TIP-1 in regulating cell migration and invasion.

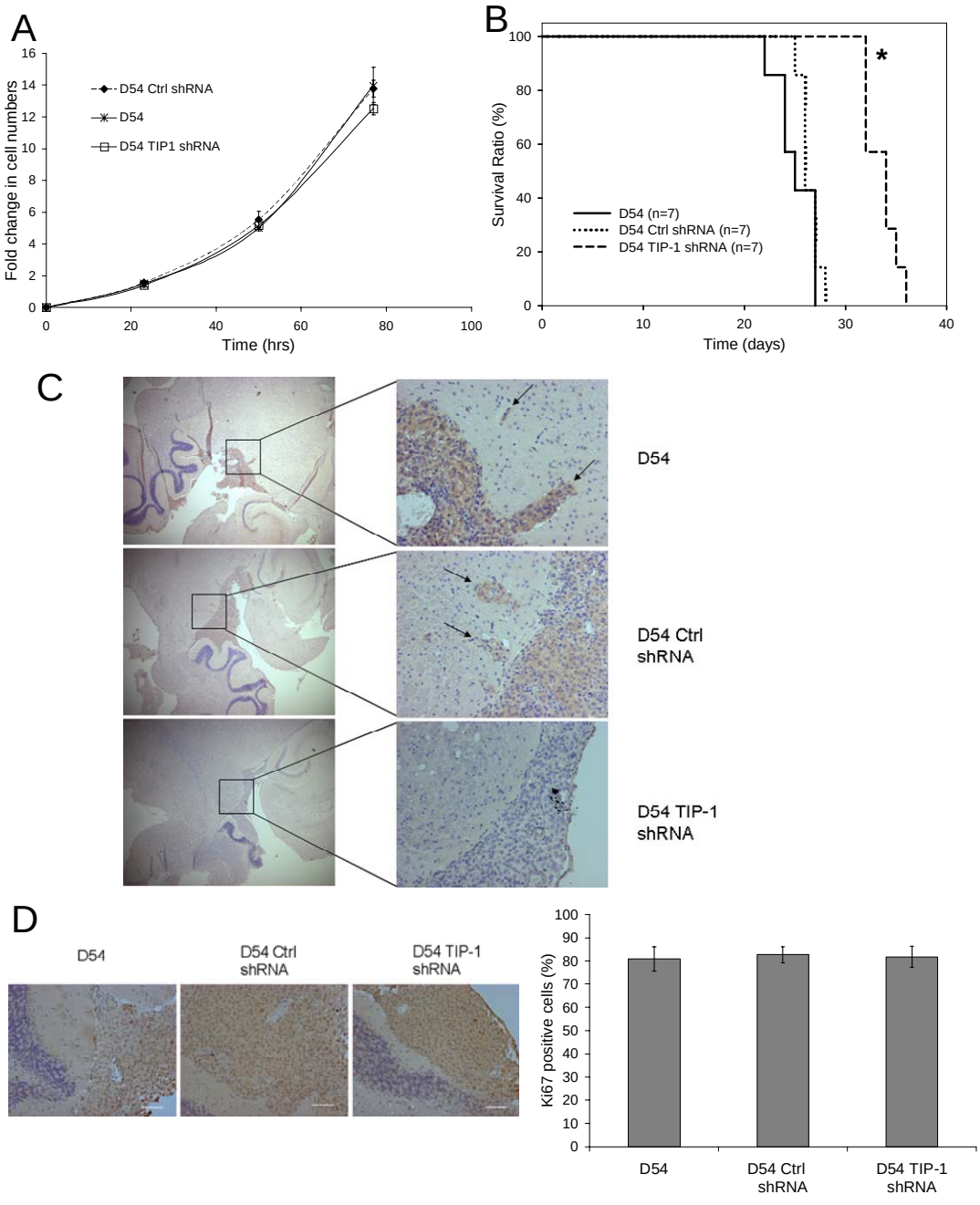
A
Fold change in cell numbers
Time (hrs)
D54 Ctrl shRNA
D54
D54 TIP1 shRNA
B
Survival Ratio (%)
Time (days)
D54 (n=7)
D54 Ctrl shRNA (n=7)
D54 TIP-1 shRNA (n=7)
*
C
D54
D54 Ctrl shRNA
D54 TIP-1 shRNA
D
D54
D54 Ctrl shRNA
D54 TIP-1 shRNA
Ki67 positive cells (%)
D54
D54 Ctrl shRNA
D54 TIP-1 shRNA

Figure 12. Downregulation of TIP-1 inhibited glioma progression in mice. (A) TIP-1 expression was stably knocked down in the human malignant glioma cell line D54 using an shRNA construct. The *in vitro* cell proliferation rates were measured by counting cell numbers every 24hrs for 3 days. (B) Same numbers of control D54 cells, D54 cell transfected with non-targeting or TIP-1 specific shRNA sequences were implanted intracranially in Athymic nude *Foxn1*^{nu} mice. The mouse survival time was monitored, and the survival data was analyzed by Kaplan Meier method (* p<0.0002). (C) At the end of the survival studies, tumors were recovered from the mice brains. The brain tumor tissues were stained with TIP-1 antibody (brown color) to confirm the efficiency of TIP-1 knockdown. Infiltration of the tumor cells into the surrounding normal brain tissues was visualized with hematoxylin staining. (D) *In vivo* tumor cell proliferation rates were determined by Ki67 staining of the brain tumor tissues. Data are expressed as mean±SD. Scale bar: 50um.

TIP-1-regulated cancer cell migration and invasion were further studied with two human glioma cell lines, D54 and T98G, which have distinct invasive capability. TIP-1 expression was stably knocked down using RNA interference approach. Two independent targeting sequences were designed to minimize the off-target effects. TIP-1 specific shRNA expression resulted in >90% inhibition of endogenous TIP-1 compared with control cells (Fig.13A). In the Boyden chamber migration assay, knockdown of TIP-1 resulted in a significant inhibition of cell migration in both cell lines (Fig. 13B). Similarly, but to a greater extent, cell invasion was inhibited in both cell lines with TIP-1 downregulation in the Boyden chamber-based invasion assays (Fig. 13C). Consistent with these results, cell motility study using the wound healing assay also revealed a similar decrease in the motility of the TIP-1 silenced cells compared with the control cells (Fig. 13D). The control cells closed the wound gaps much faster than TIP-1 knockdown cells as surveyed in 12hrs after the wound scratch.

TIP-1 regulated the MTOC orientation during the directional migration

One hallmark of the directional migration is the reorienting of the microtubule-organizing center (MTOC) and the repositioning of the Golgi apparatus toward the leading edge at the early stages of the cell migration (Kupfer et al., 1982; Ueda et al., 1997). To understand the mechanisms by which TIP-1 regulates cancer cell migration and invasion, we investigated MTOC reorientation in the control and TIP-1 knockdown T98G glioma cells. In the wound-healing assays, scratching the cell monolayer induces cell reorientation and migration in a direction perpendicular to the wound. The correctly reoriented cells will have the centrosome facing toward the scratch edge. Results from the assays revealed that TIP-1 depletion significantly perturbed scratch-induced MTOC reorientation (Fig. 13E). There were fewer cells with the correctly orientated centrosome after knockdown of TIP-1.

TIP-1 interacts with Rho GTPases GEF/effectors - beta-PIX and rhotekin

Directional migration of cells and cytoskeleton reorganization are regulated by multiple signaling pathways including the spatially and temporally orchestrated activation and inactivation of Rho GTPases. To explore the molecular mechanisms by which TIP-1 regulates cell migration and invasion, we studied TIP-1 interacting proteins. So far, there are about eleven TIP-1 interacting proteins published, with the majority identified through the yeast two hybrid method (Hampson et al., 2004; Kanamori et al., 2003; Reynaud et al., 2000; Rousset et al., 1998; Yan et al., 2009). These proteins belong to different protein families, such as oncoproteins, ion channels, cytoskeleton proteins, etc. The complexity of TIP-1 targeting proteins made it difficult to understand its functions.

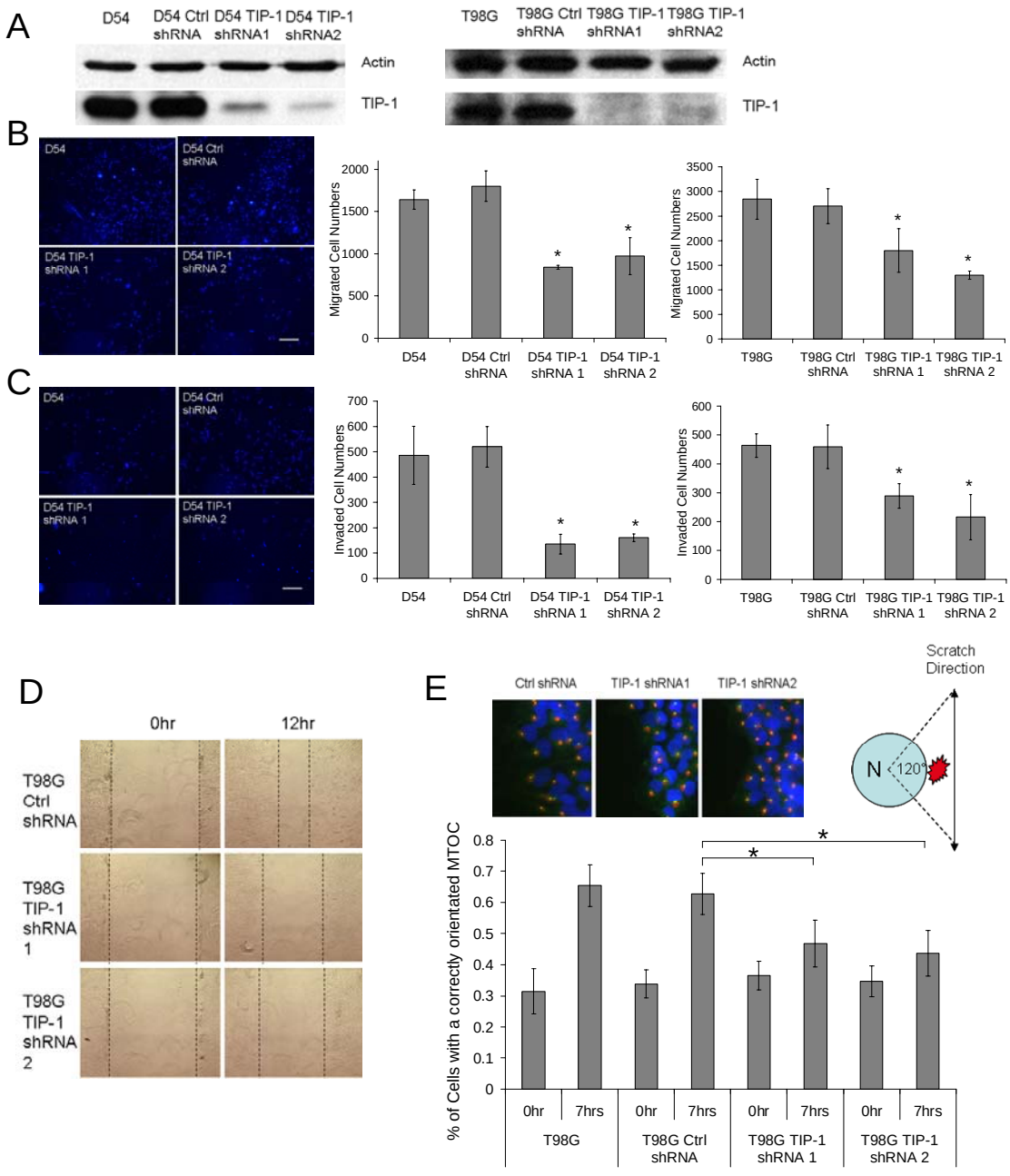
A
D54
D54 Ctrl shRNA
D54 TIP-1 shRNA1
D54 TIP-1 shRNA2
T98G
T98G Ctrl shRNA
T98G TIP-1 shRNA1
T98G TIP-1 shRNA2
Actin
TIP-1
B
C
Migrated Cell Numbers
Invaded Cell Numbers
D54 TIP-1 shRNA 1
D54 TIP-1 shRNA 2
T98G TIP-1 shRNA 1
T98G TIP-1 shRNA 2
D
0hr
12hr
T98G Ctrl shRNA
T98G TIP-1 shRNA 1
T98G TIP-1 shRNA 2
E
Ctrl shRNA
TIP-1 shRNA1
TIP-1 shRNA2
Scratch Direction
N
120°
% of Cells with a correctly orientated MTOC
0hr
7hrs

Figure 13. Depletion of TIP-1 restrained glioma cell migration and invasion. (A) Western blot showing TIP-1 expression in two glioma cell lines (D54 and T98G) with stably expressing TIP-1 shRNAs or control shRNA, respectively. (B) Migration of D54 and T98G with or without TIP-1 knocking down were studied using Boyden chamber assay as described in Materials and Methods. Bar graph represents the number of migrated cells at 12hrs after seeding the cells on the top of the membrane. Results shown are mean ± SD of 3 independent experiments (*, $p<0.01$). Representative images showed the migrated cells across the membrane. Cell nuclei were stained with DAPI (blue). (C) Invasion of D54 and T98G with or without TIP-1 knock down were studied using Boyden chamber assay. The bar graph represents the number of invaded cells at 16hrs after seeding the cells on the top of the membrane. Results shown are mean±SD of 3 independent experiments (*$p<0.01$). Representative images showed the invaded cells on the membrane. Cell nuclei were stained with DAPI (blue). Scale bar: 150um. (D) Tumor cell migration analyzed by the wound healing assay. T98G monolayer cells were scratched and monitored for 12hrs to study TIP-1 functions in migration. (E) MTOC reorientation assay. Seven hours after scratch wounding, T98G cells were fixed and stained with anti-pericentrin (centrosome, green) and GM130 antibodies (Golgi, red) and DAPI (nucleus, blue). The bar graph represents percentage of wound-edge cells having their MTOC facing toward the scratch orientation. Results shown are mean ± SD of 3-5 independent experiments with at least 500 cells being scored (*$p<0.01$).

Recently, the structure of TIP-1 was resolved with X-ray crystallography and nuclear magnetic resonance spectroscopy (NMR). Besides the classic type I PDZ binding motif, a tryptophan residue at the -5 position to the c-terminus was identified as critical for TIP-1 specific binding (Durney et al., 2009; Yan et al., 2009; Zhang et al., 2008). With this information, we searched a PDZ protein database (Beuming et al., 2005) and discovered three proteins that have this binding motif (Table 1). Of these three proteins, beta-PIX has not previously been described as interacting with TIP-1. Beta-Pix is a guanine nucleotide exchange factor (GEF) for Rho GTPases Rac1 and Cdc42, and it is involved in regulating actin cytoskeleton reorganization and cell migration (Campa et al., 2006; Feng et al.,

2010; Nayal et al., 2006; Za et al., 2006). Another protein, rhotekin, is an effector protein that can only bind to GTP bound active form of RhoA (Reid et al., 1996). A couple of studies indicated that rhotekin plays a role in cytoskeleton and focal adhesion reorganization (Ito et al., 2005; Nagata et al., 2009). The third protein, beta-catenin, also interacts with actin cytoskeleton through alpha-catenin. Therefore, all three TIP-1 interacting proteins further suggested the potential functions of TIP-1 in cytoskeleton reorganization.

Because Rho GTPases are directly involved in regulating MTOC reorientation and cell migration and invasion (Osmani et al., 2006), we focused on the interactions of TIP-1 with beta-PIX and rhotekin in this study. In immunoprecipitation assays, all three proteins were pulled down with TIP-1 wild type proteins, but not with the TIP-1 mutant with a dysfunctional PDZ domain (Fig. 14A), confirming the published data showing that TIP-1 interaction with beta-catenin and rhotekin is mediated by the PDZ domain (Kanamori et al., 2003; Reynaud et al., 2000). We further show that TIP-1 binds to beta-PIX at the c-terminal PDZ binding motif, and that mutation within the PDZ binding motif of beta-PIX from -WLQSPV to -ALQAPV abolished its interaction with TIP-1 (Fig. 14B). Inside the migrating T98G cells, TIP-1 was located at the trailing edge, in the cell body, and it was also found associated with the plasma membrane at the leading edge (Figs.14C, D). TIP-1 was found colocalized with beta-PIX at the leading edge and in the cell body (Fig. 14D). On the other hand, rhotekin was spotted mainly in the cell body and trailing edge, and it was colocalized with TIP-1 at these two intracellular locations (Figs. 14C, D).

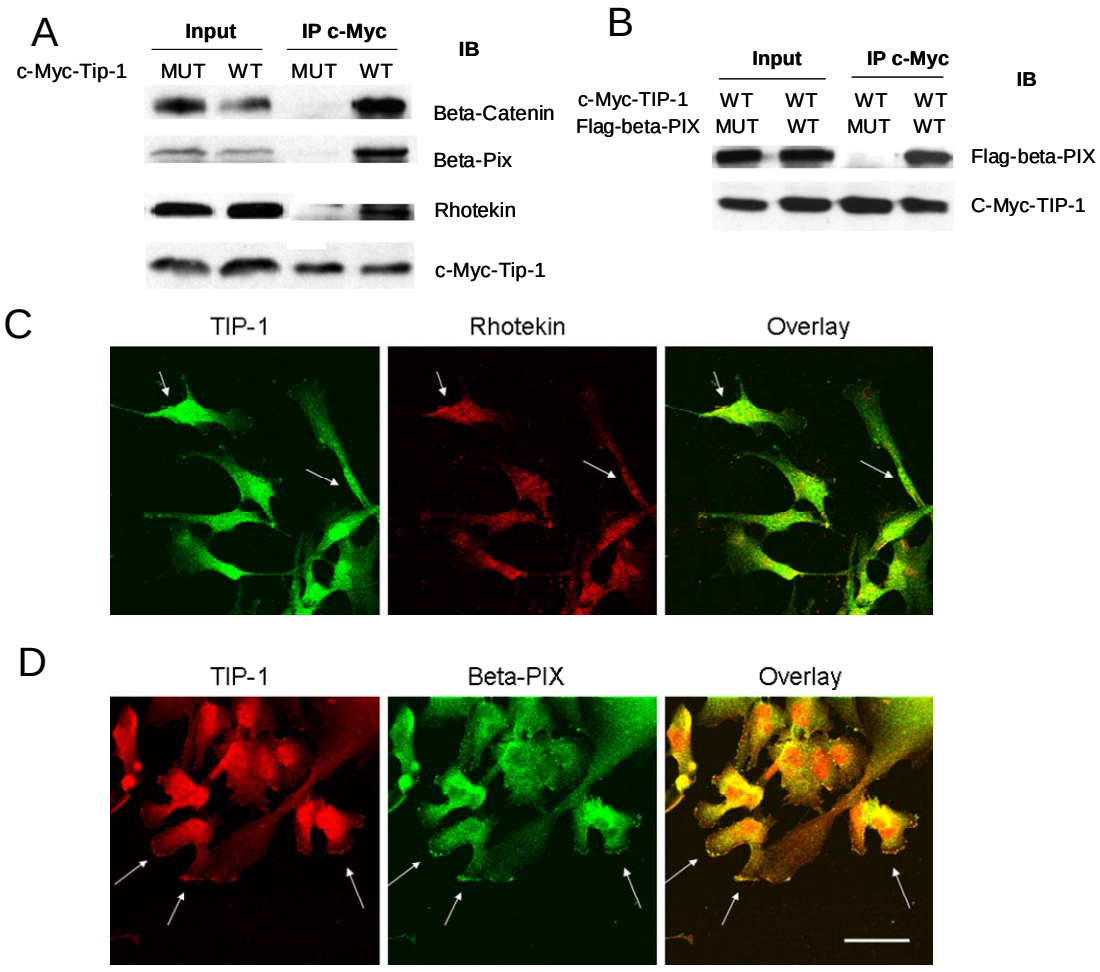

Figure 14. TIP-1 interacts with beta-PIX and rhotekin. (A) Western blot results of immnuoprecipitation of cMyc-TIP-1 in the cells transfected with either cMyc tagged TIP-1 wild type or a mutant with a dysfunctional PDZ domain. Beta-catenin, rhotekin and beta-PIX were blotted with specific antibody, respectively. (B) Immunoprecipitation of cMyc-TIP-1 in cells co-transfected with cMyc-TIP-1 (wild type) and flag-beta-PIX (wild type) or a flag-beta-PIX mutant with mutations in the c-terminal PDZ binding motif. (C) Immunofluorescent staining of T98G cells with TIP-1 antibody (green) and Rhotekin antibody (red). Arrows indicate the colocalization of both proteins. (D) Immunofluorescent staining of T98G cells with TIP-1 antibody (red) and beta-PIX antibody (green). Arrows indicate the colocalization of both proteins. Scale bars: (C and D) 50um.

Table 1: TIP-1 interacting proteins

Protein	PDZ binding motif*	Functions
Rhotekin	-**W**DE**T**N**L**	RhoA effector
Beta-PIX	-**W**LQ**S**P**V**	GEF for Rac1/Cdc42
Beta-catenin	-**W**FD**T**D**L**	Wnt pathway; bind to alpha-catenin and actin cytoskeleton

* Letters in Bold indicate the specific TIP-1 recognition motif

TIP-1 affects the interaction between beta-PIX and rhotekin with PDZ scaffold proteins

The PDZ binding motif on beta-PIX and rhotekin is used to associate these proteins to PDZ scaffold proteins (Audebert et al., 2004; Ito et al., 2006). Scribble is a PDZ scaffold proteins that guides the establishment of cell polarity in various organisms. It has been reported that scribble can interact with beta-PIX or beta-catenin and locate them to certain parts of the cell (Audebert et al., 2004; Osmani et al., 2006; Sun et al., 2009). Therefore, we used scribble as the referral protein to study how TIP-1 regulates the protein interactions and intracellular localization of beta-PIX and rhotekin.

The results from Western blot of total cell lysates showed that depletion of TIP-1 protein did not change the level of either beta-PIX or rhotekin in T98G cells (Fig.15A),

suggesting TIP-1 did not directly regulate the stability or expression of these proteins. To investigate the impact of TIP-1 on the location of these proteins, we first studied the interaction between beta-PIX, rhotekin and scribble. In a wound scratch-induced cell migration assay, scribble was pulled down with anti-Scrib antibody from cell lysates before and after the scratch wound. Besides beta-PIX, rhotekin was also shown to bind to scribble, the first time such an interaction has been reported. The bar graph shows the densitometry quantification of the results (Fig.15B). In the control cells, the scratch wound induced twice as much beta-PIX and rhotekin binding to scribble protein. Interestingly, in TIP-1 depleted cells, the basal level of the scribble interaction was increased for both beta-PIX and rhotekin. However, compared with the more than 2 fold increase of rhotekin binding to scribble, beta-PIX interaction with scribble did not change after the scratch wound (Fig. 15B). The changes in the interactions were also confirmed by immunofluorescent staining of glioma cells after a scratch wound. An increased leading edge localization of beta-PIX and rhotekin was found associated with TIP-1 depletion (Fig.15D). In contrast to the equal distribution at the leading edge in control cells, beta-PIX was only discretely located at tips of the leading edge of TIP-1 knockdown cells (Fig. 15C). The cells also showed a highly branched morphology compared with the control cells (Figs. 15C, D, 18A,B). As for rhotekin, it was mainly located in the cell body and trailing edge in the control cells, but associated with leading edge (~2 folds increase) after knocking down TIP-1 (Fig.15D). Therefore, the robust changes in protein interactions and intracellular localization of beta-PIX and rhotekin indicated that TIP-1 controlled cell migration through regulating the intracellular location of two effector/GEFs of Rho GTPases.

TIP-1 regulated Rho GTPases location and activation

Rho GTPases regulate the cytoskeleton rearrangement. The effectors/GEFs decide the location and activation of Rho GTPases. Because TIP-1 interacts with two effector/GEFs, we decided to investigate TIP-1's impact on Rho GTPase location and activation. In the control cells with high level expression of TIP-1, scratching on the cell monolayer induced a robust activation of Rac1 (2 fold increase), and to a lesser extent activation of Cdc42. RhoA activity did not show significant change. While in TIP-1 depleted cells, Rac1 and Cdc42 activities were slightly decreased after wounding. However, RhoA activity showed a robust increase (>2 fold) (Fig. 16A). Similar to the location change of beta-PIX and rhotekin, more Rac1 and Cdc42 were associated with cell leading edge. They were located to the tips of branched membrane structure in TIP-1 depleted cells, and colocalized with beta-PIX at these spots (Fig. 16B, C). Significantly more RhoA protein was found concentrated at spots at the leading edge where rhotekin was binding (Fig.16D). The active RhoA can stimulate stress fiber formation (Nobes and Hall, 1995; Ridley and Hall, 1992). Consistent with the increased activity of RhoA, there were more cells (~80%) forming stress fibers in TIP-1 depleted cells (Fig. 16E). Also, without the continuous distribution of Rac1 and Cdc42 at the leading edge, there were no actin fibers formed along the leading edge (Fig.16E).

Discussion

TIP-1 is a unique PDZ domain containing protein in that almost the entire protein is a

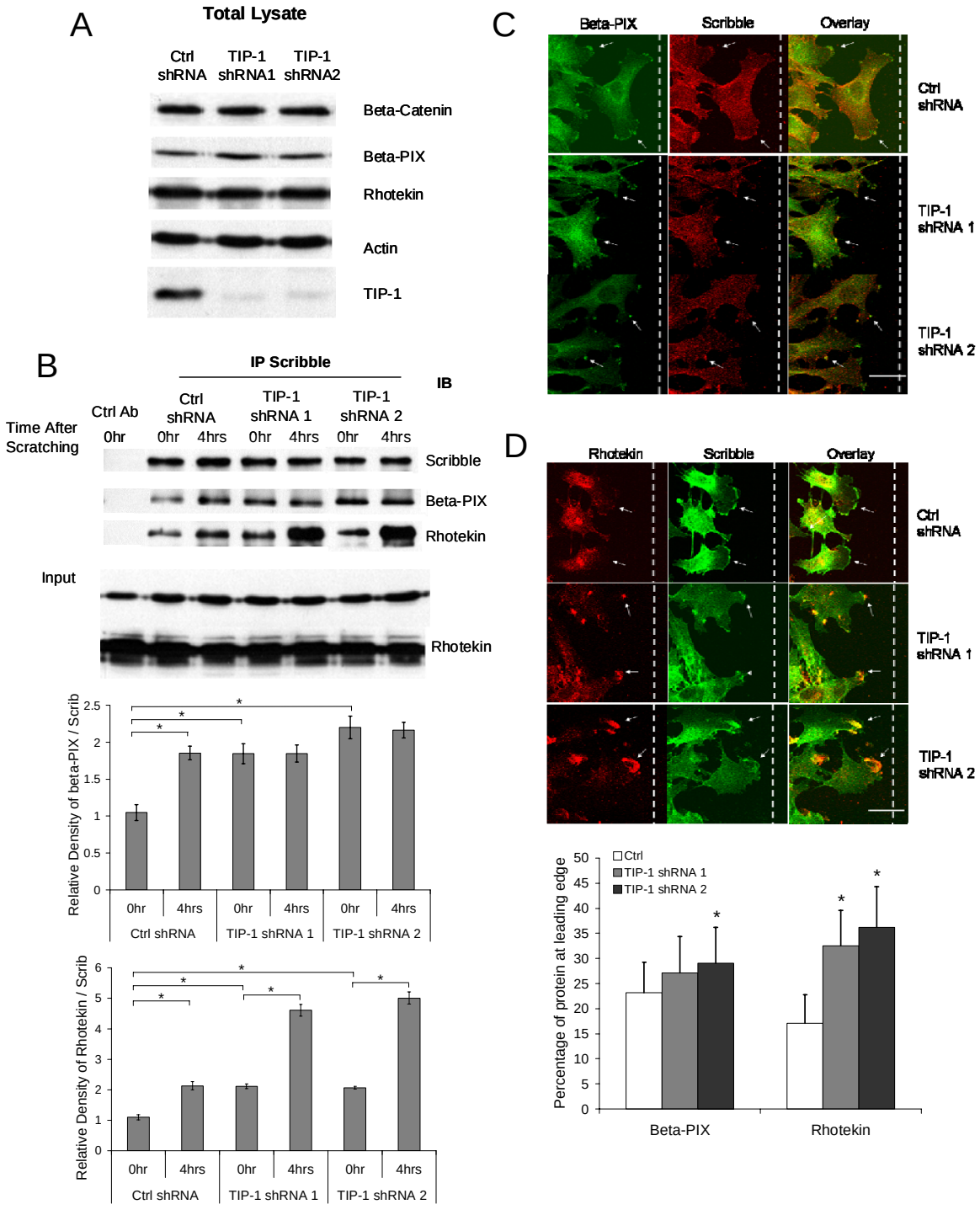
A
Total Lysate
Ctrl shRNA
TIP-1 shRNA1
TIP-1 shRNA2
Beta-Catenin
Beta-PIX
Rhotekin
Actin
TIP-1
B
IP Scribble
IB
Time After Scratching
Ctrl Ab
0hr
Ctrl shRNA
TIP-1 shRNA 1
TIP-1 shRNA 2
0hr
4hrs
Scribble
Beta-PIX
Rhotekin
Input
Rhotekin
Relative Density of beta-PIX / Scrib
Relative Density of Rhotekin / Scrib
Ctrl shRNA
TIP-1 shRNA 1
TIP-1 shRNA 2
C
Beta-PIX
Scribble
Overlay
Ctrl shRNA
TIP-1 shRNA 1
TIP-1 shRNA 2
D
Rhotekin
Scribble
Overlay
Ctrl shRNA
TIP-1 shRNA 1
TIP-1 shRNA 2
Percentage of protein at leading edge
Ctrl
TIP-1 shRNA 1
TIP-1 shRNA 2
Beta-PIX
Rhotekin

Figure 15. TIP-1 affects the interactions of scribble with beta-PIX and rhotekin. (A) Western blot analysis of beta-catenin, beta-PIX and rhotekin protein levels within total cell lysates of control or TIP-1 depleted T98G glioma cells. (B) Cells were lysed at the indicated time after scratch wounding. Immunoprecipitations with anti-Scrib or irrelevant (Ctrl Ab) antibodies were performed and analyzed by western blot with the antibodies against beta-pix, rhotekin and scribble, respectively. Blots shown are representative of three independent experiments. The bar graph is the densitometry quantification of the blot results. (* $p<0.001$) (C) 4hrs after scratch wounding, cells were fixed and co-stained with both beta-PIX antibody (green) and Scribble antibody (red) to study their location inside the cells. (Scale bar: 50um) (D) 4hrs after wounding, cells were fixed and co-stained with both rhotekin antibody (red) and Scribble antibody (green). (Scale bar: 50um). The percentages of each protein located at the leading edge were quantified by measuring fluorescence intersity and results were shown in the bar graph. (* $p<0.05$, ANOVA)

PDZ domain. With no extra domains, TIP-1 supposedly can not carry out functions like classic PDZ proteins which serve as scaffolds to assemble large structures or signaling complexes. Instead, TIP-1 was considered to function as an antagonist (Alewine et al., 2006; Kanamori et al., 2003). In this study, we report a novel function of TIP-1 in progression of human malignant glioma and directional cell migration. Tissue array studies revealed a correlation between TIP-1 protein expression and human glioma malignancy. The positive correlation between TIP-1 expression and glioma progression was further supported by a survival study using murine orthotopic glioma xenograft models in which down-regulation of tumor TIP-1 significantly increased mouse survival. Histological examination of the resected tumor tissues indicated that TIP-1 depletion restrained tumor cell migration and invasion, that was further confirmed with in vitro

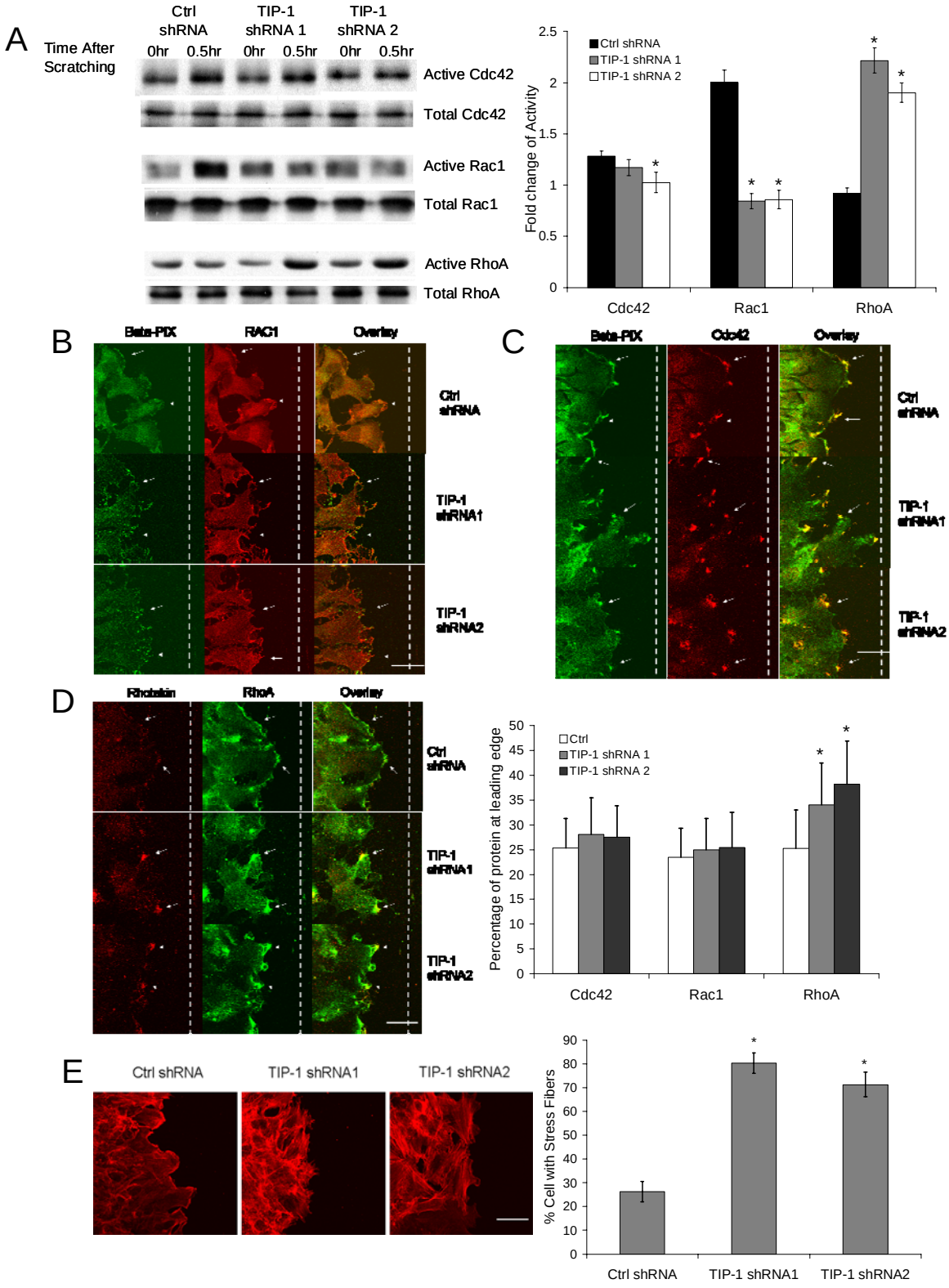
A
Time After Scratching
Ctrl shRNA
TIP-1 shRNA 1
TIP-1 shRNA 2
0hr 0.5hr 0hr 0.5hr 0hr 0.5hr
Active Cdc42
Total Cdc42
Active Rac1
Total Rac1
Active RhoA
Total RhoA
Ctrl shRNA
TIP-1 shRNA 1
TIP-1 shRNA 2
Fold change of Activity
Cdc42
Rac1
RhoA
B
Beta-PIX
RAC1
Overlay
Ctrl shRNA
TIP-1 shRNA1
TIP-1 shRNA2
C
Beta-PIX
Cdc42
Overlay
Ctrl shRNA
TIP-1 shRNA1
TIP-1 shRNA2
D
Rhotekin
RhoA
Overlay
Ctrl shRNA
TIP-1 shRNA1
TIP-1 shRNA2
Ctrl
TIP-1 shRNA 1
TIP-1 shRNA 2
Percentage of protein at leading edge
Cdc42
Rac1
RhoA
E
Ctrl shRNA
TIP-1 shRNA1
TIP-1 shRNA2
% Cell with Stress Fibers
Ctrl shRNA
TIP-1 shRNA1
TIP-1 shRNA2

Figure 16. TIP-1 regulates subcellular localization and activation of Rho GTPases. (A) Monolayer of T98G cells stably transfected with control shRNA or TIP-1 shRNAs were lysed 0 min or 30 min after wounding. Lysates were incubated with agarose beads coupled to PAK1-PBD peptide or Rhotekin-RBD peptide to pull down the active Rac1/Cdc42 or RhoA, respectively. The affinity precipitated active Rac1/Cdc42/RhoA and total Rac1/Cdc42/RhoA were analyzed with western blotting. Results are representative of 3 independent experiments. Bar graph is the densitometry quantification of the blot results. (* $p<0.02$) (B) 4hrs after wounding, cells were fixed and co-stained with both beta-PIX antibody (green) and Rac1 antibody (red) to study their subcellular localization within the T98G cells. Arrows indicate the colocalization of both proteins. (Scale bar: 50um) The cells were also stained to colocalize beta-PIX (green) and Cdc42 (red) (C), rhotekin (red), RhoA (green) (D). The fluorescent intensities of each protein were measured, and the percentages of individual proteins located at the leading edge were calculated. (*$p<0.002$, ANOVA). (E) Staining of actin (red) with phalloitoxins to visualize stress fiber formation. (Scale bar: 50um). The percentages of cells with strong stress fiber staining were quantified. (*$p<0.001$, ANOVA)

migration and invasion assays. Therefore, our results support the potential utility of TIP-1 as a molecular marker and therapeutic target of malignant glioma.

Interestingly, TIP-1 level did not show any further increase in the two highest grades of gliomas (grade III vs. grade IV glioma) (Fig.11B), which indicates a threshold TIP-1 protein level associated with tumor malignancy. These results were consistent with previous studies showing ectopic expression of TIP-1 reduced the proliferation and anchorage-independent growth of colorectal cancer cells (Kanamori et al., 2003).

The highly conserved amino acid sequence across species (Fig.17) suggests essential biological roles of TIP-1 in molecular and cellular processes. However, with only one simple but very common PDZ domain and a variety of interacting proteins, it is challenging to understand how TIP-1 regulates migration and invasion of glioma cells. Recently, the crystal structure of TIP-1 was resolved and it provided us some insight into the structural requirement for a highly selective protein association between TIP-1 and

the its interacting partners (Yan et al., 2009; Zhang et al., 2008). From the protein complex structure, a tryptophan residue at the -5 position to the C-terminus of PDZ binding motif was found critical for the TIP-1 specific binding. With this information, we searched a PDZ protein database and discovered two new proteins (beta-PIX and rhotekin) containing this binding motif. The specific interactions were confirmed by immunoprecipitation assays and colocalization of these proteins at leading or trailing edges of the migrating glioma cells. Both proteins belong to a family of guanine nucleotide exchange factor (GEF) / effector for Rho GTPases, with beta-PIX associating with active Rac1/Cdc42 and rhotekin binding to active RhoA. Among all Rho GTPases, Rac1, Cdc42 and RhoA are the three most studied in cytoskeleton reorganization and cell migration. Rac1 induces the formation of lamellipodia and membrane ruffles, Cdc42 induces the formation of filapodia, and RhoA triggers actin stress fiber formation and the retraction of the cell body (Amano et al., 1997; Hall, 1998; Kimura et al., 1996). Considering TIP-1 knockdown caused cell morphological changes with more membrane 'spikes' (Figs.15C & 18A,B), we postulated that TIP-1 regulates the cell motility through those Rho GTPases.

It is generally accepted that temporally and spatially regulated GTPase activation is required for the proper initiation of downstream signaling events including protrusion at the leading edge and rear retraction of cell body, although the molecular mechanisms that control these temporally and spatially activation of Rho GTPases are not comprehensively understood yet (Pertz et al., 2006; ten Klooster et al., 2006). In recent years, accumulating evidences indicate that Rho-GEF/Effectors can locate and direct the

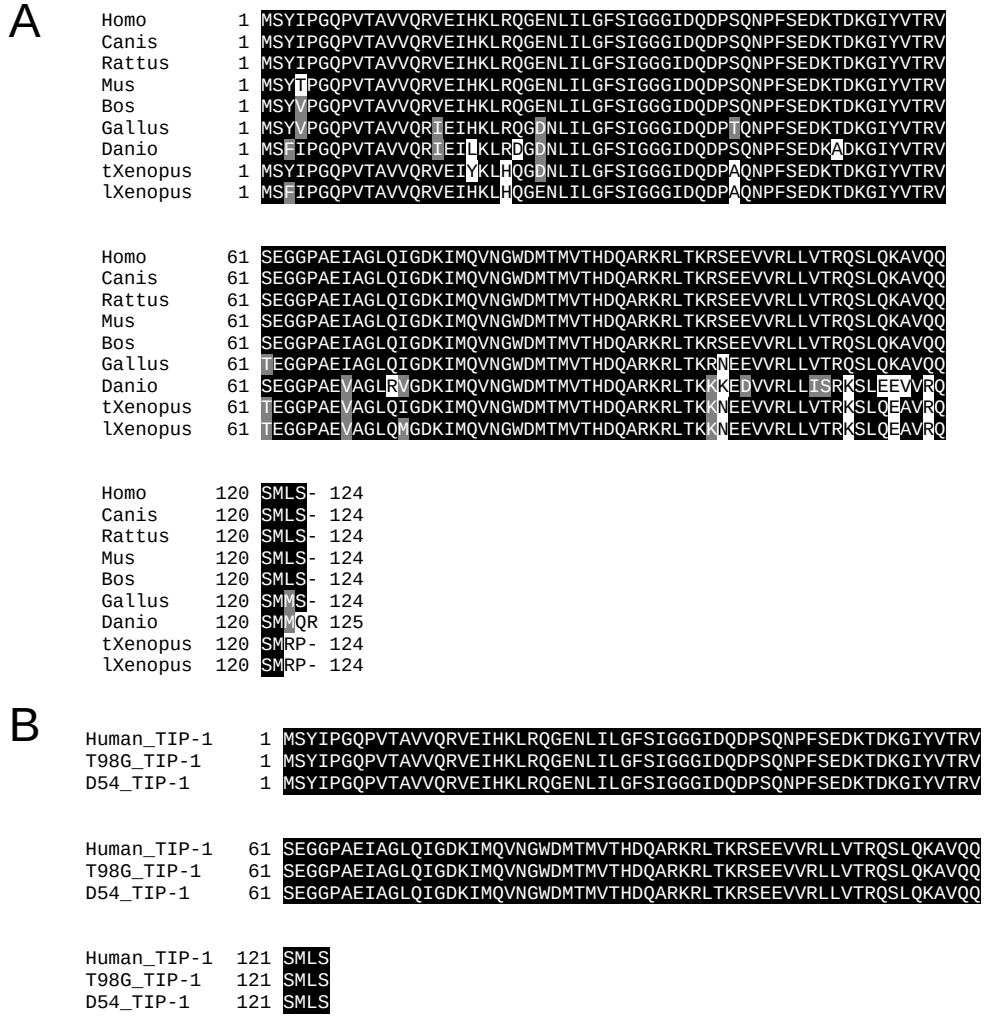

Figure 17. (A) Multiple sequence alignment of TIP-1 protein across several species, and (B) TIP-1 Sequences in glioma cell lines D54 and T98G

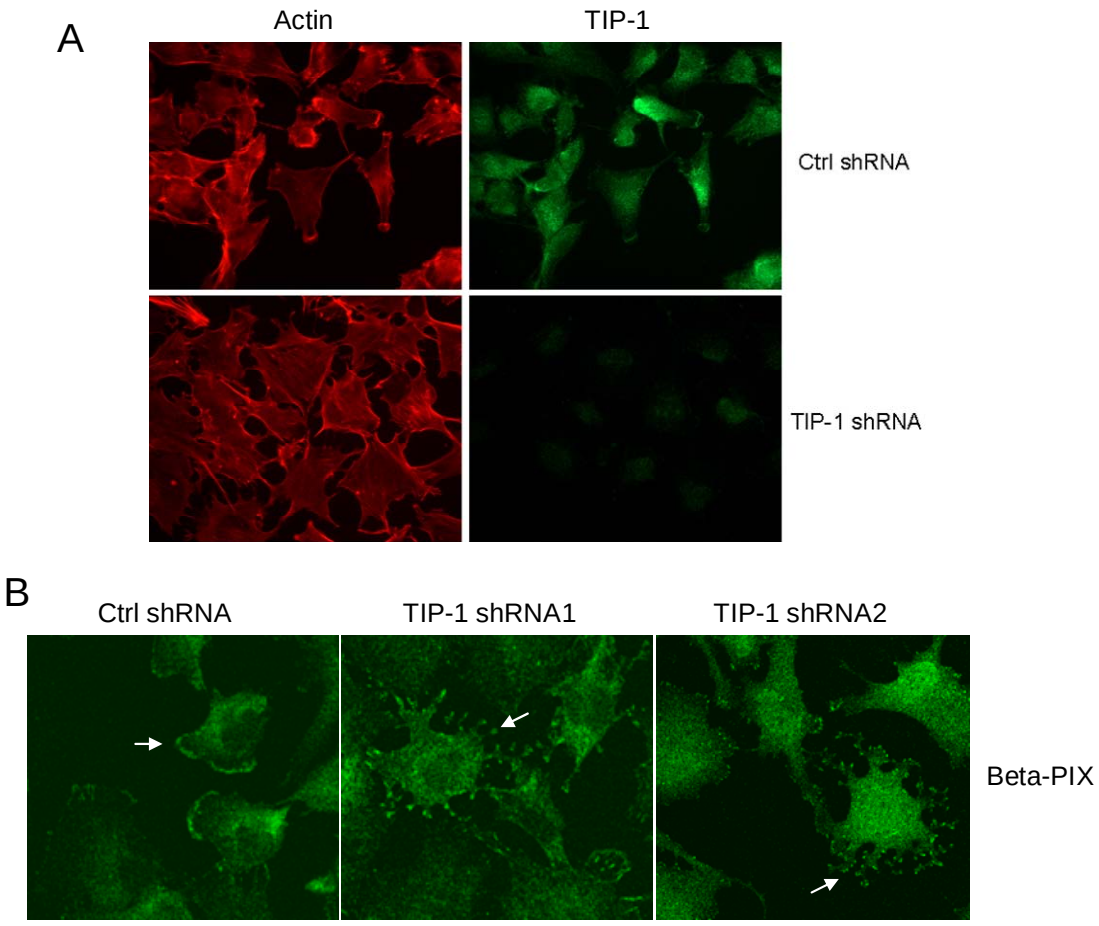

Figure 18. (A) Cell morphology change after TIP-1 knockdown in T98G cells. Red: Actin; Green: TIP-1, (B) Highly Branched Structure formed in TIP-1 knockdown T98G cells, with beta-PIX located at the tips of branches. Green: beta-PIX.

Rho GTPases signal output through their interaction with scaffold proteins (Garcia-Mata and Burridge, 2007; Jaffe and Hall, 2005; Marinissen and Gutkind, 2005). Scribble is a PDZ scaffold protein that is required for establishing epithelial polarity and limiting cell proliferation (Bilder et al., 2000). It has been reported that scribble works as a scaffold protein by interacting with beta-PIX through the PDZ domain, which controls the localization of activated Cdc42 and Rac1 to the leading edge (Audebert et al., 2004; Osmani et al., 2006; ten Klooster et al., 2006). However, almost nothing is known about roles of rhotekin in these molecular events.

Using scribble as a referral protein, we investigated the impact of TIP-1 on the temporally and spatially regulated location of the Rho GEF/effectors and activation of RhoA, Rac1 and Cdc42. The results showed that TIP-1 knockdown significantly increased the basal level of scribble protein interaction with beta-PIX and rhotekin. However, after scratch wounding, only the association between rhotekin and scribble was significantly increased. Beta-PIX did not show any increased interaction with scribble after wounding (Fig. 15B). In addition to changes in levels of interaction, the locations of beta-PIX and rhotekin inside the cells were also dramatically changed. The results illustrated that PDZ binding motifs are important for proper localization of GEF/Effectors, and indicated that TIP-1 can regulate the selective interaction and subcellular localization of beta-PIX and rhotekin inside the migrating cells. Regarding the differential binding pattern between beta-PIX and rhotekin, we speculate that the high concentration of rhotekin in glioma cells might give it some advantages to compete with beta-PIX for scribble binding (Figs.15A,B). Although we can not rule out the possibilities that

rhotekin interacts with scribble with a higher affinity, more studies are needed to further elucidate the detailed mechanisms governing these differential protein interactions. Within the TIP-1 knockdown glioma cells, the changes in the associations of beta-PIX and rhotekin with membrane associated scaffold proteins provide the basis for the irregular activation of Rac1, Cdc42 or RhoA. Consistent with this, more RhoA was located to the leading edge especially to the spots where rhotekin is localized, and it was strongly activated after wounding. On the other hand, there was barely any change of the level of Rac1/Cdc42 associated with the leading edge, except that their distribution patterns were dramatically altered, and their activities were decreased. It is also interesting to notice that the activity decrease of Rac1 is much greater than that of Cdc42, which is probably caused by the counteraction between RhoA and Rac1 (Yamaguchi et al., 2001). With the disorganized Rho GTPases activities after TIP-1 depletion, the cell did not form normal actin fiber structures along the lamellipodia at the leading edge, and MTOC reorientation was much delayed. There were more stress fibers formed, and cell motility was dramatically decreased.

Taken together, we propose that TIP-1 orchestrates cell migration through directing beta-PIX and rhotekin to the corresponding subcellular locations for temporally and spatially activation of Rho GTPases - RhoA, Rac1 and Cdc42. However, the molecular mechanisms by which TIP-1 coordinately regulates the location of beta-PIX and rhotekin remain to be defined. Further studies on the potential posttranslational modifications of TIP-1 and roles in selective protein interactions are needed to elucidate the structural basis of the protein interactions required for temporal and spatial regulation of Rho

GTPases activation in cell migration. It is interesting to notice that the third TIP-1 interacting protein, beta-catenin, also interacts with actin through alpha-catenin, and may help to stabilize the cytoskeleton. Therefore, further studies on the mechanisms by which TIP-1 regulates beta-catenin activities will provide more insights into TIP-1's contributions to cell migration and malignancy of brain tumors.

CHAPTER IV

GENERAL DISCUSSION AND FUTURE DIRECTION

Peptide Receptor Identification

Cancer targeted imaging has become an indispensable tool in modern diagnostics because it provides accurate and fast diagnosis of cancer. Peptides are small molecules with great target permeability, and they will not elicit an immune response (Ladner et al., 2004). Therefore, peptide-based imaging probes have been increasingly used in cancer targeted imaging. In our previous studies, we identified one peptide (-HVGGSSV) specifically binds to radiation treatment responsive tumors (Han et al., 2008). Several following studies already demonstrated that nanoparticles/vesicles conjugated with HVGGSSV peptide showed an increased tumor-specific delivery and bioavailability of drugs in tumors after radiation treatment (Hariri et al., 2010a; Hariri et al., 2010b).

To understand the physiological impact that underlies peptide binding, we need to know the targets of the peptide. However, due to peptides small size and low binding force, it is a great challenge to identify peptides' targeting proteins. In Chapter II of this thesis study, besides the traditional affinity purification methods, we explored several new techniques for isolating the target of HVGGSSV peptide. To increase binding affinity between the peptide and its receptor, we first conjugated a photoactive linker (4-(N-Maleimido)benzophenone, Sigma) on the peptide, which can be activated by UV light and form a covalent bond between the peptide and its target protein. However, in both *in*

vivo and *in vitro* experiments, the proteins pulled down using this method were predominantly nonspecific binding proteins. It is probably because that the conjugated photoactive linker changed the surface hydrophobicity of the whole peptide molecules. With no better chemical linkers available, we turned to a different method – phage display. Different from the phage peptide library we used for isolating HVGGSSV peptide, a phage cDNA library was screened to identify the target protein of the peptide. After several rounds of screening, the target protein with specific interactions was dramatically enriched in the pool of phage eluted from the HVGGSSV peptide. And we identified TIP-1 as the target of HVGGSSV peptide. The specific interaction was confirmed by *in vitro* biochemical assays. Therefore, our results demonstrated the potentials of screening phage-displayed cDNA library in discovery of molecular targets of the peptides with simple structure and low affinity.

TIP-1 Is A Biomarker For Assessment Of Tumor Response To Ionizing Radiation Treatment

In Chapter II of this thesis research, we have demonstrated that TIP-1 protein mediated binding of the HVGGSSV peptide within irradiated tumors, and radiation could induce TIP-1 translocation onto the cell surface. Therefore, TIP-1 can be used as a biomarker for evaluation of tumor response to ionizing radiation. However, the mechanisms of TIP-1 translocation onto the cell surface and the physiological impact of this translocation are still not clear. Based on TIP-1 function analysis in Chapter III, we assume that the translocation could sequester TIP-1 from the cytosol and inhibit cell migration and invasion. Furthermore, the exposure of TIP-1 on the cell surface might also provide a

stimulatory signal to activate the immune system. But elucidation of the exact mechanisms and functions of the translocation requires further investigation.

TIP-1 Can Serve As A Target For Radiation Guided Immunotherapy

Monoclonal antibodies are the most widely used form of immunotherapy to treat cancer. Monoclonal antibodies can be used all by itself or attached with drug or toxins or radioactive substances to kill cancer cells (Lin et al., 2005). The studies from Chapter II have shown that TIP-1 specific antibody exhibited similar binding patterns as the HVGGSSV peptide within irradiated tumors. These results indicate that TIP-1 is available for antibody binding *in vivo*, and provided the basis for monoclonal antibodies production and further investigation of TIP-1 targeted radiation guided immunotherapy.

Regulation of TIP-1 Protein Function

Almost entire TIP-1 protein forms a single PDZ domain. This unique structure indicates that TIP-1 can not function as a scaffold protein like other PDZ proteins. Studies carried out in Chapter III of this thesis research revealed that TIP-1 interacted with beta-PIX and rhotekin through the PDZ domain, and regulated the spatial and temporal activation of RhoA, Rac1 and Cdc42. Although PDZ proteins have been reported to interact with Rho GEF/effectors and control Rho GEF/effectors targeting and activation, all of these PDZ proteins are membrane associated scaffold proteins that recruit Rho GEF/effectors to appropriate subcellular destinations (Audebert et al., 2004; Park et al., 2003; Penzes et al., 2001). With our current knowledge, TIP-1 probably functions as an antagonizer to interfere with the binding of Rho GEF/effector to PDZ scaffold proteins. The

mechanisms by which TIP-1 coordinately regulate three major Rho GTPases need to be further investigated. It is probably cell type specific due to the different expression pattern of beta-PIX and rhotekin in different tissues. The phosphorylation site predicted from structure analysis is located inside the PDZ motif binding pocket on TIP-1 and may play an important role in regulating the dynamic interaction between TIP-1 and its binding proteins. Furthermore, dimmerizaton of TIP-1 or a second domain on TIP-1 are both possible mechanisms that regulate TIP-1 functions. Further investigation will provide us more insight into TIP-1 functions.

REFERENCE

Adamson, P., Marshall, C. J., Hall, A., and Tilbrook, P. A. (1992). Post-translational modifications of p21rho proteins. The Journal of biological chemistry *267*, 20033-20038.

Adey, N. B., Huang, L., Ormonde, P. A., Baumgard, M. L., Pero, R., Byreddy, D. V., Tavtigian, S. V., and Bartel, P. L. (2000). Threonine phosphorylation of the MMAC1/PTEN PDZ binding domain both inhibits and stimulates PDZ binding. Cancer research *60*, 35-37.

Aledo, J. C., Rosado, A., Olalla, L., Campos, J. A., and Marquez, J. (2001). Overexpression, purification, and characterization of glutaminase-interacting protein, a PDZ-domain protein from human brain. Protein expression and purification *23*, 411-418.

Alewine, C., Olsen, O., Wade, J. B., and Welling, P. A. (2006). TIP-1 has PDZ scaffold antagonist activity. Molecular biology of the cell *17*, 4200-4211.

Aloj, L., and Morelli, G. (2004). Design, synthesis and preclinical evaluation of radiolabeled peptides for diagnosis and therapy. Current pharmaceutical design *10*, 3009-3031.

Amano, M., Chihara, K., Kimura, K., Fukata, Y., Nakamura, N., Matsuura, Y., and Kaibuchi, K. (1997). Formation of actin stress fibers and focal adhesions enhanced by Rho-kinase. Science (New York, NY *275*, 1308-1311.

Arap, W., Haedicke, W., Bernasconi, M., Kain, R., Rajotte, D., Krajewski, S., Ellerby, H. M., Bredesen, D. E., Pasqualini, R., and Ruoslahti, E. (2002a). Targeting the prostate for destruction through a vascular address. Proceedings of the National Academy of Sciences of the United States of America *99*, 1527-1531.

Arap, W., Kolonin, M. G., Trepel, M., Lahdenranta, J., Cardo-Vila, M., Giordano, R. J., Mintz, P. J., Ardelt, P. U., Yao, V. J., Vidal, C. I.*, et al.* (2002b). Steps toward mapping the human vasculature by phage display. Nature medicine *8*, 121-127.

Asaba, N., Hanada, T., Takeuchi, A., and Chishti, A. H. (2003). Direct interaction with a kinesin-related motor mediates transport of mammalian discs large tumor suppressor homologue in epithelial cells. The Journal of biological chemistry *278*, 8395-8400.

Audebert, S., Navarro, C., Nourry, C., Chasserot-Golaz, S., Lecine, P., Bellaiche, Y., Dupont, J. L., Premont, R. T., Sempere, C., Strub, J. M.*, et al.* (2004). Mammalian Scribble forms a tight complex with the betaPIX exchange factor. Curr Biol *14*, 987-995.

Ben-Neriah, Y., Daley, G. Q., Mes-Masson, A. M., Witte, O. N., and Baltimore, D. (1986). The chronic myelogenous leukemia-specific P210 protein is the product of the bcr/abl hybrid gene. Science (New York, NY *233*, 212-214.

Benitah, S. A., Valeron, P. F., van Aelst, L., Marshall, C. J., and Lacal, J. C. (2004). Rho GTPases in human cancer: an unresolved link to upstream and downstream transcriptional regulation. Biochimica et biophysica acta *1705*, 121-132.

Bennasroune, A., Gardin, A., Aunis, D., Cremel, G., and Hubert, P. (2004). Tyrosine kinase receptors as attractive targets of cancer therapy. Critical reviews in oncology/hematology *50*, 23-38.

Besser, J., Leito, J. T., van der Meer, D. L., and Bagowski, C. P. (2007). Tip-1 induces filopodia growth and is important for gastrulation movements during zebrafish development. Development, growth & differentiation *49*, 205-214.

Beuming, T., Skrabanek, L., Niv, M. Y., Mukherjee, P., and Weinstein, H. (2005). PDZBase: a protein-protein interaction database for PDZ-domains. Bioinformatics (Oxford, England) *21*, 827-828.

Bilder, D. (2004). Epithelial polarity and proliferation control: links from the Drosophila neoplastic tumor suppressors. Genes & development *18*, 1909-1925.

Bilder, D., Li, M., and Perrimon, N. (2000). Cooperative regulation of cell polarity and growth by Drosophila tumor suppressors. Science (New York, NY *289*, 113-116.

Blume-Jensen, P., and Hunter, T. (2001). Oncogenic kinase signalling. Nature *411*, 355-365.

Bos, J. L., Rehmann, H., and Wittinghofer, A. (2007). GEFs and GAPs: critical elements in the control of small G proteins. Cell *129*, 865-877.

Boureux, A., Vignal, E., Faure, S., and Fort, P. (2007). Evolution of the Rho family of ras-like GTPases in eukaryotes. Molecular biology and evolution *24*, 203-216.

Bradford, M. M. (1976). A rapid and sensitive method for the quantitation of microgram quantities of protein utilizing the principle of protein-dye binding. Analytical biochemistry *72*, 248-254.

Brenman, J. E., Chao, D. S., Gee, S. H., McGee, A. W., Craven, S. E., Santillano, D. R., Wu, Z., Huang, F., Xia, H., Peters, M. F., *et al.* (1996). Interaction of nitric oxide synthase with the postsynaptic density protein PSD-95 and alpha1-syntrophin mediated by PDZ domains. Cell *84*, 757-767.

Bromberg, Y., Shani, E., Joseph, G., Gorzalczany, Y., Sperling, O., and Pick, E. (1994). The GDP-bound form of the small G protein Rac1 p21 is a potent activator of the

superoxide-forming NADPH oxidase of macrophages. The Journal of biological chemistry *269*, 7055-7058.

Cai, W., Niu, G., and Chen, X. (2008). Imaging of integrins as biomarkers for tumor angiogenesis. Current pharmaceutical design *14*, 2943-2973.

Campa, F., Machuy, N., Klein, A., and Rudel, T. (2006). A new interaction between Abi-1 and betaPIX involved in PDGF-activated actin cytoskeleton reorganisation. Cell research *16*, 759-770.

Cassimeris, L. (2002). The oncoprotein 18/stathmin family of microtubule destabilizers. Current opinion in cell biology *14*, 18-24.

Chen, B. S., Braud, S., Badger, J. D., 2nd, Isaac, J. T., and Roche, K. W. (2006). Regulation of NR1/NR2C N-methyl-D-aspartate (NMDA) receptors by phosphorylation. The Journal of biological chemistry *281*, 16583-16590.

Cheng, H., Li, J., Fazlieva, R., Dai, Z., Bu, Z., and Roder, H. (2009). Autoinhibitory interactions between the PDZ2 and C-terminal domains in the scaffolding protein NHERF1. Structure *17*, 660-669.

Christian, S., Pilch, J., Akerman, M. E., Porkka, K., Laakkonen, P., and Ruoslahti, E. (2003). Nucleolin expressed at the cell surface is a marker of endothelial cells in angiogenic blood vessels. The Journal of cell biology *163*, 871-878.

Chung, H. J., Huang, Y. H., Lau, L. F., and Huganir, R. L. (2004). Regulation of the NMDA receptor complex and trafficking by activity-dependent phosphorylation of the NR2B subunit PDZ ligand. J Neurosci *24*, 10248-10259.

Coso, O. A., Chiariello, M., Yu, J. C., Teramoto, H., Crespo, P., Xu, N., Miki, T., and Gutkind, J. S. (1995). The small GTP-binding proteins Rac1 and Cdc42 regulate the activity of the JNK/SAPK signaling pathway. Cell *81*, 1137-1146.

Cui, H., Hayashi, A., Sun, H.-S., Belmares, M. P., Cobey, C., Phan, T., Schweizer, J., Salter, M. W., Wang, Y. T., Tasker, R. A., *et al.* (2007). PDZ Protein Interactions Underlying NMDA Receptor-Mediated Excitotoxicity and Neuroprotection by PSD-95 Inhibitors. J Neurosci *27*, 9901-9915.

Daley, G. Q., Van Etten, R. A., and Baltimore, D. (1990). Induction of chronic myelogenous leukemia in mice by the P210bcr/abl gene of the Philadelphia chromosome. Science (New York, NY *247*, 824-830.

Daub, H., Gevaert, K., Vandekerckhove, J., Sobel, A., and Hall, A. (2001). Rac/Cdc42 and p65PAK regulate the microtubule-destabilizing protein stathmin through phosphorylation at serine 16. The Journal of biological chemistry *276*, 1677-1680.

Davies, S. P., Reddy, H., Caivano, M., and Cohen, P. (2000). Specificity and mechanism of action of some commonly used protein kinase inhibitors. The Biochemical journal *351*, 95-105.

Dovas, A., and Couchman, J. R. (2005). RhoGDI: multiple functions in the regulation of Rho family GTPase activities. The Biochemical journal *390*, 1-9.

Dowsett, M., and Dunbier, A. K. (2008). Emerging biomarkers and new understanding of traditional markers in personalized therapy for breast cancer. Clin Cancer Res *14*, 8019-8026.

Durney, M. A., Birrane, G., Anklin, C., Soni, A., and Ladias, J. A. (2009). Solution structure of the human Tax-interacting protein-1. Journal of biomolecular NMR *45*, 329-334.

Etienne-Manneville, S. (2006). In vitro assay of primary astrocyte migration as a tool to study Rho GTPase function in cell polarization. Methods in enzymology *406*, 565-578.

Etienne-Manneville, S., and Hall, A. (2002). Rho GTPases in cell biology. Nature *420*, 629-635.

Felgner, P. L., Gadek, T. R., Holm, M., Roman, R., Chan, H. W., Wenz, M., Northrop, J. P., Ringold, G. M., and Danielsen, M. (1987). Lipofection: a highly efficient, lipid-mediated DNA-transfection procedure. Proceedings of the National Academy of Sciences of the United States of America *84*, 7413-7417.

Feng, Q., Baird, D., Yoo, S., Antonyak, M., and Cerione, R. A. (2010). Phosphorylation of the Cool-1/{beta}-Pix protein serves as a regulatory signal for the migration and invasive activity of Src-transformed cells. The Journal of biological chemistry.

Fernandez-Gacio, A., Uguen, M., and Fastrez, J. (2003). Phage display as a tool for the directed evolution of enzymes. Trends in biotechnology *21*, 408-414.

Frangioni, J. V. (2003). In vivo near-infrared fluorescence imaging. Current opinion in chemical biology *7*, 626-634.

Frese, K. K., Lee, S. S., Thomas, D. L., Latorre, I. J., Weiss, R. S., Glaunsinger, B. A., and Javier, R. T. (2003). Selective PDZ protein-dependent stimulation of phosphatidylinositol 3-kinase by the adenovirus E4-ORF1 oncoprotein. Oncogene *22*, 710-721.

Fritz, G., Just, I., and Kaina, B. (1999). Rho GTPases are over-expressed in human tumors. International journal of cancer *81*, 682-687.

Fukata, M., Watanabe, T., Noritake, J., Nakagawa, M., Yamaga, M., Kuroda, S., Matsuura, Y., Iwamatsu, A., Perez, F., and Kaibuchi, K. (2002a). Rac1 and Cdc42 capture microtubules through IQGAP1 and CLIP-170. Cell *109*, 873-885.

Fukata, Y., Itoh, T. J., Kimura, T., Menager, C., Nishimura, T., Shiromizu, T., Watanabe, H., Inagaki, N., Iwamatsu, A., Hotani, H., and Kaibuchi, K. (2002b). CRMP-2 binds to tubulin heterodimers to promote microtubule assembly. Nature cell biology *4*, 583-591.

Gaggioli, C., Hooper, S., Hidalgo-Carcedo, C., Grosse, R., Marshall, J. F., Harrington, K., and Sahai, E. (2007). Fibroblast-led collective invasion of carcinoma cells with differing roles for RhoGTPases in leading and following cells. Nature cell biology *9*, 1392-1400.

Garcia-Mata, R., and Burridge, K. (2007). Catching a GEF by its tail. Trends in cell biology *17*, 36-43.

Gazit, A., Yaish, P., Gilon, C., and Levitzki, A. (1989). Tyrphostins I: synthesis and biological activity of protein tyrosine kinase inhibitors. Journal of medicinal chemistry *32*, 2344-2352.

Geng, L., Shinohara, E. T., Kim, D., Tan, J., Osusky, K., Shyr, Y., and Hallahan, D. E. (2006). STI571 (Gleevec) improves tumor growth delay and survival in irradiated mouse models of glioblastoma. International journal of radiation oncology, biology, physics *64*, 263-271.

Goga, A., McLaughlin, J., Afar, D. E., Saffran, D. C., and Witte, O. N. (1995). Alternative signals to RAS for hematopoietic transformation by the BCR-ABL oncogene. Cell *82*, 981-988.

Gomez del Pulgar, T., Benitah, S. A., Valeron, P. F., Espina, C., and Lacal, J. C. (2005). Rho GTPase expression in tumourigenesis: evidence for a significant link. Bioessays *27*, 602-613.

Gommans, W. M., Haisma, H. J., and Rots, M. G. (2005). Engineering zinc finger protein transcription factors: the therapeutic relevance of switching endogenous gene expression on or off at command. Journal of molecular biology *354*, 507-519.

Gouw, L. G., Reading, N. S., Jenson, S. D., Lim, M. S., and Elenitoba-Johnson, K. S. (2005). Expression of the Rho-family GTPase gene RHOF in lymphocyte subsets and malignant lymphomas. British journal of haematology *129*, 531-533.

Gramates, L. S., and Budnik, V. (1999). Assembly and maturation of the Drosophila larval neuromuscular junction. International review of neurobiology *43*, 93-117.

Hall, A. (1998). Rho GTPases and the actin cytoskeleton. Science (New York, NY *279*, 509-514.

Hall, W. W., and Fujii, M. (2005). Deregulation of cell-signaling pathways in HTLV-1 infection. Oncogene *24*, 5965-5975.

Hallahan, D., Geng, L., Qu, S., Scarfone, C., Giorgio, T., Donnelly, E., Gao, X., and Clanton, J. (2003). Integrin-mediated targeting of drug delivery to irradiated tumor blood vessels. Cancer cell *3*, 63-74.

Hallahan, D., Kuchibhotla, J., and Wyble, C. (1996). Cell adhesion molecules mediate radiation-induced leukocyte adhesion to the vascular endothelium. Cancer research *56*, 5150-5155.

Hallahan, D. E., Staba-Hogan, M. J., Virudachalam, S., and Kolchinsky, A. (1998). X-ray-induced P-selectin localization to the lumen of tumor blood vessels. Cancer research *58*, 5216-5220.

Hampson, L., Li, C., Oliver, A. W., Kitchener, H. C., and Hampson, I. N. (2004). The PDZ protein Tip-1 is a gain of function target of the HPV16 E6 oncoprotein. International journal of oncology *25*, 1249-1256.

Han, Z., Fu, A., Wang, H., Diaz, R., Geng, L., Onishko, H., and Hallahan, D. E. (2008). Noninvasive assessment of cancer response to therapy. Nature medicine *14*, 343-349.

Han, Z., Karatan, E., Scholle, M. D., McCafferty, J., and Kay, B. K. (2004a). Accelerated screening of phage-display output with alkaline phosphatase fusions. Combinatorial chemistry & high throughput screening *7*, 55-62.

Han, Z., Simpson, J. T., Fivash, M. J., Fisher, R., and Mori, T. (2004b). Identification and characterization of peptides that bind to cyanovirin-N, a potent human immunodeficiency virus-inactivating protein. Peptides *25*, 551-561.

Han, Z., Wang, H., and Hallahan, D. E. (2006). Radiation-guided gene therapy of cancer. Technology in cancer research & treatment *5*, 437-444.

Han, Z., Xiong, C., Mori, T., and Boyd, M. R. (2002). Discovery of a stable dimeric mutant of cyanovirin-N (CV-N) from a T7 phage-displayed CV-N mutant library. Biochemical and biophysical research communications *292*, 1036-1043.

Hariri, G., Wellons, M. S., Morris, W. H., 3rd, Lukehart, C. M., and Hallahan, D. E. (2010a). Multifunctional FePt Nanoparticles for Radiation-Guided Targeting and Imaging of Cancer. Annals of biomedical engineering.

Hariri, G., Yan, H., Wang, H., Han, Z., and Hallahan, D. E. (2010b). Radiation-guided drug delivery to mouse models of lung cancer. Clin Cancer Res *16*, 4968-4977.

Hillier, B. J., Christopherson, K. S., Prehoda, K. E., Bredt, D. S., and Lim, W. A. (1999). Unexpected modes of PDZ domain scaffolding revealed by structure of nNOS-syntrophin complex. Science (New York, NY *284*, 812-815.

Houshmand, P., and Zlotnik, A. (2003). Targeting tumor cells. Current opinion in cell biology *15*, 640-644.

Hwang, S. L., Hong, Y. R., Sy, W. D., Lieu, A. S., Lin, C. L., Lee, K. S., and Howng, S. L. (2004). Rac1 gene mutations in human brain tumours. Eur J Surg Oncol *30*, 68-72.

Iden, S., and Collard, J. G. (2008). Crosstalk between small GTPases and polarity proteins in cell polarization. Nat Rev Mol Cell Biol *9*, 846-859.

Im, Y. J., Lee, J. H., Park, S. H., Park, S. J., Rho, S. H., Kang, G. B., Kim, E., and Eom, S. H. (2003a). Crystal structure of the Shank PDZ-ligand complex reveals a class I PDZ interaction and a novel PDZ-PDZ dimerization. The Journal of biological chemistry *278*, 48099-48104.

Im, Y. J., Park, S. H., Rho, S. H., Lee, J. H., Kang, G. B., Sheng, M., Kim, E., and Eom, S. H. (2003b). Crystal structure of GRIP1 PDZ6-peptide complex reveals the structural basis for class II PDZ target recognition and PDZ domain-mediated multimerization. The Journal of biological chemistry *278*, 8501-8507.

Ito, H., Iwamoto, I., Morishita, R., Nozawa, Y., Asano, T., and Nagata, K. (2006). Identification of a PDZ protein, PIST, as a binding partner for Rho effector Rhotekin: biochemical and cell-biological characterization of Rhotekin-PIST interaction. The Biochemical journal *397*, 389-398.

Ito, H., Iwamoto, I., Morishita, R., Nozawa, Y., Narumiya, S., Asano, T., and Nagata, K. (2005). Possible role of Rho/Rhotekin signaling in mammalian septin organization. Oncogene *24*, 7064-7072.

Jaffe, A. B., and Hall, A. (2005). Rho GTPases: biochemistry and biology. Annual review of cell and developmental biology *21*, 247-269.

Javier, R. T. (2008). Cell polarity proteins: common targets for tumorigenic human viruses. Oncogene *27*, 7031-7046.

Joneson, T., and Bar-Sagi, D. (1998). A Rac1 effector site controlling mitogenesis through superoxide production. The Journal of biological chemistry *273*, 17991-17994.

Jordan, P., Brazao, R., Boavida, M. G., Gespach, C., and Chastre, E. (1999). Cloning of a novel human Rac1b splice variant with increased expression in colorectal tumors. Oncogene *18*, 6835-6839.

Joyce, J. A., Laakkonen, P., Bernasconi, M., Bergers, G., Ruoslahti, E., and Hanahan, D. (2003). Stage-specific vascular markers revealed by phage display in a mouse model of pancreatic islet tumorigenesis. Cancer cell *4*, 393-403.

Kanamori, M., Sandy, P., Marzinotto, S., Benetti, R., Kai, C., Hayashizaki, Y., Schneider, C., and Suzuki, H. (2003). The PDZ protein tax-interacting protein-1 inhibits beta-catenin transcriptional activity and growth of colorectal cancer cells. The Journal of biological chemistry *278*, 38758-38764.

Kay, B. K., and Kehoe, J. W. (2004). PDZ domains and their ligands. Chemistry & biology *11*, 423-425.

Kim, E., and Sheng, M. (2004). PDZ domain proteins of synapses. Nature reviews *5*, 771-781.

Kimura, K., Ito, M., Amano, M., Chihara, K., Fukata, Y., Nakafuku, M., Yamamori, B., Feng, J., Nakano, T., Okawa, K.*, et al.* (1996). Regulation of myosin phosphatase by Rho and Rho-associated kinase (Rho-kinase). Science (New York, NY *273*, 245-248.

Korner, M., Stockli, M., Waser, B., and Reubi, J. C. (2007). GLP-1 receptor expression in human tumors and human normal tissues: potential for in vivo targeting. J Nucl Med *48*, 736-743.

Kranjec, C., and Banks, L. (2010). A Systematic Analysis of Human Papillomavirus (HPV) E6 PDZ Substrates Identifies MAGI-1 as a Major Target of HPV Type 16 (HPV-16) and HPV-18 Whose Loss Accompanies Disruption of Tight Junctions. Journal of virology *85*, 1757-1764.

Krumpe, L. R., Atkinson, A. J., Smythers, G. W., Kandel, A., Schumacher, K. M., McMahon, J. B., Makowski, L., and Mori, T. (2006). T7 lytic phage-displayed peptide libraries exhibit less sequence bias than M13 filamentous phage-displayed peptide libraries. Proteomics *6*, 4210-4222.

Kung, A. L., Wang, S., Klco, J. M., Kaelin, W. G., and Livingston, D. M. (2000). Suppression of tumor growth through disruption of hypoxia-inducible transcription. Nature medicine *6*, 1335-1340.

Kupfer, A., Louvard, D., and Singer, S. J. (1982). Polarization of the Golgi apparatus and the microtubule-organizing center in cultured fibroblasts at the edge of an experimental wound. Proceedings of the National Academy of Sciences of the United States of America *79*, 2603-2607.

Ladner, R. C., Sato, A. K., Gorzelany, J., and de Souza, M. (2004). Phage display-derived peptides as therapeutic alternatives to antibodies. Drug discovery today *9*, 525-529.

LaLonde, D. P., and Bretscher, A. (2009). The scaffold protein PDZK1 undergoes a head-to-tail intramolecular association that negatively regulates its interaction with EBP50. Biochemistry *48*, 2261-2271.

Li, J., Poulikakos, P. I., Dai, Z., Testa, J. R., Callaway, D. J., and Bu, Z. (2007). Protein kinase C phosphorylation disrupts Na+/H+ exchanger regulatory factor 1 autoinhibition and promotes cystic fibrosis transmembrane conductance regulator macromolecular assembly. The Journal of biological chemistry *282*, 27086-27099.

Lin, M. Z., Teitell, M. A., and Schiller, G. J. (2005). The evolution of antibodies into versatile tumor-targeting agents. Clin Cancer Res *11*, 129-138.

Liu, M., and Horowitz, A. (2006). A PDZ-binding motif as a critical determinant of Rho guanine exchange factor function and cell phenotype. Molecular biology of the cell *17*, 1880-1887.

Long, J. F., Feng, W., Wang, R., Chan, L. N., Ip, F. C., Xia, J., Ip, N. Y., and Zhang, M. (2005). Autoinhibition of X11/Mint scaffold proteins revealed by the closed conformation of the PDZ tandem. Nature structural & molecular biology *12*, 722-728.

Lorenz, H. M. (2002). Technology evaluation: adalimumab, Abbott laboratories. Current opinion in molecular therapeutics *4*, 185-190.

Lowery, A., Onishko, H., Hallahan, D. E., and Han, Z. (2010). Tumor-targeted delivery of liposome-encapsulated doxorubicin by use of a peptide that selectively binds to irradiated tumors. J Control Release.

Lozano, E., Betson, M., and Braga, V. M. (2003). Tumor progression: Small GTPases and loss of cell-cell adhesion. Bioessays *25*, 452-463.

Ludford-Menting, M. J., Oliaro, J., Sacirbegovic, F., Cheah, E. T., Pedersen, N., Thomas, S. J., Pasam, A., Iazzolino, R., Dow, L. E., Waterhouse, N. J.*, et al.* (2005). A network of PDZ-containing proteins regulates T cell polarity and morphology during migration and immunological synapse formation. Immunity *22*, 737-748.

Machacek, M., Hodgson, L., Welch, C., Elliott, H., Pertz, O., Nalbant, P., Abell, A., Johnson, G. L., Hahn, K. M., and Danuser, G. (2009). Coordination of Rho GTPase activities during cell protrusion. Nature *461*, 99-103.

Manning, H. C., Merchant, N. B., Foutch, A. C., Virostko, J. M., Wyatt, S. K., Shah, C., McKinley, E. T., Xie, J., Mutic, N. J., Washington, M. K.*, et al.* (2008). Molecular imaging of therapeutic response to epidermal growth factor receptor blockade in colorectal cancer. Clin Cancer Res *14*, 7413-7422.

Margolis, B., and Borg, J. P. (2005). Apicobasal polarity complexes. Journal of cell science *118*, 5157-5159.

Marinissen, M. J., and Gutkind, J. S. (2005). Scaffold proteins dictate Rho GTPase-signaling specificity. Trends in biochemical sciences *30*, 423-426.

Matos, P., and Jordan, P. (2006). Rac1, but not Rac1B, stimulates RelB-mediated gene transcription in colorectal cancer cells. The Journal of biological chemistry *281*, 13724-13732.

Mauceri, D., Gardoni, F., Marcello, E., and Di Luca, M. (2007). Dual role of CaMKII-dependent SAP97 phosphorylation in mediating trafficking and insertion of NMDA receptor subunit NR2A. Journal of neurochemistry *100*, 1032-1046.

Mayhew, M. W., Webb, D. J., Kovalenko, M., Whitmore, L., Fox, J. W., and Horwitz, A. F. (2006). Identification of protein networks associated with the PAK1-betaPIX-GIT1-paxillin signaling complex by mass spectrometry. Journal of proteome research *5*, 2417-2423.

McCafferty, J., Griffiths, A. D., Winter, G., and Chiswell, D. J. (1990). Phage antibodies: filamentous phage displaying antibody variable domains. Nature *348*, 552-554.

Miao, Y., and Quinn, T. P. (2007). Alpha-melanocyte stimulating hormone peptide-targeted melanoma imaging. Front Biosci *12*, 4514-4524.

Miles, F. L., Pruitt, F. L., van Golen, K. L., and Cooper, C. R. (2008). Stepping out of the flow: capillary extravasation in cancer metastasis. Clinical & experimental metastasis *25*, 305-324.

Minden, A., Lin, A., Claret, F. X., Abo, A., and Karin, M. (1995). Selective activation of the JNK signaling cascade and c-Jun transcriptional activity by the small GTPases Rac and Cdc42Hs. Cell *81*, 1147-1157.

Mishra, P., Socolich, M., Wall, M. A., Graves, J., Wang, Z., and Ranganathan, R. (2007). Dynamic scaffolding in a G protein-coupled signaling system. Cell *131*, 80-92.

Mok, H., Shin, H., Kim, S., Lee, J. R., Yoon, J., and Kim, E. (2002). Association of the kinesin superfamily motor protein KIF1Balpha with postsynaptic density-95 (PSD-95), synapse-associated protein-97, and synaptic scaffolding molecule PSD-95/discs large/zona occludens-1 proteins. J Neurosci *22*, 5253-5258.

Molek, P., Strukelj, B., and Bratkovic, T. (2011). Peptide phage display as a tool for drug discovery: targeting membrane receptors. Molecules (Basel, Switzerland) *16*, 857-887.

Montell, C. (2000). A PDZ protein ushers in new links. Nature genetics *26*, 6-7.

Morales, F. C., Takahashi, Y., Momin, S., Adams, H., Chen, X., and Georgescu, M. M. (2007). NHERF1/EBP50 head-to-tail intramolecular interaction masks association with PDZ domain ligands. Molecular and cellular biology *27*, 2527-2537.

Mori, H., Manabe, T., Watanabe, M., Satoh, Y., Suzuki, N., Toki, S., Nakamura, K., Yagi, T., Kushiya, E., Takahashi, T.*, et al.* (1998). Role of the carboxy-terminal region of the GluR epsilon2 subunit in synaptic localization of the NMDA receptor channel. Neuron *21*, 571-580.

Nagata, K., Ito, H., Iwamoto, I., Morishita, R., and Asano, T. (2009). Interaction of a multi-domain adaptor protein, vinexin, with a Rho-effector, Rhotekin. Medical molecular morphology *42*, 9-15.

Nayal, A., Webb, D. J., Brown, C. M., Schaefer, E. M., Vicente-Manzanares, M., and Horwitz, A. R. (2006). Paxillin phosphorylation at Ser273 localizes a GIT1-PIX-PAK complex and regulates adhesion and protrusion dynamics. The Journal of cell biology *173*, 587-589.

Niessen, C. M. (2007). Tight junctions/adherens junctions: basic structure and function. The Journal of investigative dermatology *127*, 2525-2532.

Nobes, C. D., and Hall, A. (1995). Rho, rac, and cdc42 GTPases regulate the assembly of multimolecular focal complexes associated with actin stress fibers, lamellipodia, and filopodia. Cell *81*, 53-62.

Obenauer, J. C., Denson, J., Mehta, P. K., Su, X., Mukatira, S., Finkelstein, D. B., Xu, X., Wang, J., Ma, J., Fan, Y.*, et al.* (2006). Large-scale sequence analysis of avian influenza isolates. Science (New York, NY *311*, 1576-1580.

Oellers, P., Schroer, U., Senner, V., Paulus, W., and Thanos, S. (2009). ROCKs are expressed in brain tumors and are required for glioma-cell migration on myelinated axons. Glia *57*, 499-509.

Oh, P., Li, Y., Yu, J., Durr, E., Krasinska, K. M., Carver, L. A., Testa, J. E., and Schnitzer, J. E. (2004). Subtractive proteomic mapping of the endothelial surface in lung and solid tumours for tissue-specific therapy. Nature *429*, 629-635.

Okarvi, S. M. (2004). Peptide-based radiopharmaceuticals: future tools for diagnostic imaging of cancers and other diseases. Medicinal research reviews *24*, 357-397.

Olalla, L., Aledo, J. C., Bannenberg, G., and Marquez, J. (2001). The C-terminus of human glutaminase L mediates association with PDZ domain-containing proteins. FEBS letters *488*, 116-122.

Olalla, L., Gutierrez, A., Jimenez, A. J., Lopez-Tellez, J. F., Khan, Z. U., Perez, J., Alonso, F. J., de la Rosa, V., Campos-Sandoval, J. A., Segura, J. A.*, et al.* (2008).

Expression of the scaffolding PDZ protein glutaminase-interacting protein in mammalian brain. Journal of neuroscience research *86*, 281-292.

Oslo (2010). WHO Collaborating Centre for Drug Statistics Methodology, Guidelines for ATC classification and DDD assignment, 2011. In.

Osmani, N., Vitale, N., Borg, J. P., and Etienne-Manneville, S. (2006). Scrib controls Cdc42 localization and activity to promote cell polarization during astrocyte migration. Curr Biol *16*, 2395-2405.

Palazzo, A. F., Cook, T. A., Alberts, A. S., and Gundersen, G. G. (2001). mDia mediates Rho-regulated formation and orientation of stable microtubules. Nature cell biology *3*, 723-729.

Park, E., Na, M., Choi, J., Kim, S., Lee, J. R., Yoon, J., Park, D., Sheng, M., and Kim, E. (2003). The Shank family of postsynaptic density proteins interacts with and promotes synaptic accumulation of the beta PIX guanine nucleotide exchange factor for Rac1 and Cdc42. The Journal of biological chemistry *278*, 19220-19229.

Pasqualini, R., Koivunen, E., and Ruoslahti, E. (1995). A peptide isolated from phage display libraries is a structural and functional mimic of an RGD-binding site on integrins. The Journal of cell biology *130*, 1189-1196.

Pasqualini, R., and Ruoslahti, E. (1996). Organ targeting in vivo using phage display peptide libraries. Nature *380*, 364-366.

Passarella, R. J., Spratt, D. E., van der Ende, A. E., Phillips, J. G., Wu, H., Sathiyakumar, V., Zhou, L., Hallahan, D. E., Harth, E., and Diaz, R. (2010). Targeted nanoparticles that deliver a sustained, specific release of Paclitaxel to irradiated tumors. Cancer research *70*, 4550-4559.

Passarella, R. J., Zhou, L., Phillips, J. G., Wu, H., Hallahan, D. E., and Diaz, R. (2009). Recombinant peptides as biomarkers for tumor response to molecular targeted therapy. Clin Cancer Res *15*, 6421-6429.

Pedersen, H., Holder, S., Sutherlin, D. P., Schwitter, U., King, D. S., and Schultz, P. G. (1998). A method for directed evolution and functional cloning of enzymes. Proceedings of the National Academy of Sciences of the United States of America *95*, 10523-10528.

Penzes, P., Johnson, R. C., Sattler, R., Zhang, X., Huganir, R. L., Kambampati, V., Mains, R. E., and Eipper, B. A. (2001). The neuronal Rho-GEF Kalirin-7 interacts with PDZ domain-containing proteins and regulates dendritic morphogenesis. Neuron *29*, 229-242.

Perea, S. E., Reyes, O., Puchades, Y., Mendoza, O., Vispo, N. S., Torrens, I., Santos, A., Silva, R., Acevedo, B., Lopez, E.*, et al.* (2004). Antitumor effect of a novel proapoptotic

peptide that impairs the phosphorylation by the protein kinase 2 (casein kinase 2). Cancer research *64*, 7127-7129.

Perona, R., Montaner, S., Saniger, L., Sanchez-Perez, I., Bravo, R., and Lacal, J. C. (1997). Activation of the nuclear factor-kappaB by Rho, CDC42, and Rac-1 proteins. Genes & development *11*, 463-475.

Pertz, O., Hodgson, L., Klemke, R. L., and Hahn, K. M. (2006). Spatiotemporal dynamics of RhoA activity in migrating cells. Nature *440*, 1069-1072.

Peters, G. J., van der Wilt, C. L., van Moorsel, C. J., Kroep, J. R., Bergman, A. M., and Ackland, S. P. (2000). Basis for effective combination cancer chemotherapy with antimetabolites. Pharmacology & therapeutics *87*, 227-253.

Ponting, C. P. (1997). Evidence for PDZ domains in bacteria, yeast, and plants. Protein Sci *6*, 464-468.

Pulecio, J., Petrovic, J., Prete, F., Chiaruttini, G., Lennon-Dumenil, A. M., Desdouets, C., Gasman, S., Burrone, O. R., and Benvenuti, F. (2010). Cdc42-mediated MTOC polarization in dendritic cells controls targeted delivery of cytokines at the immune synapse. The Journal of experimental medicine *207*, 2719-2732.

Qian, Y., Luo, J., Leonard, S. S., Harris, G. K., Millecchia, L., Flynn, D. C., and Shi, X. (2003). Hydrogen peroxide formation and actin filament reorganization by Cdc42 are essential for ethanol-induced in vitro angiogenesis. The Journal of biological chemistry *278*, 16189-16197.

Radziwill, G., Erdmann, R. A., Margelisch, U., and Moelling, K. (2003). The Bcr kinase downregulates Ras signaling by phosphorylating AF-6 and binding to its PDZ domain. Molecular and cellular biology *23*, 4663-4672.

Rajotte, D., Arap, W., Hagedorn, M., Koivunen, E., Pasqualini, R., and Ruoslahti, E. (1998). Molecular heterogeneity of the vascular endothelium revealed by in vivo phage display. The Journal of clinical investigation *102*, 430-437.

Reid, T., Furuyashiki, T., Ishizaki, T., Watanabe, G., Watanabe, N., Fujisawa, K., Morii, N., Madaule, P., and Narumiya, S. (1996). Rhotekin, a new putative target for Rho bearing homology to a serine/threonine kinase, PKN, and rhophilin in the rho-binding domain. The Journal of biological chemistry *271*, 13556-13560.

Reubi, J. C. (2003). Peptide receptors as molecular targets for cancer diagnosis and therapy. Endocrine reviews *24*, 389-427.

Reubi, J. C. (2007). Targeting CCK receptors in human cancers. Current topics in medicinal chemistry *7*, 1239-1242.

Reubi, J. C., and Maecke, H. R. (2008). Peptide-based probes for cancer imaging. J Nucl Med *49*, 1735-1738.

Reynaud, C., Fabre, S., and Jalinot, P. (2000). The PDZ protein TIP-1 interacts with the Rho effector rhotekin and is involved in Rho signaling to the serum response element. The Journal of biological chemistry *275*, 33962-33968.

Ridley, A. J., and Hall, A. (1992). The small GTP-binding protein rho regulates the assembly of focal adhesions and actin stress fibers in response to growth factors. Cell *70*, 389-399.

Ridley, A. J., Paterson, H. F., Johnston, C. L., Diekmann, D., and Hall, A. (1992). The small GTP-binding protein rac regulates growth factor-induced membrane ruffling. Cell *70*, 401-410.

Riento, K., and Ridley, A. J. (2003). Rocks: multifunctional kinases in cell behaviour. Nat Rev Mol Cell Biol *4*, 446-456.

Roberts, P. J., Mitin, N., Keller, P. J., Chenette, E. J., Madigan, J. P., Currin, R. O., Cox, A. D., Wilson, O., Kirschmeier, P., and Der, C. J. (2008). Rho Family GTPase modification and dependence on CAAX motif-signaled posttranslational modification. The Journal of biological chemistry *283*, 25150-25163.

Rogelj, B., Mitchell, J. C., Miller, C. C., and McLoughlin, D. M. (2006). The X11/Mint family of adaptor proteins. Brain research reviews *52*, 305-315.

Rossman, K. L., Der, C. J., and Sondek, J. (2005). GEF means go: turning on RHO GTPases with guanine nucleotide-exchange factors. Nat Rev Mol Cell Biol *6*, 167-180.

Rousset, R., Fabre, S., Desbois, C., Bantignies, F., and Jalinot, P. (1998). The C-terminus of the HTLV-1 Tax oncoprotein mediates interaction with the PDZ domain of cellular proteins. Oncogene *16*, 643-654.

Ruoslahti, E. (1996). RGD and other recognition sequences for integrins. Annual review of cell and developmental biology *12*, 697-715.

Schlessinger, J. (2000). Cell signaling by receptor tyrosine kinases. Cell *103*, 211-225.

Schmidt, A., and Hall, A. (2002). Guanine nucleotide exchange factors for Rho GTPases: turning on the switch. Genes & development *16*, 1587-1609.

Scott, R. B. (1970). Cancer chemotherapy--the first twenty-five years. British medical journal *4*, 259-265.

Singh, A., Karnoub, A. E., Palmby, T. R., Lengyel, E., Sondek, J., and Der, C. J. (2004). Rac1b, a tumor associated, constitutively active Rac1 splice variant, promotes cellular transformation. Oncogene *23*, 9369-9380.

Smith, G. P. (1985). Filamentous fusion phage: novel expression vectors that display cloned antigens on the virion surface. Science (New York, NY *228*, 1315-1317.

Smith, G. P., and Petrenko, V. A. (1997). Phage Display. Chemical reviews *97*, 391-410.

Smith, K., Fennelly, J. A., Neal, D. E., Hall, R. R., and Harris, A. L. (1989). Characterization and quantitation of the epidermal growth factor receptor in invasive and superficial bladder tumors. Cancer research *49*, 5810-5815.

Spaller, M. R. (2006). Act globally, think locally: systems biology addresses the PDZ domain. ACS chemical biology *1*, 207-210.

Spanos, W. C., Geiger, J., Anderson, M. E., Harris, G. F., Bossler, A. D., Smith, R. B., Klingelhutz, A. J., and Lee, J. H. (2008). Deletion of the PDZ motif of HPV16 E6 preventing immortalization and anchorage-independent growth in human tonsil epithelial cells. Head & neck *30*, 139-147.

Steiner, P., Higley, M. J., Xu, W., Czervionke, B. L., Malenka, R. C., and Sabatini, B. L. (2008). Destabilization of the postsynaptic density by PSD-95 serine 73 phosphorylation inhibits spine growth and synaptic plasticity. Neuron *60*, 788-802.

Stern, M., and Herrmann, R. (2005). Overview of monoclonal antibodies in cancer therapy: present and promise. Critical reviews in oncology/hematology *54*, 11-29.

Su, J. L., Lai, K. P., Chen, C. A., Yang, C. Y., Chen, P. S., Chang, C. C., Chou, C. H., Hu, C. L., Kuo, M. L., Hsieh, C. Y., and Wei, L. H. (2005). A novel peptide specifically binding to interleukin-6 receptor (gp80) inhibits angiogenesis and tumor growth. Cancer research *65*, 4827-4835.

Suetsugu, S., Miki, H., and Takenawa, T. (2002). Spatial and temporal regulation of actin polymerization for cytoskeleton formation through Arp2/3 complex and WASP/WAVE proteins. Cell motility and the cytoskeleton *51*, 113-122.

Sugahara, K. N., Teesalu, T., Karmali, P. P., Kotamraju, V. R., Agemy, L., Greenwald, D. R., and Ruoslahti, E. (2010). Coadministration of a tumor-penetrating peptide enhances the efficacy of cancer drugs. Science (New York, NY *328*, 1031-1035.

Sugi, T., Oyama, T., Muto, T., Nakanishi, S., Morikawa, K., and Jingami, H. (2007). Crystal structures of autoinhibitory PDZ domain of Tamalin: implications for metabotropic glutamate receptor trafficking regulation. The EMBO journal *26*, 2192-2205.

Sun, Y., Aiga, M., Yoshida, E., Humbert, P. O., and Bamji, S. X. (2009). Scribble interacts with beta-catenin to localize synaptic vesicles to synapses. Molecular biology of the cell *20*, 3390-3400.

Suzuki, A., and Ohno, S. (2006). The PAR-aPKC system: lessons in polarity. Journal of cell science *119*, 979-987.

Takimoto CH, C. E. (2008). Principles of Oncologic Pharmacotherapy. In Cancer Management: A Multidisciplinary Approach, W.L. Pazdur R, Camphausen KA, Hoskins WJ ed.

Tapon, N., Nagata, K., Lamarche, N., and Hall, A. (1998). A new rac target POSH is an SH3-containing scaffold protein involved in the JNK and NF-kappaB signalling pathways. The EMBO journal *17*, 1395-1404.

Teesalu, T., Sugahara, K. N., Kotamraju, V. R., and Ruoslahti, E. (2009). C-end rule peptides mediate neuropilin-1-dependent cell, vascular, and tissue penetration. Proceedings of the National Academy of Sciences of the United States of America *106*, 16157-16162.

ten Klooster, J. P., Jaffer, Z. M., Chernoff, J., and Hordijk, P. L. (2006). Targeting and activation of Rac1 are mediated by the exchange factor {beta}-Pix. J Cell Biol *172*, 759-769.

Tenzer, A., Hofstetter, B., Sauser, C., Bodis, S., Schubiger, A. P., Bonny, C., and Pruschy, M. (2004). Profiling treatment-specific post-translational modifications in a complex proteome with subtractive substrate phage display. Proteomics *4*, 2796-2804.

Thiery, J. P. (2002). Epithelial-mesenchymal transitions in tumour progression. Nat Rev Cancer *2*, 442-454.

Tian, Q. B., Suzuki, T., Yamauchi, T., Sakagami, H., Yoshimura, Y., Miyazawa, S., Nakayama, K., Saitoh, F., Zhang, J. P., Lu, Y., *et al.* (2006). Interaction of LDL receptor-related protein 4 (LRP4) with postsynaptic scaffold proteins via its C-terminal PDZ domain-binding motif, and its regulation by Ca/calmodulin-dependent protein kinase II. The European journal of neuroscience *23*, 2864-2876.

Tomaic, V., Gardiol, D., Massimi, P., Ozbun, M., Myers, M., and Banks, L. (2009). Human and primate tumour viruses use PDZ binding as an evolutionarily conserved mechanism of targeting cell polarity regulators. Oncogene *28*, 1-8.

Tonikian, R., Zhang, Y., Boone, C., and Sidhu, S. S. (2007). Identifying specificity profiles for peptide recognition modules from phage-displayed peptide libraries. Nature protocols *2*, 1368-1386.

Tonikian, R., Zhang, Y., Sazinsky, S. L., Currell, B., Yeh, J. H., Reva, B., Held, H. A., Appleton, B. A., Evangelista, M., Wu, Y., *et al.* (2008). A specificity map for the PDZ domain family. PLoS biology *6*, e239.

Ueda, M., Graf, R., MacWilliams, H. K., Schliwa, M., and Euteneuer, U. (1997). Centrosome positioning and directionality of cell movements. Proceedings of the National Academy of Sciences of the United States of America *94*, 9674-9678.

Uematsu, K., Kanazawa, S., You, L., He, B., Xu, Z., Li, K., Peterlin, B. M., McCormick, F., and Jablons, D. M. (2003). Wnt pathway activation in mesothelioma: evidence of Dishevelled overexpression and transcriptional activity of beta-catenin. Cancer research *63*, 4547-4551.

Umeda, K., Ikenouchi, J., Katahira-Tayama, S., Furuse, K., Sasaki, H., Nakayama, M., Matsui, T., Tsukita, S., Furuse, M., and Tsukita, S. (2006). ZO-1 and ZO-2 independently determine where claudins are polymerized in tight-junction strand formation. Cell *126*, 741-754.

Utepbergenov, D. I., Fanning, A. S., and Anderson, J. M. (2006). Dimerization of the scaffolding protein ZO-1 through the second PDZ domain. The Journal of biological chemistry *281*, 24671-24677.

Valadon, P., Garnett, J. D., Testa, J. E., Bauerle, M., Oh, P., and Schnitzer, J. E. (2006). Screening phage display libraries for organ-specific vascular immunotargeting in vivo. Proceedings of the National Academy of Sciences of the United States of America *103*, 407-412.

van Hengel, J., D'Hooge, P., Hooghe, B., Wu, X., Libbrecht, L., De Vos, R., Quondamatteo, F., Klempt, M., Brakebusch, C., and van Roy, F. (2008). Continuous cell injury promotes hepatic tumorigenesis in cdc42-deficient mouse liver. Gastroenterology *134*, 781-792.

Visvikis, O., Lores, P., Boyer, L., Chardin, P., Lemichez, E., and Gacon, G. (2008). Activated Rac1, but not the tumorigenic variant Rac1b, is ubiquitinated on Lys 147 through a JNK-regulated process. The FEBS journal *275*, 386-396.

Wall, M. E., Wani, M. C., Cook, C. E., Palmer, K. H., McPhail, A. I., and Sim, G. A. (1966). Plant antitumor agents. 1. The isolation and structure of camptothecin, a novel alkaloidal leukemia nad tumor inhibitor from camptotheca acuminate. J Am Chem Soc *88*, 3888-3890.

Wang, H., Yan, H., Fu, A., Han, M., Hallahan, D., and Han, Z. (2010). TIP-1 translocation onto the cell plasma membrane is a molecular biomarker of tumor response to ionizing radiation. PloS one *5*, e12051.

Weiss, R. B. (1992). The anthracyclines: will we ever find a better doxorubicin? Seminars in oncology *19*, 670-686.

Wong, A. J., Bigner, S. H., Bigner, D. D., Kinzler, K. W., Hamilton, S. R., and Vogelstein, B. (1987). Increased expression of the epidermal growth factor receptor gene in malignant gliomas is invariably associated with gene amplification. Proceedings of the National Academy of Sciences of the United States of America *84*, 6899-6903.

Wu, H., Feng, W., Chen, J., Chan, L. N., Huang, S., and Zhang, M. (2007a). PDZ domains of Par-3 as potential phosphoinositide signaling integrators. Molecular cell *28*, 886-898.

Wu, H., Nash, J. E., Zamorano, P., and Garner, C. C. (2002). Interaction of SAP97 with minus-end-directed actin motor myosin VI. Implications for AMPA receptor trafficking. The Journal of biological chemistry *277*, 30928-30934.

Wu, J., Yang, Y., Zhang, J., Ji, P., Du, W., Jiang, P., Xie, D., Huang, H., Wu, M., Zhang, G., *et al.* (2007b). Domain-swapped dimerization of the second PDZ domain of ZO2 may provide a structural basis for the polymerization of claudins. The Journal of biological chemistry *282*, 35988-35999.

Wu, W. J., Tu, S., and Cerione, R. A. (2003). Activated Cdc42 sequesters c-Cbl and prevents EGF receptor degradation. Cell *114*, 715-725.

Yamaguchi, Y., Katoh, H., Yasui, H., Mori, K., and Negishi, M. (2001). RhoA inhibits the nerve growth factor-induced Rac1 activation through Rho-associated kinase-dependent pathway. The Journal of biological chemistry *276*, 18977-18983.

Yan, X., Zhou, H., Zhang, J., Shi, C., Xie, X., Wu, Y., Tian, C., Shen, Y., and Long, J. (2009). Molecular mechanism of inward rectifier potassium channel 2.3 regulation by tax-interacting protein-1. J Mol Biol *392*, 967-976.

Yasuda, S., Taniguchi, H., Oceguera-Yanez, F., Ando, Y., Watanabe, S., Monypenny, J., and Narumiya, S. (2006). An essential role of Cdc42-like GTPases in mitosis of HeLa cells. FEBS letters *580*, 3375-3380.

Za, L., Albertinazzi, C., Paris, S., Gagliani, M., Tacchetti, C., and de Curtis, I. (2006). betaPIX controls cell motility and neurite extension by regulating the distribution of GIT1. Journal of cell science *119*, 2654-2666.

Zavarella, S., Nakada, M., Belverud, S., Coniglio, S. J., Chan, A., Mittler, M. A., Schneider, S. J., and Symons, M. (2009). Role of Rac1-regulated signaling in medulloblastoma invasion. Laboratory investigation. Journal of neurosurgery *4*, 97-104.

Zhai, G. G., Malhotra, R., Delaney, M., Latham, D., Nestler, U., Zhang, M., Mukherjee, N., Song, Q., Robe, P., and Chakravarti, A. (2006). Radiation enhances the invasive

potential of primary glioblastoma cells via activation of the Rho signaling pathway. Journal of neuro-oncology *76*, 227-237.

Zhang, J., Yan, X., Shi, C., Yang, X., Guo, Y., Tian, C., Long, J., and Shen, Y. (2008). Structural Basis of [beta]-Catenin Recognition by Tax-interacting Protein-1. Journal of Molecular Biology *384*, 255-263.

Zhang, L., Hoffman, J. A., and Ruoslahti, E. (2005). Molecular profiling of heart endothelial cells. Circulation *112*, 1601-1611.

Zigmond, S. H. (2004). Formin-induced nucleation of actin filaments. Current opinion in cell biology *16*, 99-105.

Zurita, A. J., Troncoso, P., Cardo-Vila, M., Logothetis, C. J., Pasqualini, R., and Arap, W. (2004). Combinatorial screenings in patients: the interleukin-11 receptor alpha as a candidate target in the progression of human prostate cancer. Cancer research *64*, 435-439.

Zwick, E., Bange, J., and Ullrich, A. (2002). Receptor tyrosine kinases as targets for anticancer drugs. Trends in molecular medicine *8*, 17-23.